

https://dspace.org/

An assessment of Sn-W-Nb-Ta oxide minerals from the Bugesera district of Rwanda and geological context

Buurman, Innes

2018

https://hdl.handle.net/10539/25877

Buurman, Innes, (2018) An assessment of Sn-W-Nb-Ta oxide minerals from the Bugesera district of Rwanda and geological context, University of the Witwatersrand, Johannesburg, https://hdl.handle.net/10539/25877.

Downloaded from a DSpace repository. https://dspace.org/



An assessment of Sn-W-Nb-Ta oxide minerals from the Bugesera district of Rwanda and geological context

Innes Buurman

1057988

Supervisors

Professor J.A. Kinnaird

Professor P.A.M. Nex

Declaration

I Innes Buurman declare that this document is my own work, that it has not been submitted for any degree or examination in any other university, and that all the sources I used or quoted have been indicated and acknowledged by complete references.

Innes Buurman



Signed

24 May 2018

Date

Acknowledgements

I would like to thank the following people for their guidance and assistance throughout the project. Professor J.A. Kinnaird and Professor P.A.M. Nex, my supervisors for their support as study leaders and their expertise and guidance throughout the project. Mr. Warrick Fuchsloch and Dr. Peter Horvath for their guidance with the electron microprobe analysis. I would also like to thank Mr. Richard Montjoie one of the directors of Umbono Capital for allowing this study on their Rwanda project and for his helpful insight and assistance with sampling, field trip planning, and arranging financial support from Umbono Capital for this project. Lastly, I would like to thank my wife Laetitia Buurman, for her continued support throughout this project.

Abstract

The Sn-W-Nb-Ta oxide minerals of Rwanda are rarely found in the same area and predominantly occur in different deposits. Gatumba is known for its pegmatite related Nb-Ta, and Sn mineralisation, Nyakabingo for its hydrothermal vein type W mineralisation, and Rutongo for its hydrothermal vein type Sn mineralisation. Very little geological research has been performed on the Bugesera district in Rwanda. Therefore, the aim of this study is to enhance the knowledge base on the Bugesera district by studying four mining areas (Nyagasagara, Gakurazo, Kageyo and Kageyo Extension) on the Hard Metal Rwanda (HMR) license, their locations relative to regional structures and G4 granites, and the mineral grade at each of the deposits. The mineralogy and mineral chemistry were only studied on the concentrate material from Nyagasagara, for comparison with literature and to determine whether the mineralisation was primary or secondary. The HMR license is located in between the Bugesera granite and the Bugesera syncline fold. Nyagasagara and Kageyo occur adjacent (< 4km) to known large scale structures, granites and/or pegmatites, Gakurazo is located in between Nyagasagara and Kageyo, and the Kageyo Extension is located on the rim of the Bugesera granite. No outcrops of granite and/or pegmatite were observed at any of the sites. The highest mineral grade was recorded at Nyagasagara Tunnel 1 (5.56% cassiterite) with the lowest grade recorded at Kageyo and Kageyo Extension (0.01% coltan). Around 60% of the cassiterite grains from Nyagasagara, reports to the coarser size fraction of +4 mm and +2 mm, with the shape of the grains ranging from angular to very angular. Cassiterite is the only oxide mineral of interest present at Nyagasagara, as confirmed by the whole rock chemistry and optical microscopy on the concentrate samples from Nyagasagara. The mineral chemistry of the cassiterite plots in the rare element granite and pegmatite field on the binary Nb + Ta and Fe + Mn diagram. Most of the cassiterite contains more Nb compared to Ta (Nb>Ta) and minor Fe_2O_3. The cassiterite also contained numerous coltan inclusions and exsolution products. This study concludes that the HMR license area is situated in a suitable regional geological setting for Sn-W-Ta-Nb oxide minerals to be found. However, the Nyagasagara deposit is an eluvial deposit consisting of only cassiterite minerals, which have a magmatic origin, believed to be related to rare element granites.

Table of Contents

Declaration 1
Acknowledgements 2
Abstract 3
List of Figures 6
List of Tables 8
Chapter 1: 9
Introduction 9
1.1 Regional geology 9
1.2 Granites in the KAB 11
1.3 Mineralisation 12
1.3.1 Primary mineralisation 13
1.3.2 Secondary mineralisation 18
1.4 Mining history of Rwanda and the Bugesera district 19
1.5 Aim 21
1.6 Objectives 22
Chapter 2: 23
Local geology and project location 23
2.1 Local geology 23
2.2 Project location 23
Chapter 3: 26
Material and methods 26
3.1 Field observations, surveying and mapping 26
3.2 Grade estimates of the various mining sites 26
3.3 Sample description 27
3.4 Sample preparation and analytical procedures 27
3.4.1 Size fraction analysis (dry screening) 28
3.4.2 Thin sections and optical microscopy 29
3.4.3 XRF analysis 29
3.4.4 ICP-MS analysis for lithium 29
3.4.5 Electron Microprobe Analysis 29
Chapter 4: 31
Mineralisation 31
4.1 Field observations, mapping and grade estimates 31
4.1.1. Nyagasagara 32
4.1.2. Gakurazo, Kageyo and Kageyo Extension 33

4.2 Size fraction analysis 36
4.3 XRF and ICP-MS 38
4.4 Optical microscopy 41
4.5 Electron Microprobe Analysis 42
4.5.1 Geochemistry of cassiterite 43
4.5.2 Geochemistry of the coltan inclusions and products of exsolution 48
Chapter 5: 51
Discussion 51
5.1 Introduction 51
5.2 HMR mining areas compared to other deposits in Rwanda 51
5.3 Nyagasagara deposit and its mineralisation 53
5.3.1 Geochemistry of cassiterite 54
5.3.2 Geochemistry of coltan inclusions and exsolution products 55
Chapter 6: 57
Conclusions and Recommendations 57
References 59
Appendix A: Annual exports, earnings and contribution to total exports from 1930 to 2015 (GMD, 2010; OGMR, 2010; Ngaruye, 2011; USGS, 2016) 62
Appendix B: Summary of Rwanda's mining history 63
Appendix C: Sample list from the four mining areas 64
Appendix D: Sample list sent to Setpoint and work program 66
Appendix E: List of thin sections from Nyagasagara concentrate 67
Appendix F: Cassiterite grades at the Nyagasagara and Coltan grades Kageyo, Kageyo Extension and Gakurazo mining sites. 68
Appendix G: Cassiterite Size Fraction Analysis 69
Appendix H: Whole rock chemical data from the cassiterite concentrates of Nyagasagara 70
Appendix I: Whole rock chemical data from the cassiterite concentrates of Nyagasagara 71
Appendix J: EMPA data from all the grains analysed from Nyagasagara concentrate 72

List of Figures

Figure 1. 1: Geological maps of the KIB and the KAB;(A) A simplified regional geological map including the KIB, KAB and the Rusizi belt; (B) illustrates the regional framework of the KAB with major magmatic outcrops modified after Tack et al., (2010), Koegelenberg et al., (2014) and Debruyne, (2015). 10
Figure 1. 2: General metallogenic model for granite-related deposits in Central Africa. Note that both magmatic-hydrothermal and quartz vein systems represents the fluids from the residual melt, in addition to the intragranular fluid associated with multiphase granite intrusions (Pollard and Taylor, 1986; Lehmann et al., 2014). 12
Figure 1. 3: Vein type tin mineralisation in Rwanda; (A) Geological map of a mining level 100m underground, showing steeply dipping cassiterite rich quartz veins (black) hosted predominantly in quartzite, although some veins occur in the metapelites too (Coordinates are in metres), (B) A ca. 20cm thick cassiterite rich quartz vein, crosscutting the quartzite in which it is hosted. At the bottom of the vein is a grey shale layer. Also seen in the picture is a 1cm thick alteration zone along the margins of the vein (scale bar is 9 cm) (Masoro, tunnel 7); (C) is a sketch of (B). (De Clercq, 2012; Pohl et al., 2013). 15
Figure 1. 4: Vein type tungsten mineralisation in Rwanda; (A) Alternating dark shale and quartzite units in the Rulizahene open pit mine, the dark shale contains small folded bedding-parallel quartz veins as illustrated in (B) (De Clercq, 2012; Dewaele et al., 2016). 15
Figure 1. 5: Geological map, illustrating the zonation of the Gatumba pegmatite field and the location of important outcrops relative to the Gitarama granite on the bottom right. The biotite zone occurs the closest to the granite, with each subsequent zone occurring a little further away from the granite. The mineralised zone is the furthest away from the granite (Hulsbosch et al., 2014). 17
Figure 1. 6: Paragenesis of the Gatumba, cassiterite and coltan mineralisation (Dewaele et al., 2007; Dewaele et al., 2011) 18
Figure 1. 7: Illustrations of (A) artisanal miners at Gatumba extracting minerals from secondary mineralisation whereas (B) is an old entrance to an abandoned underground mine extracting minerals from primary mineralisation (Montjoie, 2014; Muchez et al., 2014). 20
Figure 1. 8: Cassiterite contribution in percent to total exports from 1930 to 2015 (GMD, 2010; OGMR, 2010; Ngaruye, 2011; USGS, 2016). 20
Figure 2. 1: Geological map of Rwanda, indicating the location of the study area, owned by Hard Metal Rwanda (HMR). Other known cassiterite and coltan mining areas, such as Gatumba, Nyakabingo and Rutongo are also indicated on the map. Modified from Schlüter, (2008). 23
Figure 2. 2: Location map of known cassiterite and/or coltan mines, such as Gatumba, Rutongo, Musha, Nemba and the Hard Metal Rwanda project area situated in the Bugesera district of Rwanda modified from Buurman and Montjoie (2016). 24
Figure 2. 3: Map of the Bugesera district indicating various discoveries and historical mines. Note that the location of the Hard Metal Rwanda project is situation south of a tin discovery and historical mine modified after Buurman & Montjoie (2016) and Baudin et al., (1982). 25
Figure 3. 1: A) The weighing of the ROM before processing and drying, and B) the weighing of the concentrate after drying. 26
Figure 3. 2: Google earth images indicating the location of the four mining areas (Nyagasagara, Kageyo, Kageyo Extension and Gakurazo). Note that Kageyo Extension is located outside the HMR licence boundary (light green outline) (Buurman and Montjoie, 2016). 27
Figure 3. 3: Artisanal miners on the HMR project, A) processing the ROM and B) drying the concentrate, using traditional methods. 28

Figure 4. 1: Geological map of the HMR licence area, illustrating the mining sites and their locations relative to regional structures and the underlying geology, modified after Buurman & Montjoie (2016) and Baudin et al., (1982). 31
Figure 4. 2: Map of Nyagasagara, illustrating the locations and cassiterite grade of the various mining sites on the deposit; the Belgium miners used the Nyagasagara pit and Belgium tailings in the 1950s. The current mining areas are Tunnel 1 to 5. 32
Figure 4. 3: Cassiterite grades at the various mining sites (Tunnel I - V and Walking 1 and 2) at Nyagasagara. 33
Figure 4. 4: Map of Gakurazo, illustrating the location and cassiterite grade of the mining site. 34
Figure 4. 5: Combined cassiterite and/or coltan grade at Kageyo, Gakurazo and Kageyo Extension. 34
Figure 4. 6: Map of Kageyo, illustrating the location and coltan grade of the various mining sites. 35
Figure 4. 7: Map of Kageyo Extension, illustrating the location and coltan grade observed at the mining sites. 36
Figure 4. 8: Grain size distribution of the combined cassiterite and coltan concentrate from all four mining areas on Nyagasagara. 37
Figure 4. 9: Comparison between the average cassiterite and coltan grade and the grain size distribution on Nyagasagara. The sample ID's are ordered from top to bottom on the y-axis, from highest (NYAG07) to lowest (NYAG04) cassiterite and coltan grade. 38
Figure 4. 10: Chemical composition of the concentrate from Nyagasagara, ordered from the highest cassiterite grade (NYAG07) to the lowest cassiterite grade (NYAG04). A) Tin concentrations in the concentrate; B) Tantalum and Niobium concentrations in the concentrate. 39
Figure 4. 11: Microphotograph of the +4mm size fraction cassiterite grains from Tunnel 2, Nyagasagara under a transmitted light microscope. Most of the grains are fractured and typical colour zonation (dark brown-white) and pleochroism from dark brown to light brown can be seen in some of the grains. 41
Figure 4. 12: Microphotograph of +4mm size fraction cassiterite grains from; A) Tunnel 1; B) Tunnel 3; C) Walking 1; D) Walking 2, under a transmitted light microscope. Zoning and pleochroism from dark brown to light brown can be seen in some of the grains. 42
Figure 4. 13: Average SnO_2 content as weight percentage in cassiterite from Tunnel 1, 2, Walking 1, and 2, at Nyagasagara. The Sample ID's are ordered from highest grade (NYAG07) to lowest grade (NYAG04). 43
Figure 4. 14: A (Sn+Ti,W) - (Nb+Ta) - (Fe+Mn) ternary diagram showing chemical compositions of all analysed cassiterite at NYAG07 (green), NYAG15 (red), NYAG03 (blue), and NYAG04 (yellow). 44
Figure 4. 15: Cassiterite analyses plotted in the columbite quadrilateral showing low Nb/Ta fractionation; (B) a binary diagram of (Nb + Ta) vs (Fe +Mn) for cassiterite from all the mining sites, NYAG07 (green), NYAG15 (red), NYAG03 (blue), NYAG04 (yellow). The fields of cassiterite in rare element pegmatites and of hydrothermal cassiterite were defined by Tindle and Breaks (1998). 46
Figure 4. 16: Microphotographs of inclusions and/or exsolution products hosted in the cassiterite grains of Nyagasagara; A) zoned zircon grain, B) zoned coltan grain, C) zoned coltan grain. 47
Figure 4. 17: Coltan analyses plotted in the (Sn+Ti+W) – (Nb+Ta) – (Fe+Mn) ternary diagram 48
Figure 4. 18: Coltan minerals from the Nyagasagara mining area plotted in the columbite quadrilateral. 50

List of Tables

Table 1. 1: Major differences between the WD and ED 11
Table 1. 2: Summary of the three-well-known vein and rare element pegmatite type deposits of Rwanda (Dewaele et al., 2009; De Clercq, 2012; Pohl et al., 2013; Lehmann et al., 2014; Dewaele et al., 2016). 14
Table 3. 1: Characteristics of the CAMECA SX 5FE 30

Chapter 1:

Introduction

The Bugesera district in Rwanda has been mined artisanally in various mining pits, but very little geological research has been performed on cassiterite and coltan of this district. Information is limited to research performed on the Karagwe-Ankole belt (KAB), Rwanda in general, and on adjacent areas such as the Gatumba, Rutongo and Nyakabingo regions. This study has therefore aimed at enhancing the knowledge base on the project area by completing field work, studying the mineralogy and geochemistry of the cassiterite and coltan, and comparing it to existing literature on the KAB, Rwanda, Gatumba, Rutongo and Nyakabingo area in Rwanda.

1.1 Regional geology

Rwanda forms part of the Karagwe-Ankole belt (KAB) of Central Africa which is mainly composed of Mesoproterozoic metasedimentary and metavolcanic rocks (Tack et al., 2010). The geology of Rwanda generally consists of the Mesoproterozoic Burundian Supergroup (sandstones alternating with shales) intruded by granite bodies throughout the country (Fig. 1.1) (Schlüter, 2008). In older literature (Pohl and Günther, 1991; Pohl, 1994), the KAB was thought to form the northern part of the Kibara belt (KIB), a continuous northeast (NE) trending orogenic belt stretching over 1500 km, from the Katanga area in the Democratic Republic of Congo (DRC) through Rwanda, Burundi, and up to the Ankole region in southwest (SW) Uganda. Research by Tack et al., (2010) however, demonstrates that the KIB and KAB are in fact two separate segments, because they are separated by the Paleoproterozoic Rusizi Belt and they had an independent basin development (Fig. 1.1a) (Tack et al., 2010; Fernandez-Alonso et al., 2012). This however, is refuted by Debruyne et al., (2015), indicating that both the KIB and KAB forms part of the same orogenic system. In his paper he argues that both belts had the same ages of magmatic intrusions at (~ 1375 Ma and ~ 1000 Ma) and deformation.

In the literature, there appears to be confusion related to the term “Kibara belt”, where synonyms such as Kibaride belt, Kibaran belt, North-Eastern Kibaran belt (NKB), Kibara belt senso-strictu and Kibara belt sensu-lato are all used to describe the Kibara belt, and depending on the author, could include the KAB or not. For the sake of clarity, the term “Kibara belt” (“KIB”) and “Karagwe-Ankole belt” (“KAB”) used in this study is based on the definition by Tack et al., (2010). They defined the KIB as the part south of the Rusizi belt and the KAB as the part NE of the Rusizi belt, not including the part

in the DRC (northwest of the Rusizi belt), which is left undefined (Fig. 1.1a). Since the study area is in Rwanda further discussions will mainly be focussed on the KAB.

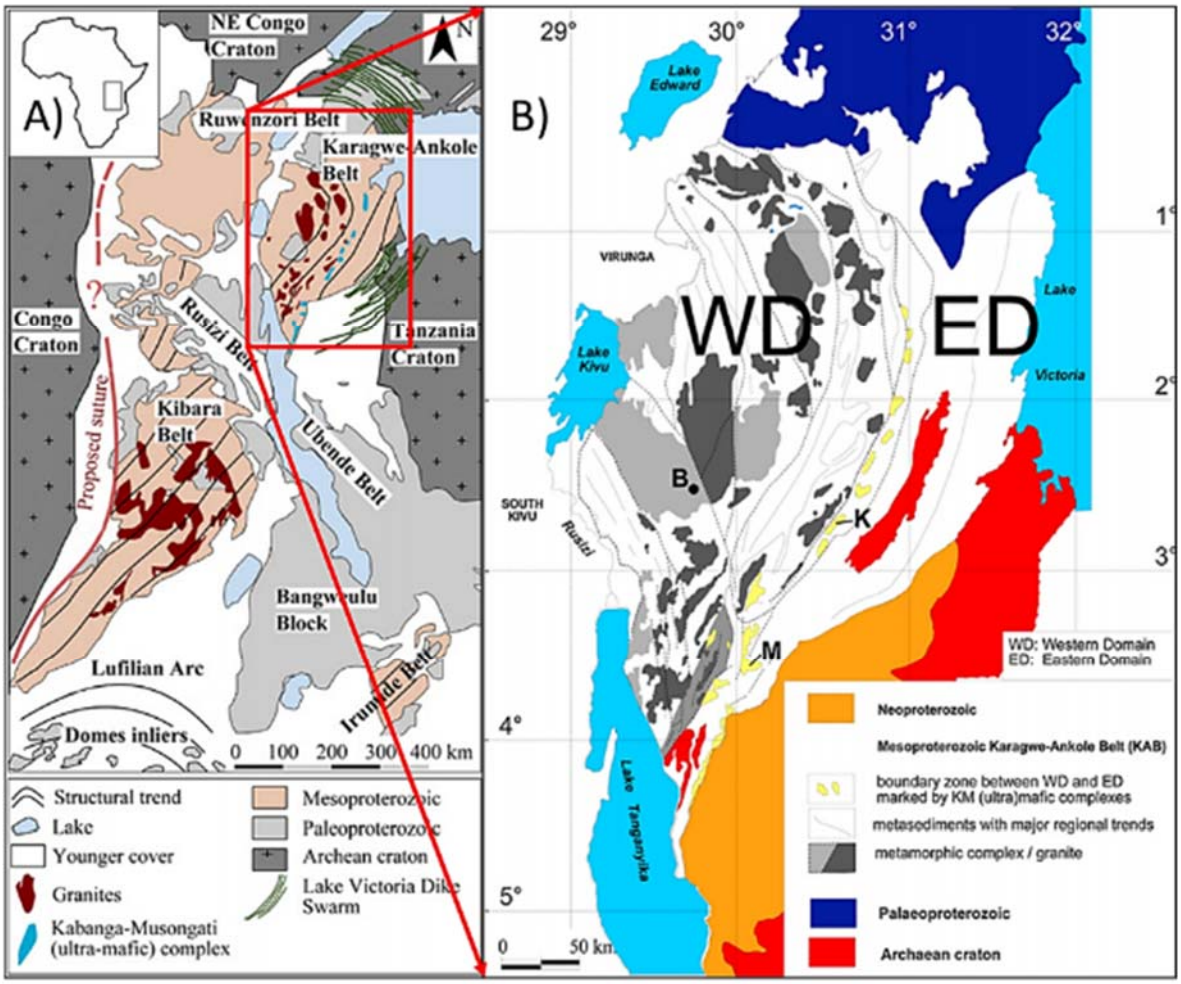


Figure 1. 1: Geological maps of the KIB and the KAB;(A) A simplified regional geological map including the KIB, KAB and the Rusizi belt; (B) illustrates the regional framework of the KAB with major magmatic outcrops modified after Tack et al., (2010), Koegelenberg et al., (2014) and Debruyne, (2015).

The KAB, according to Tack et al., (1994) can be further subdivided into two structurally contrasting domains, the Eastern Domain (ED) and the Western Domain (WD) (Fig. 1.1b). The major differences between the WD and the ED are summarized in the table below (Table 1.1). The WD and ED are separated by mafic and ultramafic layered complexes of the Kabanga-Musongati (KM) alignment (Fig. 1.1b) and the area of interest is situated in the WD of the KAB (Tack et al., 1994; Evans et al., 2000; Fernandez-Alonso et al., 2012). One distinctive difference between the domains is the presence of various granitic intrusions in the WD and the absence of granitic intrusions in the ED (Tack et al., 2010).

Table 1. 1: Major differences between the WD and ED

Domain	Western Domain (WD)	Eastern Domain (ED)
General characteristic	It is complexly evolved (Tack et al., 1994; Fernandez-Alonso and Theunissen, 1998)	It is weakly evolved and exclusively sedimentary (Tack et al., 1994; Fernandez-Alonso and Theunissen, 1998)
Supergroup	Akanyaru Supergroup (Fernandez-Alonso et al., 2012)	Kagera Supergroup (Fernandez-Alonso et al., 2012)
Deposition	Deposition started at 1.42Ga (Fernandez-Alonso et al., 2012)	Deposition started at 1.78Ga (Fernandez-Alonso et al., 2012)
Deformation and host rocks	Deformed metasedimentary rocks of greenschist to amphibolite facies (Tack et al., 2010)	Eastward decrease in both deformation and metamorphism (Tack et al., 1994; Tack et al., 2010)
Mineralisation	Locally intruded by barren homogeneous 1375Ma S-type granites and 986Ma tin-granites and associated mineralisation (Tack et al., 2010)	Absence of S-type granite intrusions and associated (Sn-Nb-Ta-W) and Au Mineralisation (Tack et al., 2010)

1.2 Granites in the KAB

The KAB had been intruded by different generations of granites and subordinate mafic bodies (Fig. 1.1) (Cahen et al., 1984; Dewaele et al., 2011). In older literature, (Klerkx et al., 1987; Fernandez-Alonso and Theunissen, 1998) the granite intrusions of Rwanda are subdivided into four different types (G1 to G4), according to their age (based on Rb/Sr data) and structural setting. However, recent studies based on U-Pb SHRIMP dating (Tack et al., 2010; Fernandez-Alonso et al., 2012) suggests the presence of only two main granite generation events in the KAB. The first event being the G1 to G3 granite emplacement at 1380 ± 10Ma, which intruded the Palaeo- and Mesoproterozoic rocks and the second event being the G4 granite ("tin granite") emplacement at 986 ± 10Ma (Dewaele et al., 2009; Tack et al., 2010; Dewaele et al., 2011). The first event is believed to have been related to the regional bimodal magmatism and extensional tectonics at 1375Ma, whereas the second event is believed to have been related to post-orogeny collapse after the compressional event in the Irumide belt at 1000Ma (Dewaele et al., 2011; Dewaele et al., 2013).

1.3 Mineralisation

Granites have the ability to concentrate a substantial number of elements into the crust and as a result form economic ore deposits of Sn, Ta, Nb, W, rare earth elements (REE), Au, Zr, Th, U, Mo, Cu, Li, Rb, Cs and Be. These economic ore deposits are also commonly referred to as granite-related ore deposits and according to Cerny et al., (2005) can be divided into three main categories, such as a) rare metal granites, b) vein and greisen and, c) rare element pegmatites (Cerny et al., 2005).

The granite related ore deposits in the KAB are known to be rich in minerals such as cassiterite (SnO_2), wolframite ($(Fe,Mn)WO_4$), columbite-tantalite ($(Nb,Ta)_2O_5$, also called coltan), spodumene ($LiAlSi_2O_6$), beryl ($Be_3Al_2Si_6O_{18}$), monazite ($(Ce,La,Y,Nd,Th)PO_4$), amblygonite ($(Li,Na)AlFPO_4$) and gold (Au), etc (Dewaele et al., 2009). They occur in a variety of mineralisation styles, but can broadly be categorised into primary and secondary mineralisation. The primary mineralisation style, associated with Sn-Nb-Ta-W deposits in the KAB, are the vein type cassiterite and wolframite mineralisation, and the rare element pegmatite type with coltan and in some cases cassiterite mineralisation (Fig 1.2), whereas the secondary mineralisation style refers to eluvial and alluvial deposits and can contain cassiterite, coltan, and tungsten mineralisation (Dewaele et al., 2009).

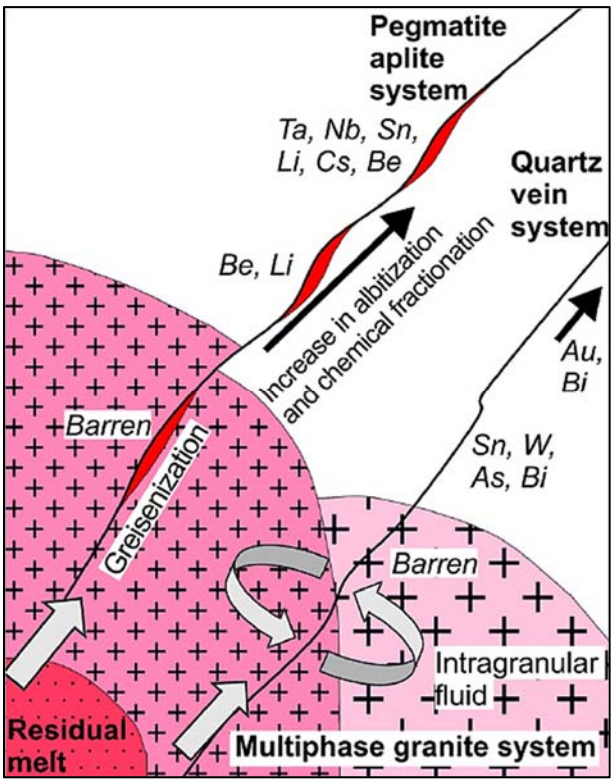


Figure 1. 2: General metallogenic model for granite-related deposits in Central Africa. Note that both magmatic-hydrothermal and quartz vein systems represents the fluids from the residual melt, in addition to the intragranular fluid associated with multiphase granite intrusions (Pollard and Taylor, 1986; Lehmann et al., 2014).

1.3.1 Primary mineralisation

In the KAB, the primary mineralisation of Sn, Nb-Ta and W do not commonly occur in the same deposits, due to different host rocks at the various deposits, which influences the precipitation mechanisms of the elements. Primary vein-type Sn mineralisation is best studied in the Rutongo area (quartzite as host rock), with no known occurrences of either W and/or Nb-Ta. Whereas, primary vein type W mineralisation is best studied in the Nyakabingo region (shale as host rock), with no known occurrence of either Sn and/or Nb-Ta. The Gatumba region is known for its pegmatite related Nb-Ta and Sn mineralisation (dolerites and metasediments as host rock). A short summary of the key characteristic of each area are presented in Table 1.2 and described below (Dewaele et al., 2009; Hulsbosch et al., 2013; Pohl et al., 2013; Dewaele et al., 2016).

Vein type mineralisation

Cassiterite and wolframite vein deposits share several similar features such as paragenesis, tectonic control and hydrothermal wall-rock alteration. Thus, it is easy to assume that both minerals occur in the same deposit. However, most deposits in Central Africa contain only one of the two minerals, with very few deposits containing both minerals (Pohl et al., 2013). The principle controlling factor for these two deposit types is lithological (host rock). This is supported by production results from Rutongo and Nyakabingo, two well-known cassiterite and wolframite mining districts in Rwanda (Table 1.2).

At Rutongo hundreds of sheeted quartz veins, rich in cassiterite, are located in brittle quartzites (Fig. 1.3(A)-(C), with only a limited number of the veins occurring in metapelites. These veins vary in size, ranging from a few centimetres up to a few metres. The average width however, ranges between 0.5 m to 1 m. These veins can extend for some meters up to hundreds of meters, with the extensions mostly controlled by the thickness of the quartzite units (Dewaele et al., 2009). The cassiterite is interpreted to have been precipitated from an aqueous-gaseous fluid, with a low to moderate salinity (6-15 mass-% NaCl eq.) and a temperature of 330^{o}C (Pohl et al., 2013).

Table 1. 2: Summary of the three-well-known vein and rare element pegmatite type deposits of Rwanda (Dewaele et al., 2009; De Clercq, 2012; Pohl et al., 2013; Lehmann et al., 2014; Dewaele et al., 2016).

Name	Rutongo	Nyakabingo	Gatumba
Location	Cassiterite mining district 10 km north of Kigali, situated on the Rutongo anticline. Mining initially focused on secondary mineralisation, but progressively moved underground to primary mineralisation.	Wolframite mining district approximately 40 km north-west of Kigali, situated on the flanks of the Bumbogo anticline. Mining originated as open pit, but progressively moved to underground.	Open pit mining (approximately 150 km^2) district 50 km west of Kigali, situated between two granitic batholiths (Gitarama pluton and the Kabaya pluton). It is located on the western limb of the Ndiza syncline.
Type	Cassiterite containing hydrothermal quartz veins hosted predominantly in quartzites (Fig. 1.3).	Wolframite containing hydrothermal quartz veins hosted predominantly in black shales (Fig. 1.2).	Coltan and cassiterite in rare metal pegmatite (lithium-caesium-tantalum, LCT) dykes, hosted in mafic dolerites and metasedimentary rocks.
Production	Historic production of 50 000 tons of cassiterite of which 65% was from primary mineralisation and 25% from secondary mineralisation. Present production is unknown.	Historic production of 8000 tons wolframite, it is unclear whether this was from primary or secondary mineralisation. Present production is less than 10 t/month	Historic production of 4000 tons coltan, in addition to 20 000 tons of cassiterite, it is unclear whether this was only from primary mineralisation. Present production is less than 10 t/month
Grade	Average of 0.6% cassiterite, with rich pockets ranging up to 5% cassiterite.	Unknown	0.5 kg/m^3 cassiterite, coltan unknown.
Activity	Active mining	Active artisanal mining	Active artisanal mining and hard rock mine in construction

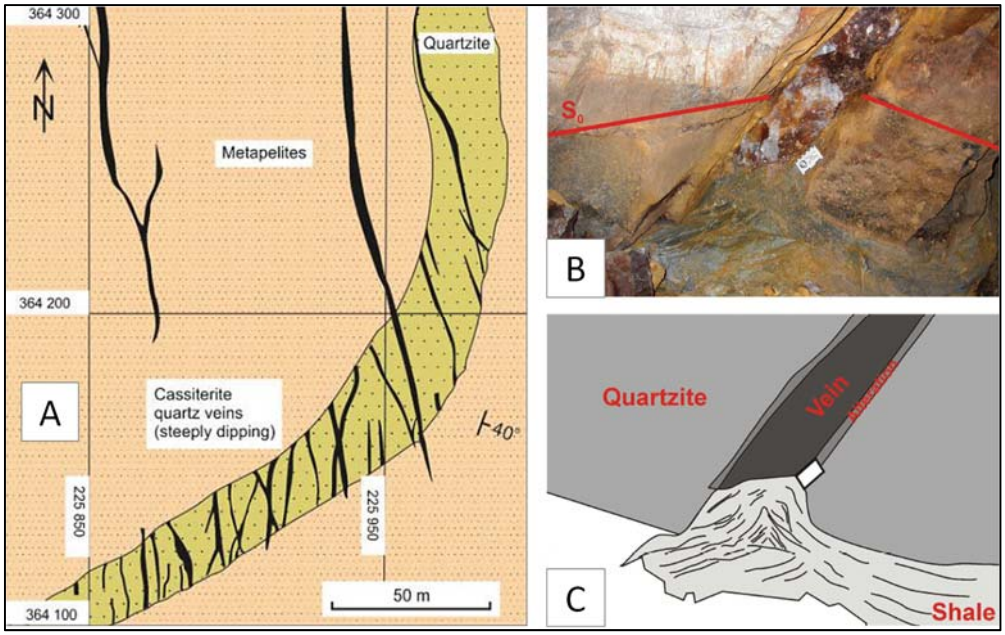


Figure 1. 3: Vein type tin mineralisation in Rwanda; (A) Geological map of a mining level 100m underground, showing steeply dipping cassiterite rich quartz veins (black) hosted predominantly in quartzite, although some veins occur in the metapelites too (Coordinates are in metres), (B) A ca. 20cm thick cassiterite rich quartz vein, crosscutting the quartzite in which it is hosted. At the bottom of the vein is a grey shale layer. Also seen in the picture is a 1cm thick alteration zone along the margins of the vein (scale bar is 9 cm) (Masoro, tunnel 7); (C) is a sketch of (B). (De Clercq, 2012; Pohl et al., 2013).

At Nyakabingo the wolframite containing quartz veins are hosted in carbon-rich shale (Fig. 1.4) instead of quartzites. The wolframite minerals precipitated from a hydrothermal fluid similar to that from which cassiterite precipitated. Thus, supporting the theory that the main difference between these two deposit types are the host rocks which host them (De Clercq, 2012). The fluids had a low to moderate salinity (0.6-13.8 eq. wt% NaCl), with a temperature between 270°C and 344°C.

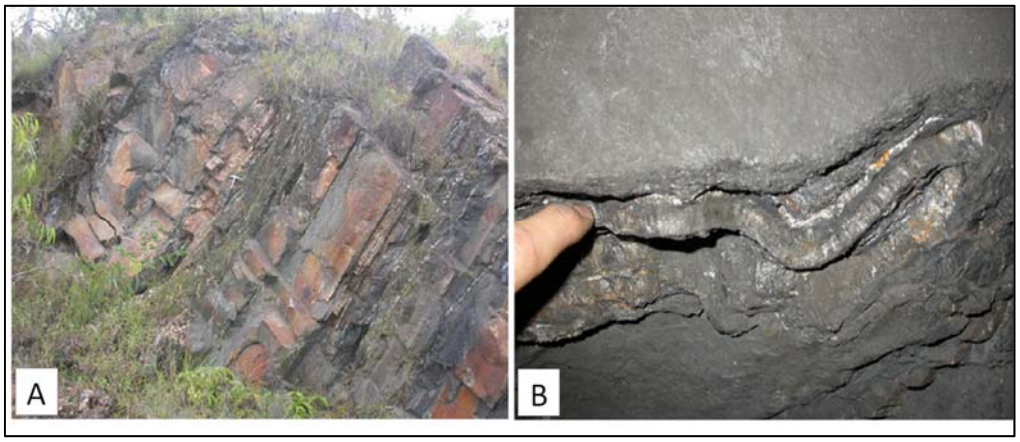


Figure 1. 4: Vein type tungsten mineralisation in Rwanda; (A) Alternating dark shale and quartzite units in the Rulizahene open pit mine, the dark shale contains small folded bedding-parallel quartz veins as illustrated in (B) (De Clercq, 2012; Dewaele et al., 2016).

Note that even though the host rocks of these deposit may differ, both minerals mostly occur along the margins and centre of quartz veins, and its contact zones with the host rocks (De Clercq, 2012; Pohl et al., 2013; Dewaele et al., 2016).

Pegmatite type mineralisation

According to Hulsbosch et al., (2014) the Gatumba pegmatite field consists of four zones of pegmatites, with only the fourth pegmatite zone (most fractionated) containing cassiterite and coltan mineralisation. The first three pegmatite zones are barren and they gradually evolve to the most fractionated, rare-element pegmatite (zone 4). These rare-element pegmatites can be classified according to the petrogenetic-geochemical classification of Cerny et al., (2005), as belonging to the lithium-caesium-tantalum (LCT) pegmatite family (Dewaele et al., 2011; Hulsbosch et al., 2013). In Gatumba, there are about 130 known and mapped pegmatite dykes (Fig. 1.5), all of which are believed to be structurally controlled and associated with structural features such as lineaments, interpreted to be fractures. These pegmatites vary in size, shape and thickness, ranging from a few centimetres to 30 m in thickness, and from a couple of metres to approximately 2400 m in length (Dewaele et al., 2007) (Dewaele et al., 2011; Hulsbosch et al., 2014). Note that the vertical extent of these pegmatites remains unknown because most of the mining activity to date focussed on the upper part of the deposits.

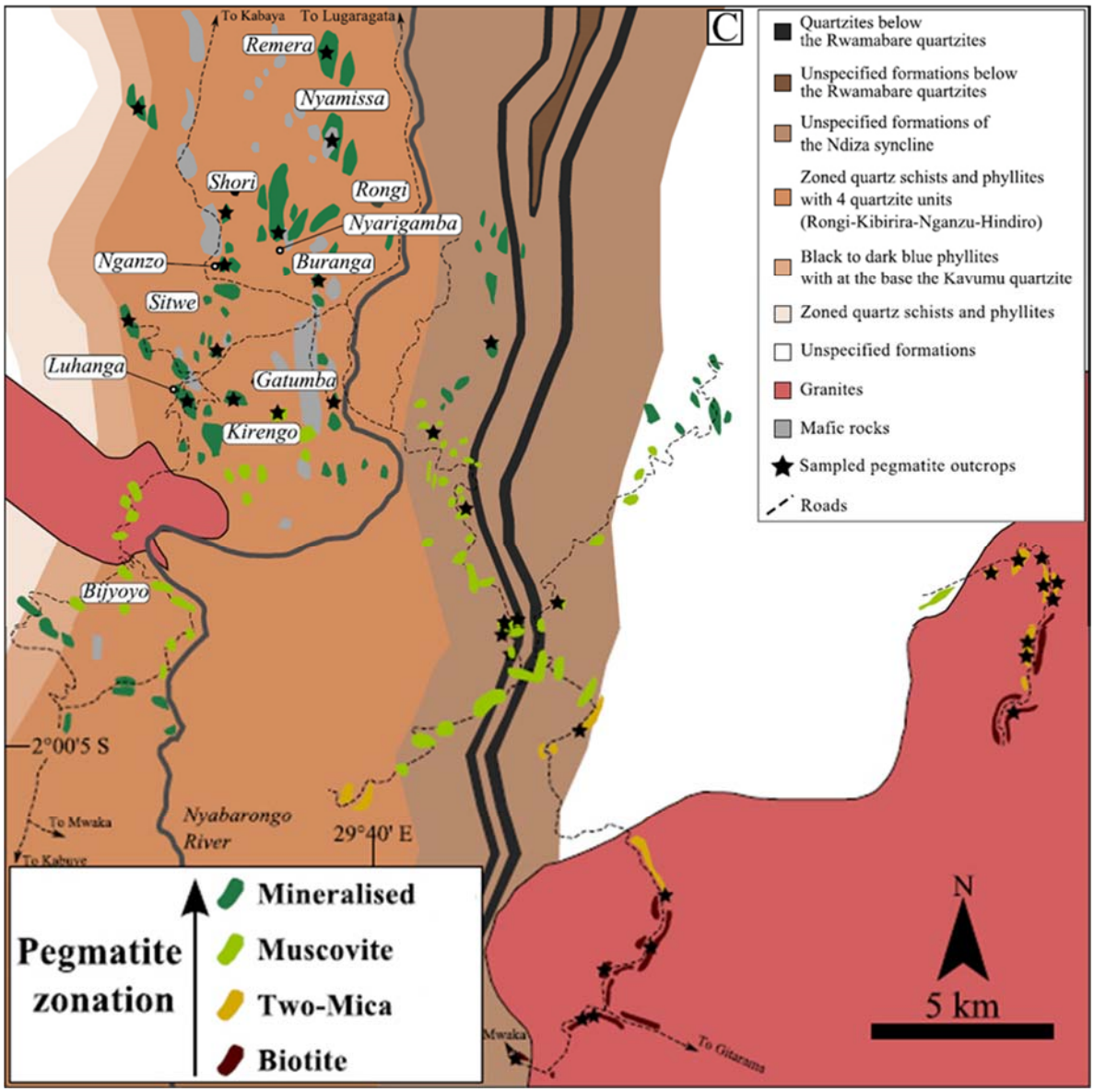


Figure 1. 5: Geological map, illustrating the zonation of the Gatumba pegmatite field and the location of important outcrops relative to the Gitarama granite on the bottom right. The biotite zone occurs the closest to the granite, with each subsequent zone occurring a little further away from the granite. The mineralised zone is the furthest away from the granite (Hulsbosch et al., 2014).

Enrichment processes for Sn-W-Nb-Ta are very similar, but their precipitation mechanisms are different. In contrast to cassiterite and wolframite, coltan is insoluble in aqueous fluids and crystallizes with the pegmatite melt phase. This explains its absence in hydrothermal alteration zones (Hulsbosch et al., 2013). According to Dewaele et al., (2007), isotopic data and petrographic observations suggest that the timing of the coltan mineralisation (965 ± 5 Ma) and pegmatite emplacement overlaps. Some of the petrographic observations supporting this, including coltan cross-cut by later alteration phases (Fig. 1.6). Even though cassiterite minerals are associated with pegmatite deposits, the timing of its mineralisation suggests that most of the minerals formed during a later metasomatic-hydrothermal stage associated with muscovitisation and sericitisation of the pegmatites (Fig. 1.6). This is supported

by evidence of cassiterite minerals in quartz veins cross-cutting the pegmatite, whereas coltan mineralisation is equally distributed throughout the pegmatite (Dewaele et al., 2007; Dewaele et al., 2011).

In addition to cassiterite and coltan, accessory minerals present in the mineralised pegmatite are: muscovite, K-feldspar, quartz, sericite, albite, apatite, spodumene, beryl and some pyrite.

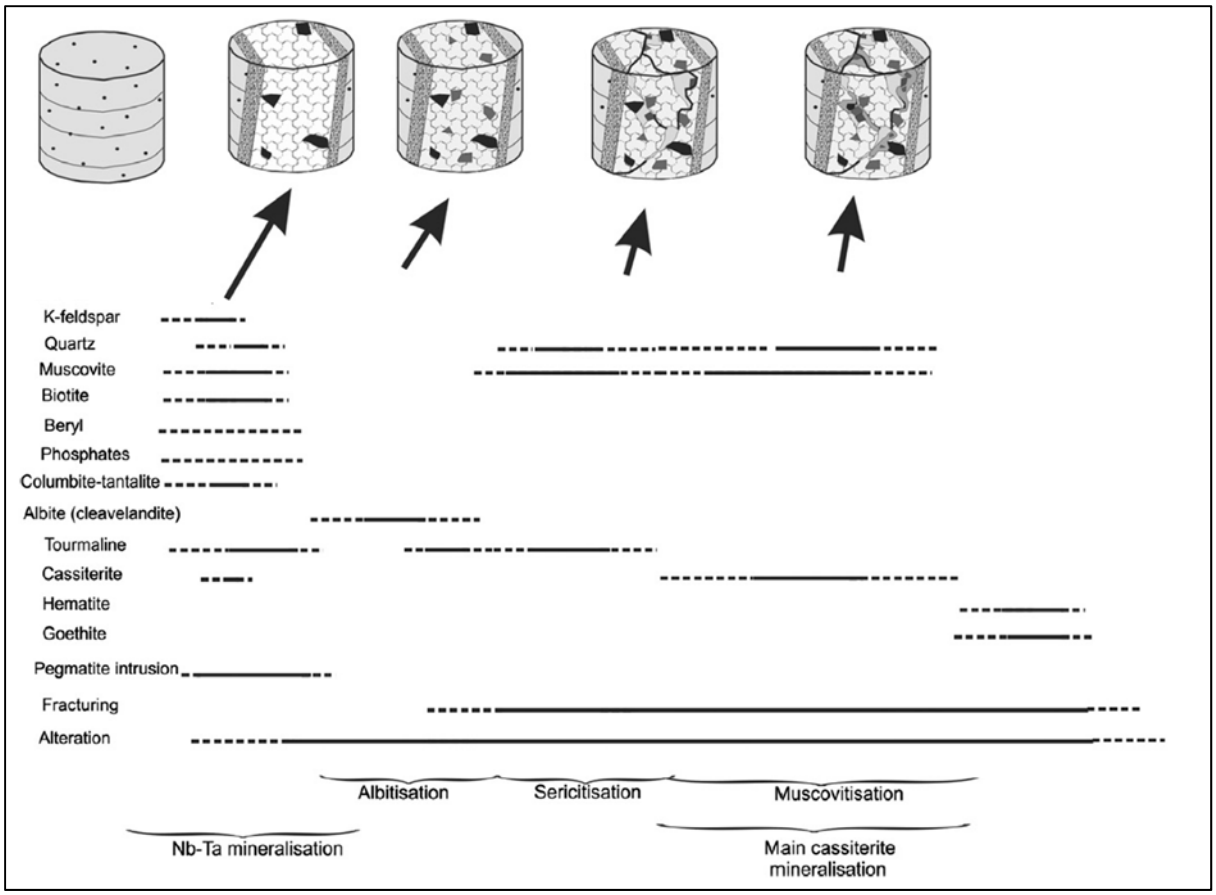


Figure 1. 6: Paragenesis of the Gatumba, cassiterite and coltan mineralisation (Dewaele et al., 2007; Dewaele et al., 2011)

1.3.2 Secondary mineralisation

Secondary mineralisation refers to deposits also known as alluvial and eluvial deposits. The latter are mainly situated very close to the primary deposit and inherited its characteristics. Alluvial deposits are dependent on the type of primary deposits, but other factors such as the morphology of the river network also plays a role (Dewaele et al., 2013). To form these type of deposits, weathering and erosion have played a big role. In Rwanda this has been very efficient, due to the abundance of water, tropical climate, and morphology of the terrain. The weathered zone normally reaches a depth of 30 m in Rwanda and in some areas even deeper. However, the weathered zone associated with schists

ranges between 5 and 10 m, and for quartzitic and doleritic rocks it is even shallower (Dewaele et al., 2013).

The ore minerals cassiterite, coltan and wolframite are resistant to chemical weathering, but have varying degrees of resistance to physical weathering. Cassiterite being the most resistant mineral to weathering is often concentrated in eluvial and alluvial deposits, with mainly its grain size affected. The cassiterite grain size in eluvial deposits is very coarse, but it reduces in size the further it is located from the primary source. The thickness of the eluvial gravel ranges between 1 to 2 m, with an average cassiterite grade between 500g/m^3 and 1500g/m^3. However, the cassiterite grade is not constant throughout the deposits, as is expected for eluvial and alluvial deposits, with the cassiterite grade varying between 200g/m^3 and 5000g/m^3 in some areas (Dewaele et al., 2013). Coltan behaves very similar to cassiterite, but it is not as resistant to physical weathering. Wolframite however, is brittle and is not as resistant to physical weathering. Thus, it only occurs 100 to 200 m from the primary deposit (Dewaele et al., 2013).

1.4 Mining history of Rwanda and the Bugesera district

The first discovery of cassiterite in Rwanda was between 1922 and 1928 in Gatumba by a Belgian exploration team (Pohl, 1994; Ngaruye, 2011; Muchez et al., 2014). The team was tasked with the geological mapping of Burundi, the Kivu Province, and Rwanda, and was led by Chanone A. Salee of the University of Louvain. The exploitation of cassiterite followed soon after the first discovery, with the earliest record of production from the 1930s (Dewaele et al., 2009; OGMR, 2010; Ngaruye, 2011; Kinnaird et al., 2016). These initial mining companies were primarily from Belgium and their production was mainly from secondary alluvial and eluvial material (Fig. 1.7a), but they later progressed to mining the underground primary mineralised deposits (Fig. 1.7b) (Dewaele et al., 2011; Hulsbosch et al., 2013; Nieder et al., 2014; Kinnaird et al., 2016).



Figure 1. 7: Illustrations of (A) artisanal miners at Gatumba extracting minerals from secondary mineralisation whereas (B) is an old entrance to an abandoned underground mine extracting minerals from primary mineralisation (Montjoie, 2014; Muchez et al., 2014).

From 1930 to 1968 mining production increased from 20% to 42.5% of total export earnings; whereas, between 1969 and 1973 the export revenues decreased from 42.5% to 21.6% (Fig. 1.8 and Appendix A). This sharp decline is believed to be a result of no new foreign investment after Rwandan independence in 1962 (GMD, 2010; OGMR, 2010; Ngaruye, 2011). This led to the government and private industry forming a joint venture (49% and 51% shareholding respectively) in February 1973, the Société Minière du Rwanda (SOMIRWA) mining company. The objectives were to firstly increase production and secondly to improve the administration and ultimately a turnaround in the country's mining industry (Ngaruye, 2011).

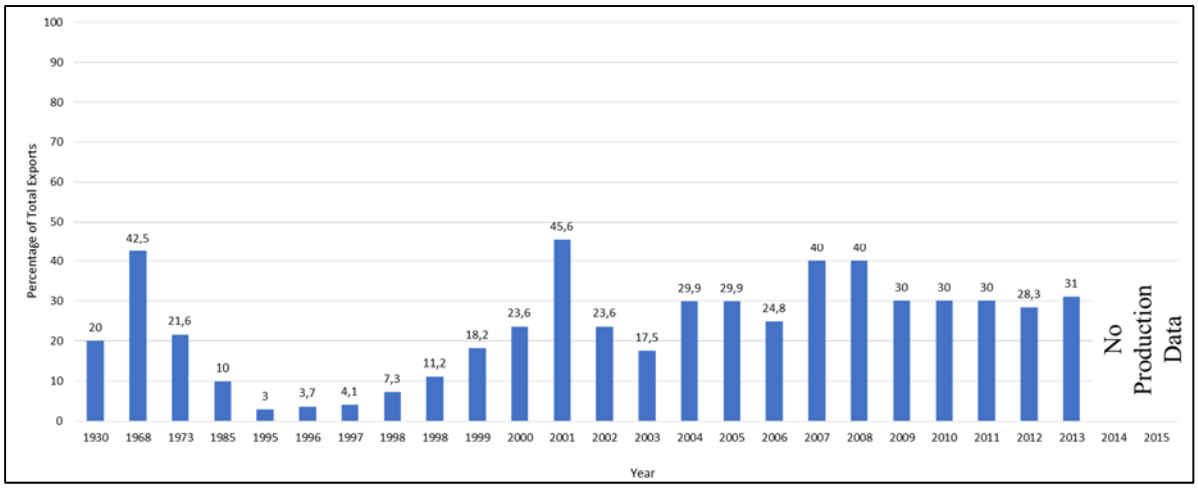


Figure 1. 8: Cassiterite contribution in percent to total exports from 1930 to 2015 (GMD, 2010; OGMR, 2010; Ngaruye, 2011; USGS, 2016). Note that although this may be more useful in cassiterite produced in tonnes, this data has only been available since 1998.

It is important to note that "Regie d'Exploitation et de Developpement des Mines" (REDEMI) is the government-controlled company referred to by some authors, and not SOMIRWA. The latter went

bankrupt in 1985 causing a collapse of the whole industry, due to the company's monopoly position and corruption (OGMR, 2010; Ngaruye, 2011; Melcher et al., 2015). SOMIRWA was subsequently replaced by the government controlled REDEMI and a private company, known as the "Cooperative de Promotion de l'Industrie Miniere Artisanale au Rwanda" (COPIMAR). This private company was mainly created for the artisanal miners of Rwanda (OGMR, 2010; Ngaruye, 2011). In literature, there is not a lot of information available for the timeframe between 1985 and 2001, this is most probably due to the Rwandan genocide of 1994, affecting the total export figures between 1994 and 1998. There appeared to be a gradual recovery of Rwanda's industry after 1998, with export mineral revenues gradually growing to approximately 45.7% of total exports in 2001 (Fig. 1.8 and Appendix A).

The government continued to own approximately 90% of all known deposits from 1985 up to 2006, but the majority of the country's production was from artisanal and small-scale mining activities (OGMR, 2010). Between 1994 and 1998 cassiterite production reaches its lowest levels in record history, due to the Rwandan genocide of 1994. In 2006 the government agreed on a policy to privatize the mining sector, resulting in all the government concessions (except Rutongo and Gatumba) being transferred to private companies and individuals by the end of 2006 (GMD, 2010; OGMR, 2010; Kinnaird et al., 2016). Although this process was only concluded in 2008, it still resulted in a capital injection into the mining sector, with the primary focus on both new discoveries and semi-industrial exploitations in the former state concessions (OGMR, 2010). After the policy change, the activities of REDEMI were transferred to "Office de la Géologie et des Mines du Rwanda" (OGMR) with their specific function to regulate the industry. In 2011, the OGMR's name was changed to the "Geology and Mines Department" (GMD), but their vision and function stayed the same. A summary of the mining history of Rwanda is presented in Appendix B (GMD, 2010).

Throughout history, artisanal activities have been the principle mining method applied in Rwanda, but at certain deposits, such as Rutongo, this has recently been changing to more semi-industrial and small scale mining activities (Perks, 2013). Currently, at other locations, such as the Bugesera district, artisanal mining remains the main method used for extraction. However, metal recoveries for this type of mining are very low, estimated to be between 10% - 30% (Muchez et al., 2014).

1.5 Aim

Very little geological research has been performed on the Bugesera district in Rwanda. Information is limited to research performed on adjacent areas such as Gatumba, Nyakabingo and Rutongo. This study will therefore endeavour to enhance the knowledge base on the Bugesera district, by studying

four mining areas (Nyagasagara, Gakurazo, Kageyo and Kageyo Extension) on the Hard Metal Rwanda license, their locations relative to regional structures and G4 granites, and the mineral grade at each of the deposits. Furthermore, it was important to study the mineralogy and mineral chemistry on the concentrate material from Nyagasagara, for comparison with literature and to determine whether the mineralisation was primary or secondary.

1.6 Objectives

1) To compile a location map of the various artisanal mining pits on the licence area relative to the location of known granites, pegmatites and structures.
2) To determine what material is being mined by the artisanal miners at Nyagasagara, whether it is related to primary mineralisation and/or secondary mineralisation.
3) To determine the mineral grades (estimates) of the artisanal mining pits across the licence area.
4) To assess the size fraction analysis on the Nyagasagara concentrate, to determine in what size fraction the bulk of the minerals occur on the different mining sites. Also, to determine whether there is a relationship between the grain size and the grade at the various deposits.
5) To undertake mineralogical, including textural and compositional studies on the Nyagasagara concentrate to determine whether it is related to primary and/or secondary mineralisation.
6) To determine the occurrence of cassiterite, coltan and wolframite minerals at the different mine sites of Nyagasagara.
7) To compare information obtained from the studies mentioned above with existing literature on the Sn-W-Ta-Nb oxide minerals in the KAB.

Chapter 2:

Local geology and project location

2.1 Local geology

The geological information of Rwanda is mainly related to the KIB and KAB (Pohl and Günther, 1991; Pohl, 1994; Melcher et al., 2009; Fernandez-Alonso et al., 2012; Dewaele et al., 2013; Dyussembayeva et al., 2014; Debruyne et al., 2015; Melcher et al., 2015), the Gatumba area (Dewaele et al., 2011; Hulsbosch et al., 2013; Lehmann et al., 2014; Nieder et al., 2014), the Rutongo area (Fig. 2.1) (Dewaele et al., 2009), and the Nyakabingo area (Dewaele et al., 2016).

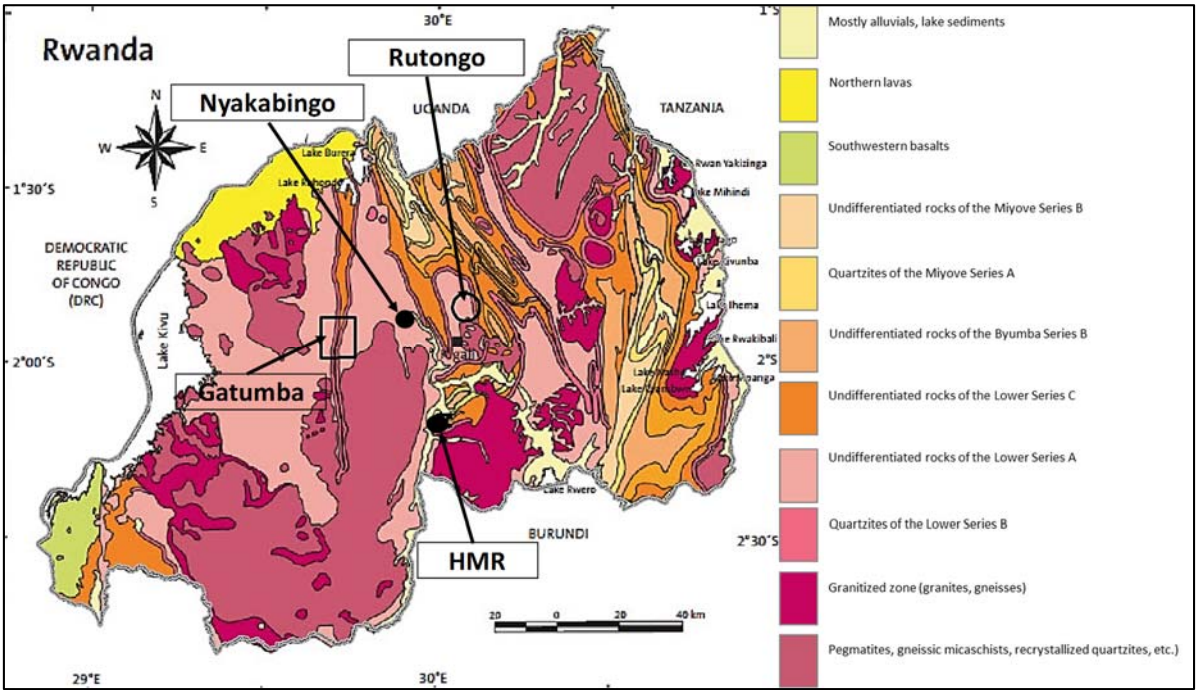


Figure 2. 1: Geological map of Rwanda, indicating the location of the study area, owned by Hard Metal Rwanda (HMR). Other known cassiterite and coltan mining areas, such as Gatumba, Nyakabingo and Rutongo are also indicated on the map. Modified from Schlüter (2008).

Although Sn and Ta production in Rwanda have been taking place since the early 1900s (Dewaele et al., 2009; Melcher et al., 2015), very little research has been performed in the Bugesera district with no published literature available on the specific project area.

2.2 Project location

The Hard Metal Rwanda (HMR) project is in the Bugesera district of Rwanda and consists of four mining areas situated in the Musenyi sector of the district, approximately 25km south of Kigali (Fig. 2.2). The

HMR licence boundary is approximately 6km west of the village of Kinazi and access to these sites are along an unpaved road.

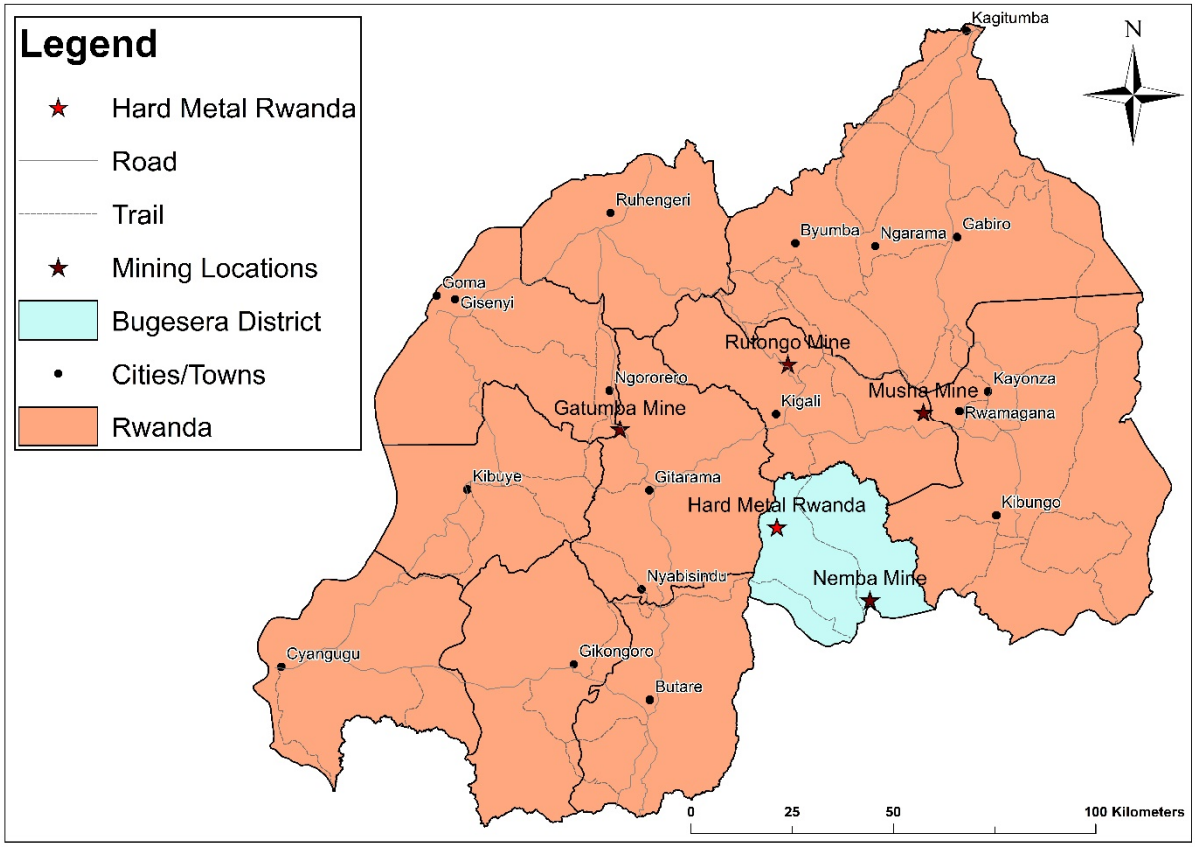


Figure 2. 2: Location map of known cassiterite and/or coltan mines, such as Gatumba, Rutongo, Musha, Nemba and the Hard Metal Rwanda project area situated in the Bugesera district of Rwanda modified from Buurman and Montjoie (2016).

The Bugesera district is not historically known as a major producer of Sn-W-Nb-Ta oxide minerals, although there have been a few tin discoveries and producers in the district throughout history (Fig. 2.3) (Baudin et al., 1982). There are reports of other mineral discoveries, such as diamond and wolframite, in the southwest of the Bugesera district, but the exact location of these discoveries remains unknown. The mining and geological information on the Bugesera district is limited to old internal company reports (unpublished) of which most are in German or French except for research performed in 2011 by Bundesanstalt für Geowissenschaften und Rohstoffe (BGR), and in 2014 and 2016 by Umbono Capital Partners. Due to virtually no research being available on the Bugesera district, literature on Gatumba, Rutongo, Nyakabingo, KIB and KAB will be used as a basis for this study and comparative purposes.

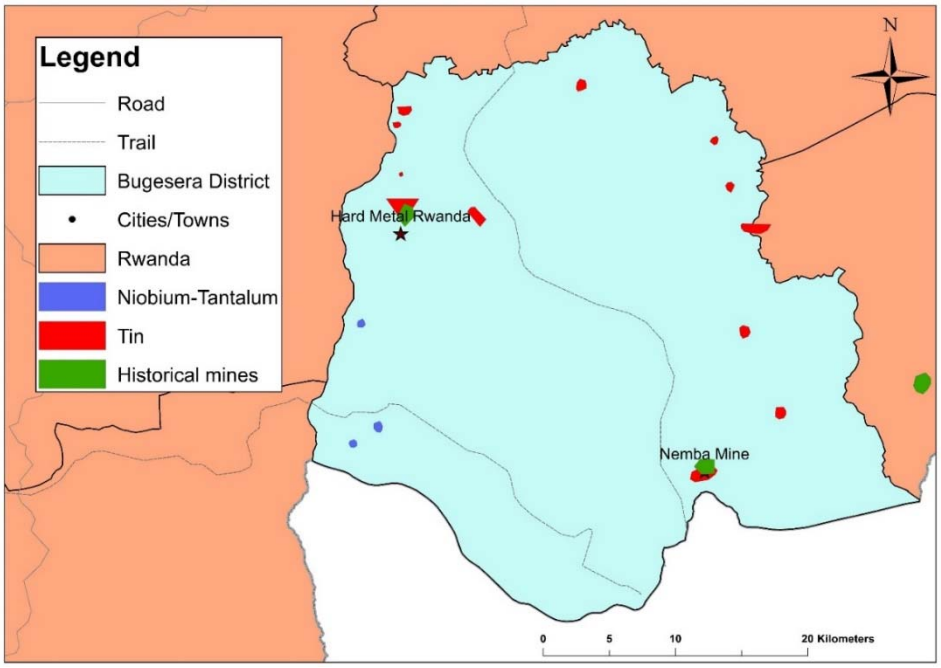


Figure 2. 3: Map of the Bugesera district indicating various discoveries and historical mines. Note that the location of the Hard Metal Rwanda project is situation south of a tin discovery and historical mine modified after Buurman & Montjoie (2016) and Baudin et al., (1982).

On the HMR licence there are four mining areas, the so-called, Nyagasagara, Kageyo, Gakurazo and Kageyo Extension. These sites are mainly exploited for cassiterite and coltan minerals. However, according to the artisanal miners, wolframite (Fe, Mn)WO_4 can also occur at these sites, but this has not been assessed yet. The artisanal miners believe that all of these sites contain both cassiterite and coltan minerals, however, the HMR production figures only indicates cassiterite for Nyagasagara and coltan for Kageyo. No production data are available for Gakurazo and Kageyo Extension, but they too are believed to contain both cassiterite and coltan minerals (Buurman and Montjoie, 2016).

Chapter 3:

Material and methods

3.1 Field observations, surveying and mapping

In 2016, the HMR project area was visited twice. The first was in February 2016 and the second in September 2016. Before the first site visit, a desktop study was carried out to create a database of all the available maps and data on the area. The main software used to compile a database of maps for this study was ArcMAP 10.

The main objectives of the first site visit in February 2016, was to determine the exact location, minerals present, grade, and collect samples from each mining site for Umbono's due diligence on the project. The samples collected would then also be used for this study.

The main objective of the second site visit in September 2016, was to try and find fresh granite and or pegmatite samples located in the project area.

3.2 Grade estimates of the various mining sites

The mineral grades for all four mining sites were estimated by dividing the concentrate weight for each site (after drying) (Fig. 3.1a) with the weight of the run of mine (ROM) material before processing and drying (Fig. 3.1b).



Figure 3. 1: A) The weighing of the ROM before processing and drying, and B) the weighing of the concentrate after drying.

3.3 Sample description

The samples investigated are from four different mining areas on the HMR prospecting licence area, they are Nyagasagara, Kageyo, Kageyo Extension and Gakurazo (Fig. 3.2). With Nyagasagara being the focus of this study. The sampling material focused on the ROM, concentrate, and tailings. The samples were kindly provided by Umbono Capital Partners LLC, a joint venture partner of the project. A total of 39 samples were sampled for further analysis (Appendix C).

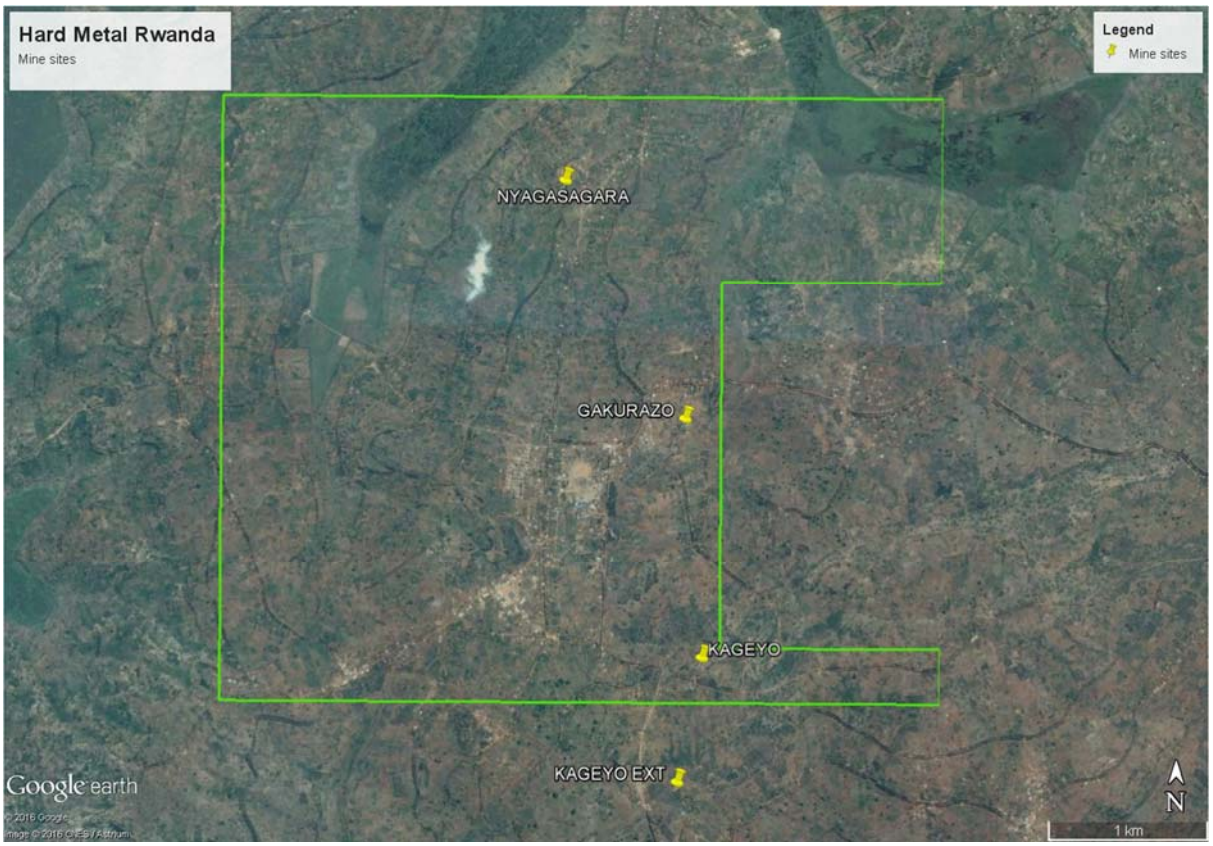


Figure 3. 2: Google earth images indicating the location of the four mining areas (Nyagasagara, Kageyo, Kageyo Extension and Gakurazo). Note that Kageyo Extension is located outside the HMR licence boundary (light green outline) (Buurman and Montjoie, 2016).

3.4 Sample preparation and analytical procedures

In this study, the samples were restricted to less than 1kg (Appendix C). The ROM and tailings, samples were collected by obtaining a spade full of material from the stockpiles (the samples are not assumed to be representative), whereas the concentrates samples were collected after the processing of the ROM, using a traditional processing and drying technique (Fig. 3.3) (Appendix C). The samples collected from Nyagasagara were analysed at Setpoint laboratories (SPL). The sample preparation for all samples included drying followed by splitting (using a riffle splitter) into a split to be analysed and

a split to be returned to Umbono. The lab analysis for the concentrate, ROM and tailings differ slightly; on the concentrate, size fraction analysis and 31 element analyses (including Sn, Ta and Nb) were performed; on the ROM, ICP-OES in addition to 31 element analyses (including Sn, Ta and Nb) were performed; on the tailings only 31 element analyses (including Sn, Ta and Nb) were performed. In addition to the analysis performed at SPL the concentrate, in its various size fractions, were mounted on thin sections (28 thin sections), which were studied with reflective (transmitted where possible) microscopy and electron microprobe analysis (Refer to Appendix D for the Setpoint sample complete list and the work programme).



Figure 3. 3: Artisanal miners on the HMR project, A) processing the ROM and B) drying the concentrate, using traditional methods.

Note that at this stage only the Nyagasagara samples have been analysed (Appendix D), mainly due to the low grade and not enough concentrate material from the other mining areas.

3.4.1 Size fraction analysis (dry screening)

The size fraction analysis was performed, only on the concentrate of Nyagasagara (sample no: NYAG07, NYAG15, NYAG08, NYAG04, and NYAG03), because the other sites did not have enough concentrate. A total mass of 200g was used for screening into 4mm, 2mm, 1mm, 500µm, 250µm, 150µm and 53µm size fractions. The screens were stacked together and placed onto a vibrating platform, with the sample introduced to the top screen. After 10 minutes, the material in each sieve was weighed and the material left in the bottom sieve was reported as 53µm. The concentrate in the various size fractions was returned to Umbono, to be used in the making of the thin sections.

3.4.2 Thin sections and optical microscopy

A total of 28 polished thin sections were prepared from the concentrate (in its various size fractions) of Nyagasagara at the University of Witwatersrand (WITS) (Refer to Appendix E, for a complete list of the thin sections). The grains for each sample were placed in moulds to create grain mounts. After which the grain mounts were mounted onto a piece of glass and ground down to the size of a thin section and subsequently polished.

Both reflective and transmitted light microscopy were used in this study, mainly for the identification of textures and structures in the various grains in each size fraction.

3.4.3 XRF analysis

The XRF analysis was performed by SPL, South Africa. It included a 31-element analysis plus the analysis for Sn, Ta and Nb. An ignited sample mass of 1.1g was fused with 9.9g flux in a clean platinum dish. This fusion melt was poured into a clean platinum mould and allowed to solidify. The solidified discs were labelled and analysed by calibrated XRF spectrometer.

The 31-element quantitative scan was obtained by the analysis of 12 elements using fusion XRF and the remainder of the elements were obtained by pressed pellets. The fusion disks for the 12 elements were prepared using the same preparation methods as for the analysis of Sn, Ta, and Nb. For the pressed pellet an aliquot of the sample (~1.3g) and wax binder (~11.7g) was milled together and the resulting liquid pressed together at 20 metric tons pressure for 15 seconds in a pellet press. The pressed pellets were labelled and analysed by calibrated XRF spectrometer.

3.4.4 ICP-MS analysis for lithium

The ICP-MS analysis for lithium was performed by SPL, South Africa. For the sample preparation, half a gram of pulp material was digested using a combination of four acids (HNO_3, HF, $HClO_4$ and HCl) in teflon tubes and a digestion block. The digested samples were then made up to a volume of 100ml and analysed for Li using inductively coupled plasma-mass spectrometry (ICP-MS).

3.4.5 Electron Microprobe Analysis

The electron probe microanalysis (EMPA) was performed at the University of the Witwatersrand using a CAMECA SX-5FE microprobe equipped with 5WDS spectrometers housed at the Microscopy and

Microanalysis Unit (MMU). The data was collected with CAMECA software. An automated X-PHI matrix algorithm was applied to correct for differential matrix effects. Oxygen was calculated by stoichiometry. EMPA was performed on 8 thin sections created from Nyagasagara concentrate material separated into +2 mm and +500 µm size fractions, specifically from Tunnel 1 (NYAG07), Tunnel 2 (NYAG15), Walking 1 (NYAG04), and Walking 2 (NYAG03). The data was collected The specifications and operating conditions of the instrument used at WITS are presented in Table 3.2.

Table 3. 1: Characteristics of the CAMECA SX 5FE

	Description
Model	CAMECA SX 5FE
Analyse	Qualitative analysis and quantitative identification of phases
Detectors	5 WDS spectrometers
Data format	Spot analysis,
Acc. Voltage Probe current	15 kV 20 nA/ variable
Standards	Natural and synthetic standards were used for calibration: Ti on rutile, Sn on cassiterite/Sn metal, Mn on rhodonite, Fe on almandine, Mg on pyrope, Si on diopside, Sc on Sc metal, W on W metal, and Nb on Nb metal.
Counting times	10 seconds on the peak, and 5 seconds total on the background

Chapter 4:

Mineralisation

4.1 Field observations, mapping and grade estimates

Field-work was carried out on the HMR license area during February and September 2016, specifically on the four mining areas, Nyagasagara, Gakurazo, Kageyo, and Kageyo Extension (Fig 4.1). The main goals were to record the grade of the four mining areas, to collect samples for further investigations, and to map each mining site. The focus of this paper is on Nyagasagara, but general observations and comparisons related to the other three sites will be mentioned.

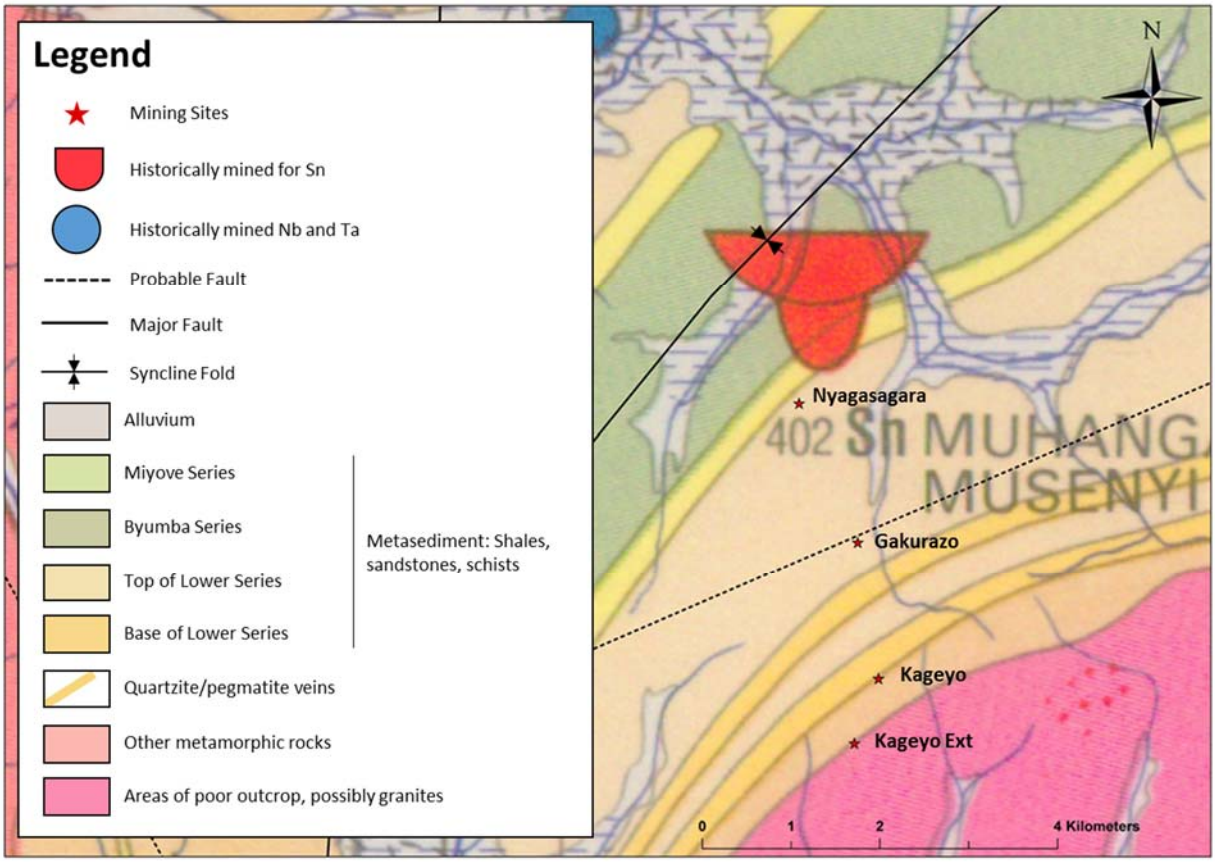


Figure 4. 1: Geological map of the HMR licence area, illustrating the mining sites and their locations relative to regional structures and the underlying geology, modified after Buurman & Montjoie (2016) and Baudin et al., (1982).

The HMR project is located between the Bugesera syncline and the Bugesera granite, with both the Nyagasagara and Kageyo mining occur adjacent (<4 km) to known large scale structures, granites and/or pegmatites (Fig. 4.1). Whereas the Gakurazo mining area is located between the two mining areas. The Kageyo Extension area is located on the rim of the Bugesera granite, but no granite outcrop has been identified at the deposit yet.

4.1.1. Nyagasagara

The Nyagasagara mining area is the biggest on the HMR license and was mined by Belgium miners in the 1950s. It is situated approximately 2 km southeast of the Bugesera syncline and 500 m south of the historically mined area (Fig. 4.1). The current mining areas on Nyagasagara are Tunnel 1 to 5 (Fig. 4.2). Note that Tunnel 2 and 3 intersect at a depth of 10 m and together represent one mining area. Walking 1 and 2 are not actively being mined. The average depth of the mining pits is 15 m below surface and the artisanal miners find it difficult to go deeper than 15 m without a water pump.



Figure 4. 2: Map of Nyagasagara, illustrating the locations and cassiterite grade of the various mining sites on the deposit; the Belgium miners used the Nyagasagara pit and Belgium tailings in the 1950s. The current mining areas are Tunnel 1 to 5.

The main mineral exploited at Nyagasagara is cassiterite, but local information suggests that coltan and wolframite are present too. The cassiterite minerals are hosted in very weathered material, appearing to be laterite. Associated minerals such as muscovite are present at all the mining sites, although kaolinite is only present at Tunnel 1. The ROM material from Tunnel 2 to 5, and Walking 1 and 2 appears very similar (reddish clay material, containing abundant muscovite), but the ROM from Tunnel 1 differs quite a bit, being mostly kaolinite. There are no visible outcrops of pegmatite(s) and/or granite on Nyagasagara and none of the mining sites intersect fresh pegmatite(s) and/or granite. Note

that Tunnel 1 is the only site with an average combined cassiterite grade above 1%, whereas the other mining sites have cassiterite grades lower than 0.3% (Fig. 4.2 and Fig 4.3).

The cassiterite grade varies quite a bit over the area, with the highest grade (5.56% cassiterite) recorded at Tunnel I, and the lowest grade (0.04% cassiterite) recorded at Tunnel IV (Fig. 4.2 and Fig 4.3). The grade from the material believed to be from the Belgium tailings sites was 0.12% and 0.18% cassiterite for Walking 1 and Walking 2 respectively. Interesting to note, what is believed to be the tailings material have higher grades than what is thought to be unmined material, such as at Tunnel 4 and 5 (For a complete list of the minerals grades for all the mining areas, refer to Appendix F).

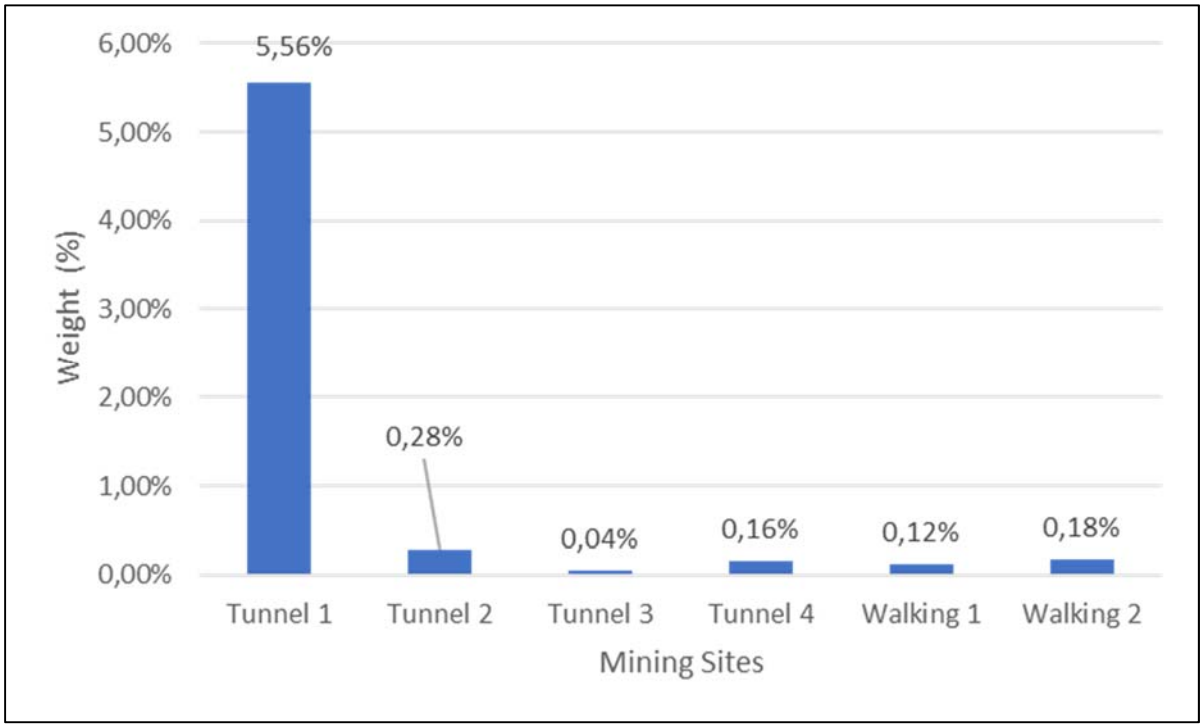


Figure 4. 3: Cassiterite grades at the various mining sites (Tunnel I - V and Walking 1 and 2) at Nyagasagara.

4.1.2. Gakurazo, Kageyo and Kageyo Extension

The Gakurazo area is the smallest mining area on the HMR license and was recently discovered by the artisanal miners. It consists of only one mining pit (Fig. 4.4) approximately 5 m deep. The site is believed to contain both cassiterite and coltan minerals. The host rock is very weathered and contains abundant kaolinite and muscovite. With the naked eye, the host rock appears similar to the host rock from Tunnel 1 at Nyagasagara. However, the combined cassiterite grade at Gakurazo of 0.08% (Fig 4.4 and 4.5) is much lower compared to the 5.56% cassiterite grade at Tunnel 1 on Nyagasagara.



Figure 4. 4: Map of Gakurazo, illustrating the location and cassiterite grade of the mining site.

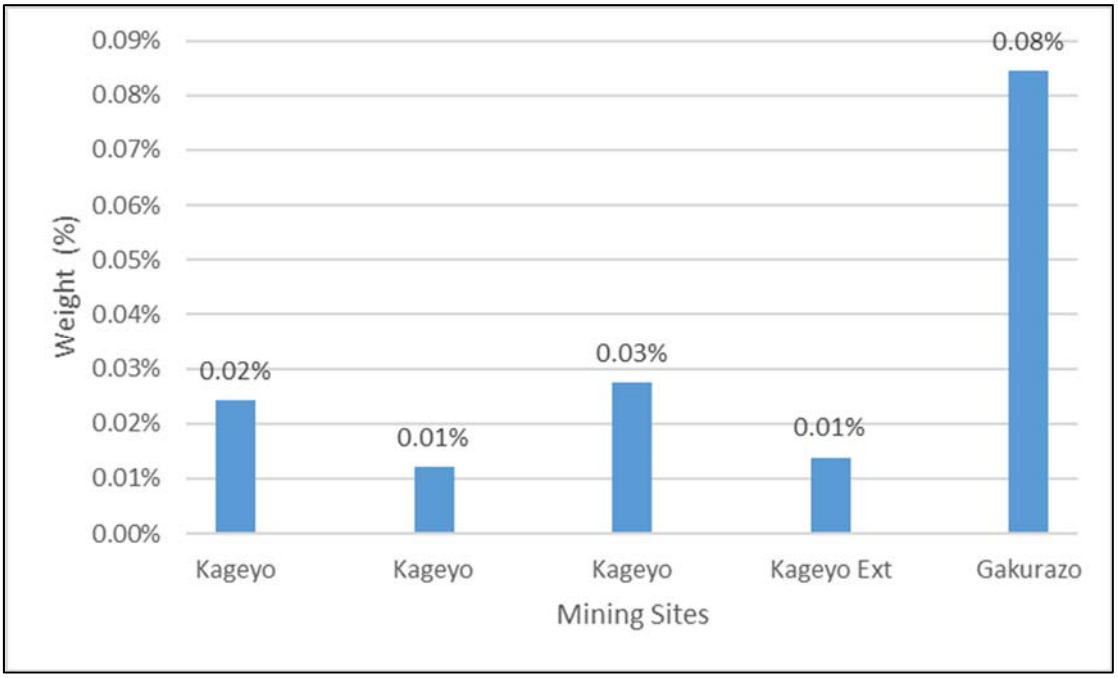


Figure 4. 5: Combined cassiterite and/or coltan grade at Kageyo, Gakurazo and Kageyo Extension.

The Kageyo mining area is the second largest mining area on the HMR license. It is situated approximately 4 km southeast of the Bugesera syncline, on the southern rim of the "quartzite/pegmatite vein" as indicated on Figure 4.1, and approximately 500 m north of the Bugesera

granite (although no outcrop of the Bugesera granite were observed during the field visits). The current mining areas on Kageyo are, Kageyo 1, Kageyo 2 and Kageyo 3 (Fig. 4.6) and the average depth of these sites is 10 m.



Figure 4. 6: Map of Kageyo, illustrating the location and coltan grade of the various mining sites.

Coltan is the main mineral extracted from the Kageyo area, but local information suggests that cassiterite is present too. A predominant quartzite layer outcrops in the area with an apparent strike of northeast and a dip of southeast (Fig. 4.6). This is most probably the "quartzite/pegmatite vein" illustrated on Figure 4.1. The host rock for both Kageyo 3 and Kageyo 2 is situated in what appears to be a very weathered pegmatite vein which intruded the quartzite layer, also dipping southeast. The combined cassiterite and coltan grade at Kageyo is very low compared to Nyagasagara, with a maximum and minimum grade of 0.03% and 0.01% respectively (Fig. 4.5 and 4.6). The coltan and cassiterite mineralisation is associated with quartz and muscovite at all three sites.

The Kageyo Extension, unlike the other three mining areas appears to be situated on the Bugesera granite (no outcrop of the Bugesera granite were observed during the site visits). It is situated 6 km southeast from the Bugesera syncline and 500 m southwest of the Kageyo mining area. The area consists of only one mining pit approximately 5 m deep (Fig. 4.7).



Figure 4. 7: Map of Kageyo Extension, illustrating the location and coltan grade observed at the mining sites.

The area appears similar to Kageyo, with coltan being the main mineral extracted, although it is believed to contain cassiterite too. The host rock appears to be weathered pegmatite that intruded a quartzite layer with a strike of northeast and a dip of south east. The coltan mineralisation is associated with muscovite.

No fresh pegmatite(s) and/or granite outcrops were observed at any of the mining sites and none of the sites intersected it either. This makes it difficult to determine whether the mineralisation style is primary and/or secondary. A combination of other methods had to be employed to try and determine whether the mineralisation style is primary and/or secondary and to further differentiate characteristics between the various mining sites. These methods included, grain size analysis, optical microscopy, and electron microscopy. Note that these methods were only applied on the concentrate material from Nyagsagara, due to the low grades at the other 3 mining areas.

4.2 Size fraction analysis

Size fraction analysis had been performed on the concentrate samples from Nyagasagara, specifically on concentrate from Tunnel 1, 2, 3, Walking 1 and 2 (NYAG07, NYAG15, NYAG08, NYAG04 and NYAG03

respectively) (For a complete list of the size fractions at the various sites, refer to Appendix G). Due to the low grade and insufficient concentrate material, size fraction analysis was not performed on the concentrate from Gakurazo, Kageyo and Kageyo Extension.

The cassiterite grain size distribution of Nyagasagara (Fig. 4.8) indicates that most of the cassiterite recovered, reports to the coarser size fractions. These include the cassiterite from the +4 mm (17.55%), +2 mm (39.67%), and the +1 mm (29.89%) size fractions. There appears to be a sharp drop in the grain size distribution below the +1 mm size fraction, which as literature suggest, could indicate the inefficiency of the traditional recovery methods in recovering cassiterite grains below +1 mm. The size distribution below +1 mm, includes the +500 µm (7.56%), +250 µm (3.51%), +150 µm (1.03%), +53 µm (0.43%), and -53 µm (0.36%) size fractions.

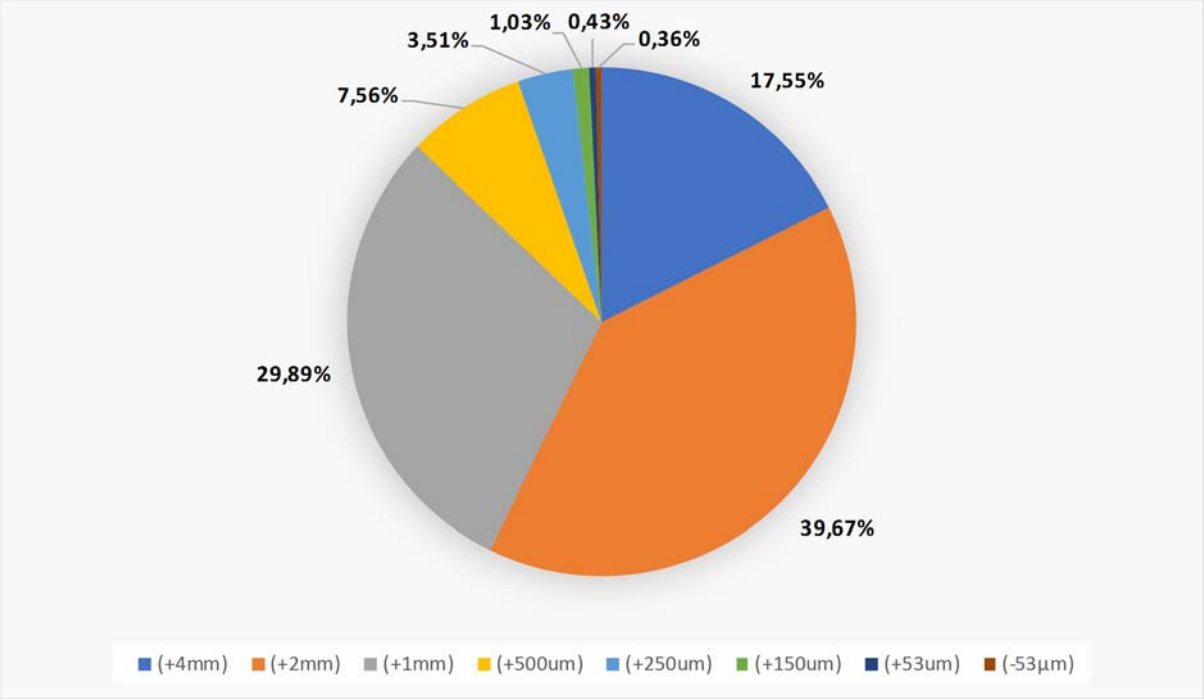


Figure 4. 8: Grain size distribution of the combined cassiterite and coltan concentrate from all four mining areas on Nyagasagara.

Comparing the average grain size distribution with the cassiterite and coltan grade, from highest (NYAG07) to lowest grade (NYAG04) (Fig. 4.9), indicates a general decrease in the size fractions with a decreasing grade. The +2 mm and +1 mm however, shows an increasing trend with decreasing grade. The presence of size fractions below +500 µm appears to be absent from NYAG03 and NYAG04, compared to its presence in NYAG07, NYAG08 and NYAG15.

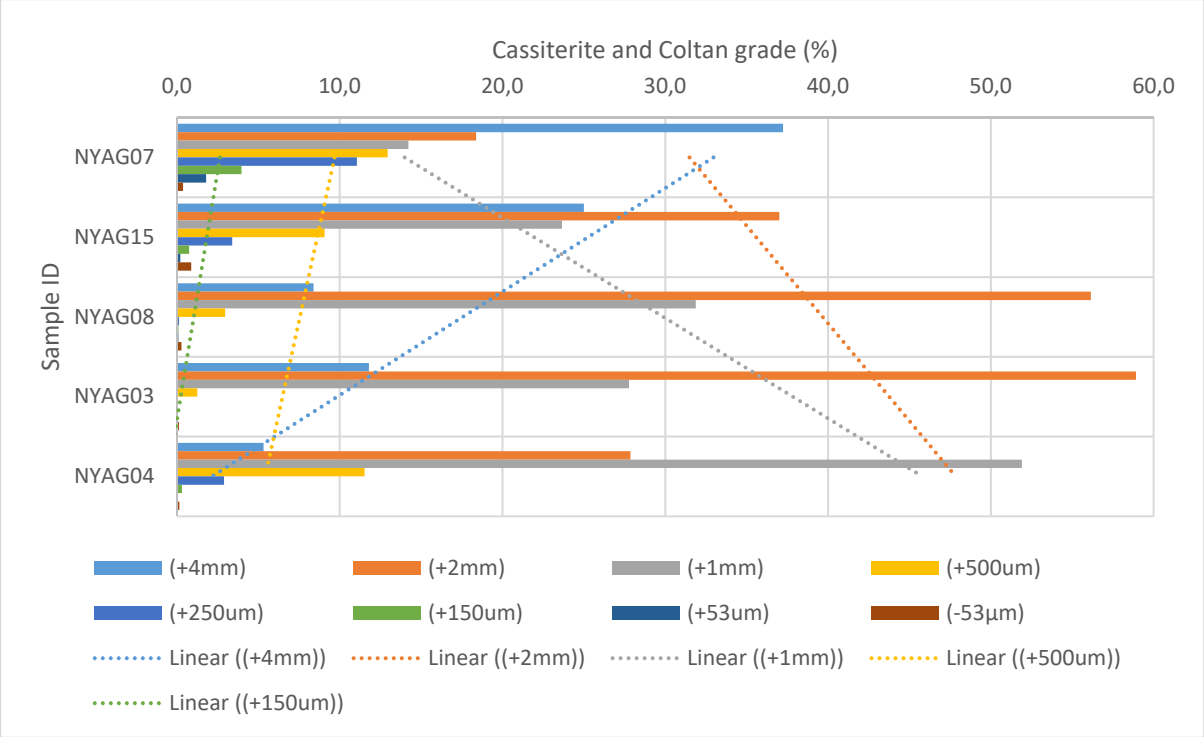


Figure 4. 9: Comparison between the average cassiterite and coltan grade and the grain size distribution on Nyagasagara. The sample ID's are ordered from top to bottom on the y-axis, from highest (NYAG07) to lowest (NYAG04) cassiterite and coltan grade.

The sample with the coarsest cassiterite and coltan size fraction (+4 mm) is NYAG07. It is also the mining site with the highest cassiterite grade. Based on the grain size analysis, there appears to be a difference between the different mining sites on Nyagasagara, but further analysis such as whole rock chemistry and optical microscopy is needed to further differentiate between the different mining sites on Nyagasagara.

4.3 XRF and ICP-MS

The concentrate material from Nyagasagara, which according to local information contained cassiterite, coltan and/or wolframite, was submitted for XRF analysis. The aim was to determine the chemical composition of the concentrate from Tunnel 1, 2, 5, Walking 1, and 2 (Fig. 4.10), and to try and determine whether there are any differences between the material from the various sites. The ICP-MS was used primarily to analyse for Li and whether it is present in significant amounts at the mining sites (For a complete list of the whole rock chemistry, refer to Appendix H and I).

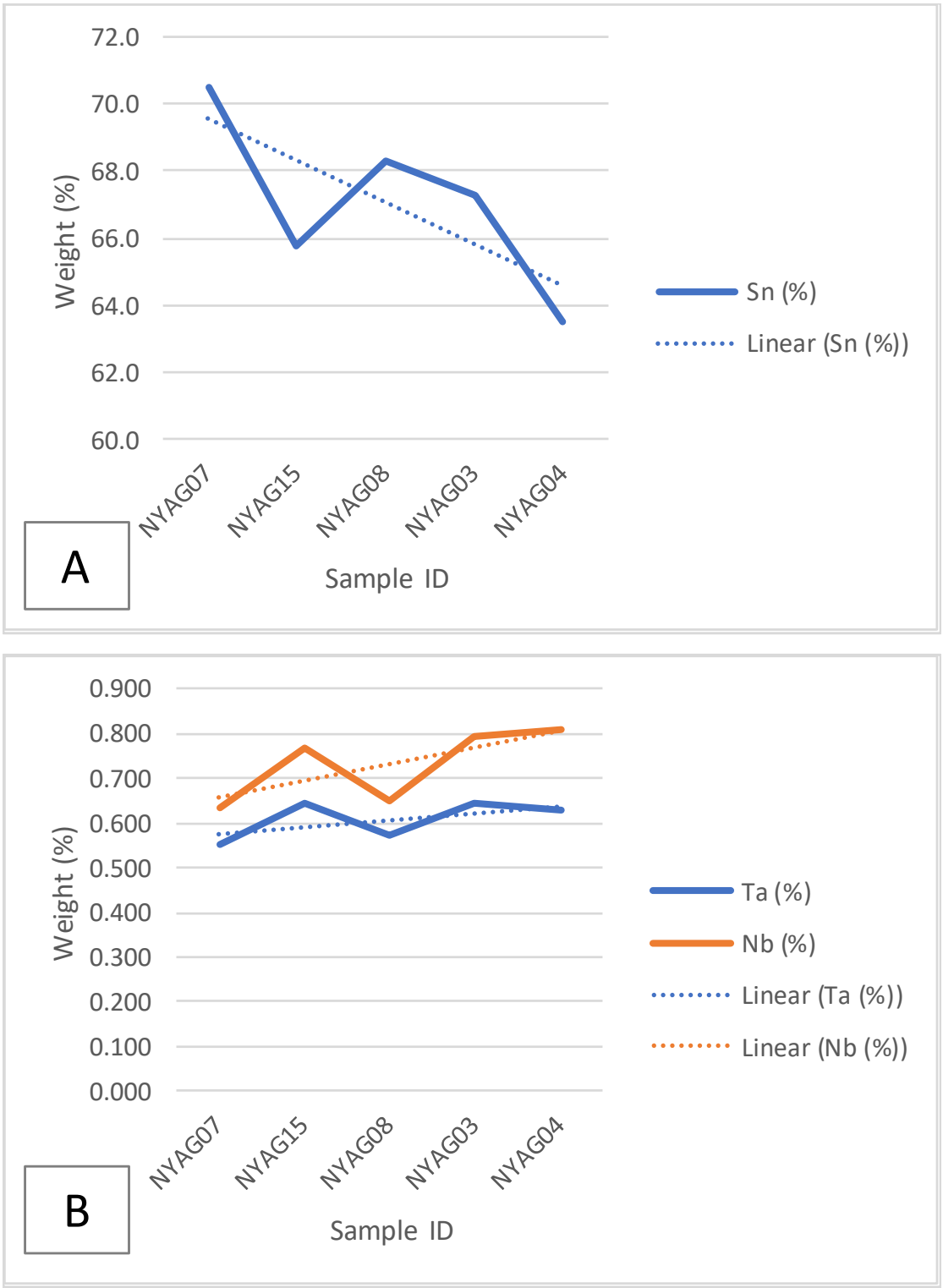


Figure 4. 10: Chemical composition of the concentrate from Nyagasagara, ordered from the highest cassiterite grade (NYAG07) to the lowest cassiterite grade (NYAG04). A) Tin concentrations in the concentrate; B) Tantalum and Niobium concentrations in the concentrate. Note that the Nb – Ta weight percentages were plotted on a separated graph to highlight the change in these elements across the mining areas. Whereas, if they were plotted on the same graph they would plot as a horizontal line relative to the change in Sn.

Sn is the most abundant element in the concentrate samples from Nyagasagara, with an average concentration of 67.08% Sn. After tin, niobium and then tantalum are the most abundant elements in

the concentrate samples at Nyagasagara with an average concentration of 0.73% and 0.61% respectively. Tungsten however, is only present in minor amounts, with an average concentration of 150 ppm recorded in the concentrate samples (Appendix H).

The highest and lowest tin concentration are recorded at NYAG07 (70.5%) and NYAG04 (63.5%) respectively (Fig 4.10A). The tin concentration has a positive correlation with the cassiterite grade, indicating a general decrease in tin concentration as the cassiterite grade decreases. Niobium and tantalum however, has a negative correlation with the cassiterite grade, illustrating a general increase in concentration as the cassiterite grade decreases. NYAG07 has the lowest niobium and tantalum concentration (0.643% and 0.551% respectively), whereas NYAG04 has the highest niobium and tantalum concentration (0.809% and 0.627% respectively) (Fig. 4.10B).

Lithium is only present in minor amounts at some of the mining sites, with the highest concentration recorded at Tunnel 2 (13.8 ppm Li) (Appendix I).

4.4 Optical microscopy

The concentrate samples from Tunnel 1,2,4,5, Walking 1, and 2 of Nyagasagara, were examined with transmitted and reflective microscopy. Interestingly, only cassiterite was identified under the microscope, with no coltan or wolframite present in any of the samples examined. The Nyagsagara cassiterite displays similar optical characteristics as described in literature. Under transmitted light the cassiterite display a variation of colours ranging from dark reddish brown to colourless (Fig. 4.11 and Fig. 4.12(A)-(D)). The grains from the various sites appeared quite similar under the microscope with no distinct differences observed, except that the cassiterite from Nyagasagara Tunnel 2 (NYAG15) were slightly darker compared to the cassiterite from the other four sites.

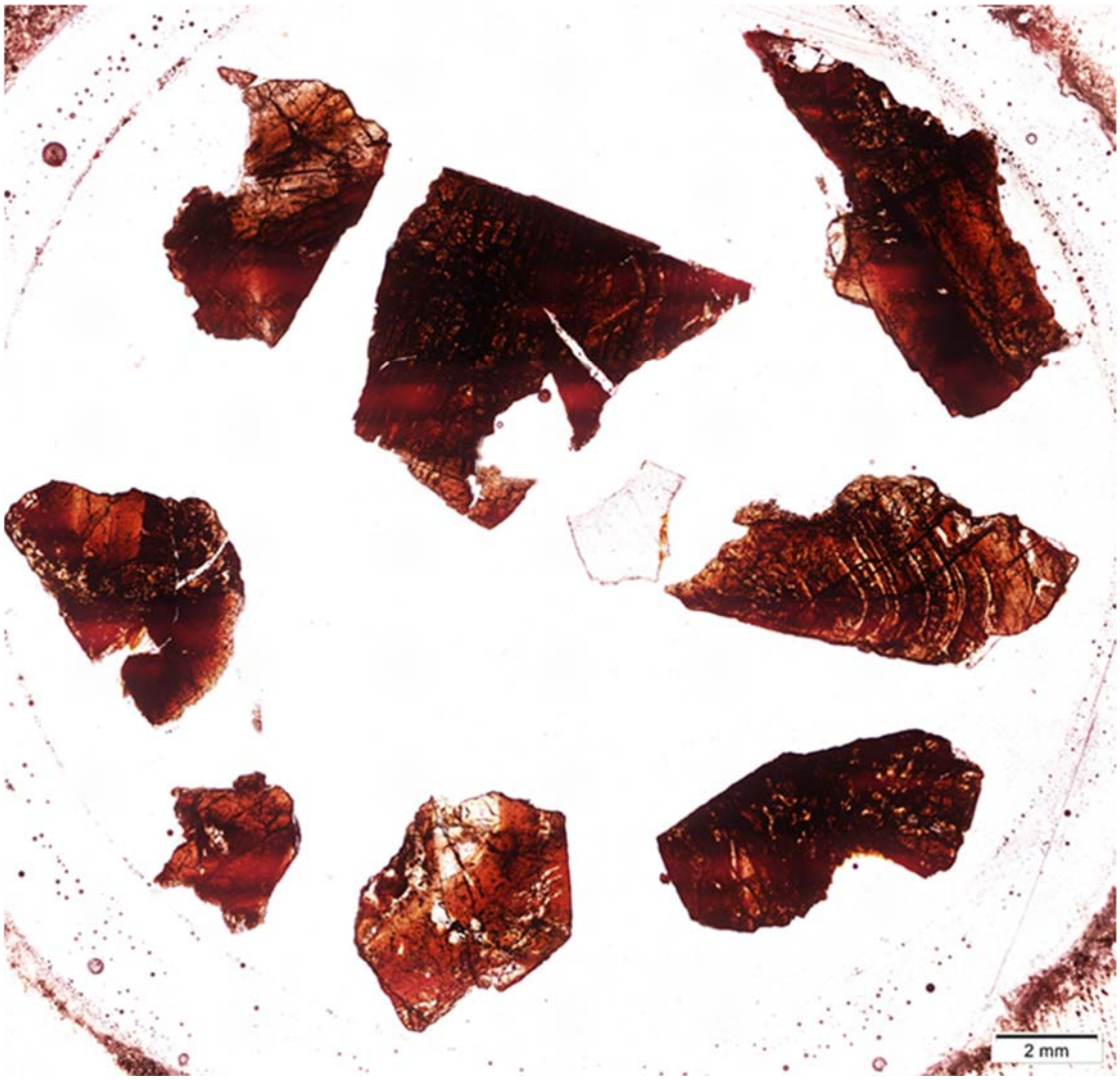


Figure 4. 11: Microphotograph of the +4mm size fraction cassiterite grains from Tunnel 2, Nyagasagara under a transmitted light microscope. Most of the grains are fractured and typical colour zonation (dark brown-white) and pleochroism from dark brown to light brown can be seen in some of the grains.

The cassiterite also displays other common characteristics, such as colour zoning and moderate to intense pleochroism (Fig 4.11 and Fig. 4.12(A)-(D)). The shape of the cassiterite grains observed in all the size fractions, ranges from very angular to angular. Note that there appears to be no correlation between the grain size and the number of alternating zones in cassiterite. The cassiterite grains, its zoning and some inclusions in the grains were further investigated with the electron microprobe.

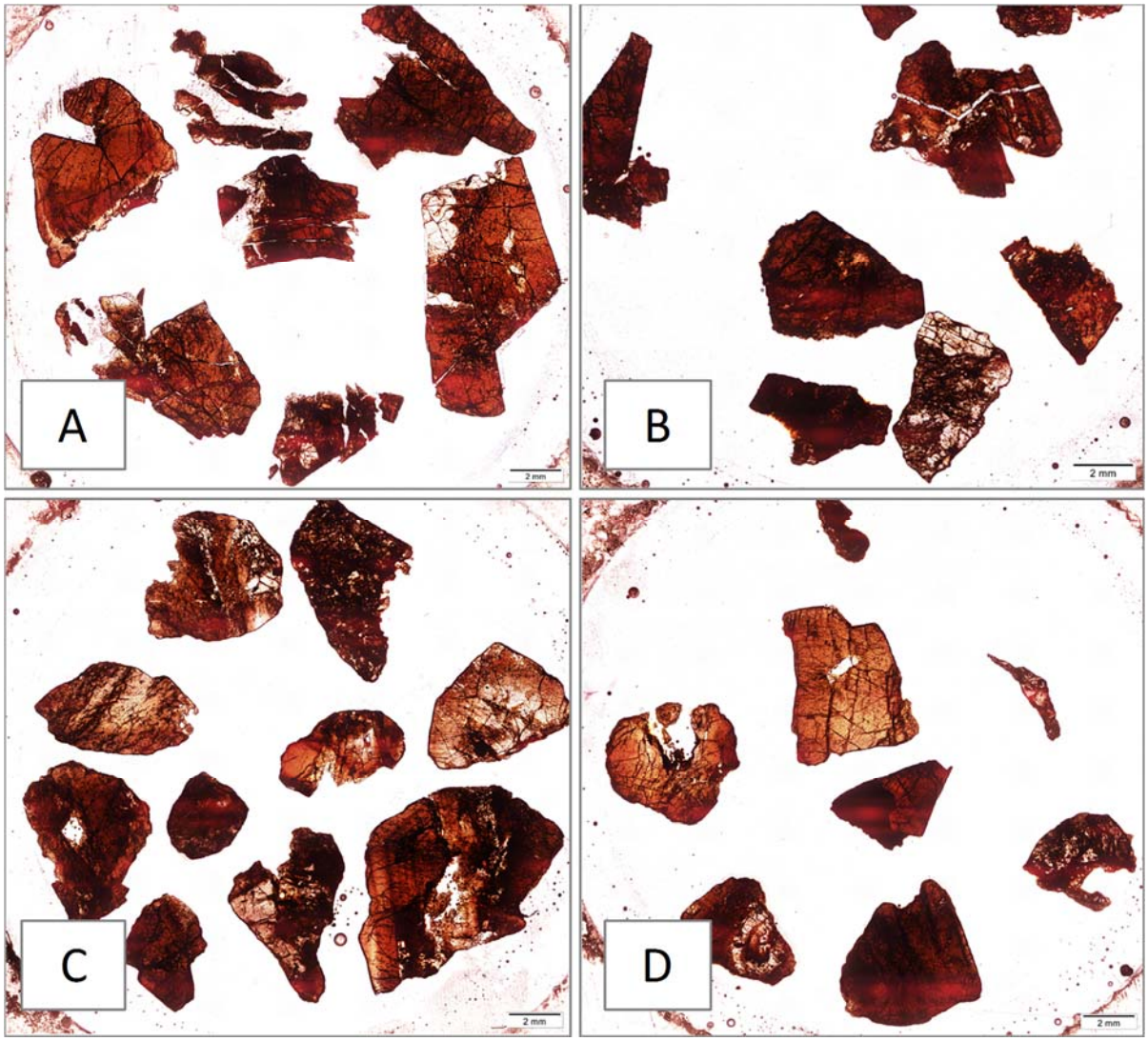


Figure 4. 12: Microphotograph of +4mm size fraction cassiterite grains from; A) Tunnel 1; B) Tunnel 3; C) Walking 1; D) Walking 2, under a transmitted light microscope. Zoning and pleochroism from dark brown to light brown can be seen in some of the grains.

4.5 Electron Microprobe Analysis

A total of 234 spot analysis (65 analysis on the +2 mm size fraction and 169 analysis on the +500 µm size fraction) were carried out on cassiterite grains and its inclusions from the Nyagasagara mining area. These samples were from Tunnel 1 (NYAG07), 2 (NYAG15), Walking 1 (NYAG04) and 2 (NYAG03)

(For a complete list of the electron microprobe results, refer to Appendix J). The aim of which were to determine the cassiterite composition by analysing for SnO_2, Ta_2O_5, Nb_2O_5, WO_3, Fe_2O_3, MnO, TiO_2, Sc_2O_3, SiO_2, and MgO. In addition, the chemical differences across zoned cassiterite were analysed to determine whether the cassiterite contained inclusions and/or exsolution products and the chemistry of these inclusions and/or exsolution products, and to determine the origin of the cassiterite based on its composition.

4.5.1 Geochemistry of cassiterite

The average SnO_2 content for cassiterite from the four mining sites ranges between 97.36% (NYAG07) and 96.42% (NYAG03) (Fig. 4.13). The SnO_2 content shows a decreasing trend as the cassiterite grade decreases. However, at NYAG04 the SnO_2 content increases slightly from 96.42% to 96.5%.

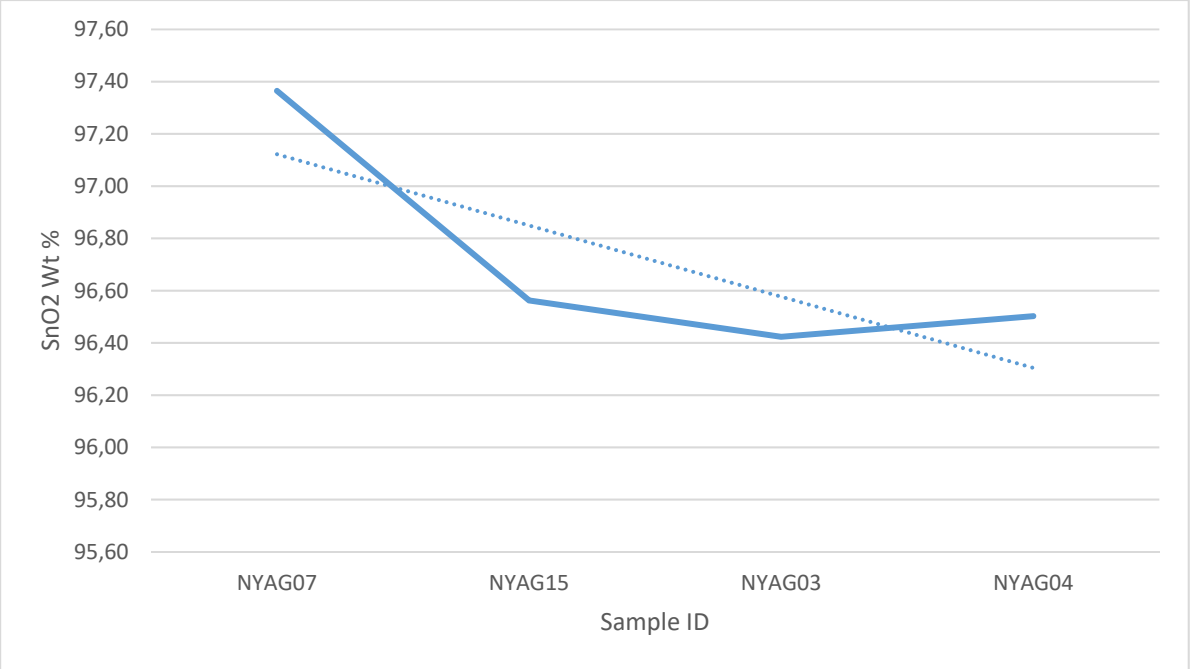


Figure 4. 13: Average SnO_2 content as weight percentage in cassiterite from Tunnel 1, 2, Walking 1, and 2, at Nyagasagara. The Sample ID's are ordered from highest grade (NYAG07) to lowest grade (NYAG04).

Even though there are slight differences in the composition of the cassiterite, all the grains analysed contained more than 90% Sn+W+Ti and has more Nb + Ta compared to Fe + Mn as illustrated in Figure 4.14. The cassiterite from NYAG03 appears to have the widest range Sn+W+Ti, ranging from 91.6% to 99.8%, whereas NYAG15 has the purest Sn+W+Ti composition, ranging from 95.4% to 100% (Fig. 4.14).

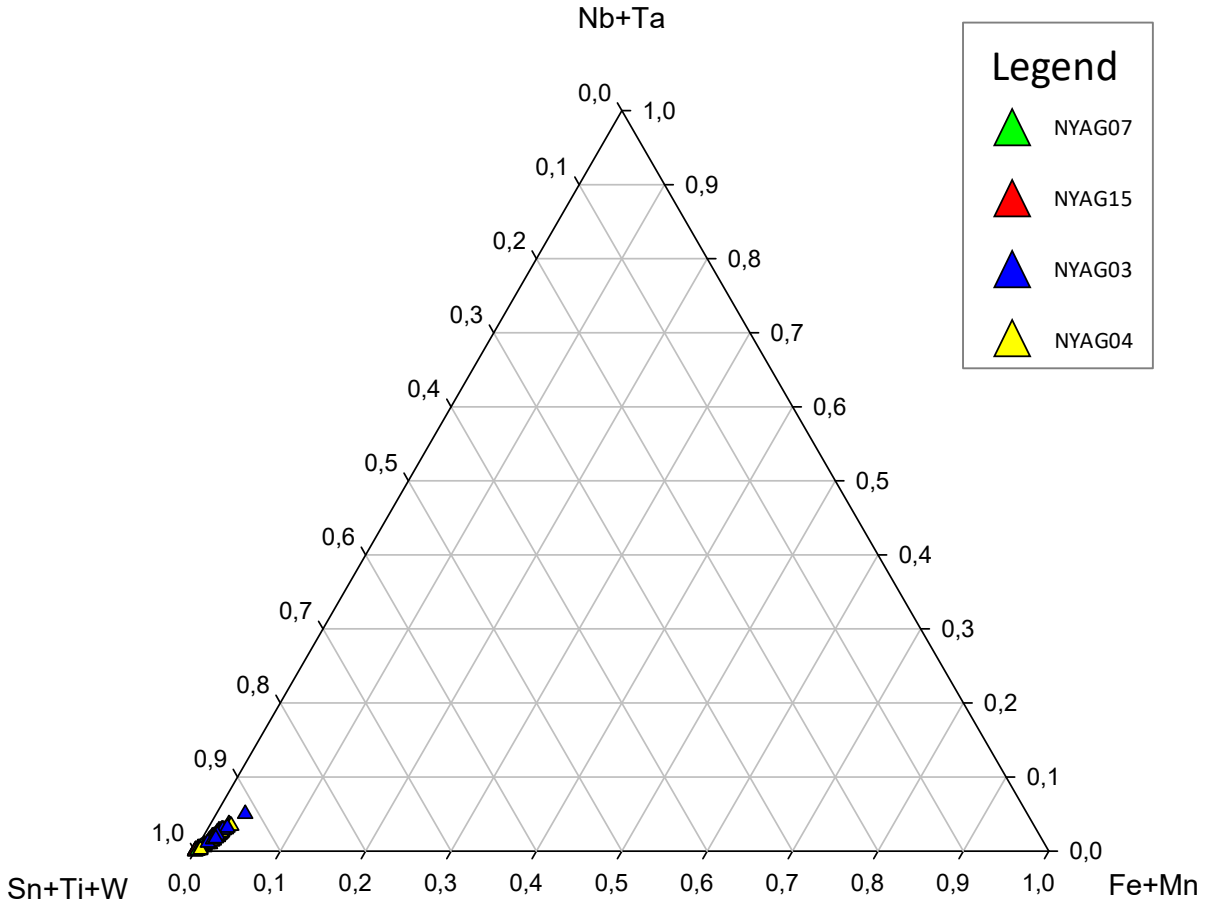


Figure 4. 14: A (Sn+Ti,W) - (Nb+Ta) - (Fe+Mn) ternary diagram showing chemical compositions of all analysed cassiterite at NYAG07 (green), NYAG15 (red), NYAG03 (blue), and NYAG04 (yellow).

In the zoned cassiterite crystals from Nyagasagara (Table 4.1), the chemical composition seems related to the colour of the cassiterite. The chemical composition of the darker and lighter zones differs from each other, the dark zones have higher Nb, Ta and Fe contents relative to the lighter zones. Of these elements, Nb concentrations are the highest and range from 0.6% to 2% Nb_2O_5. The samples with the highest Nb_2O_5 concentrations are also the samples with the lowest SnO_2 concentrations, whereas the lighter zones have the highest SnO_2 concentrations. The TiO content is not well distinguished across the colour zonation, and in some darker zones contains higher Ti content, but in other darker zones contain lower Ti content compared to the lighter zones. The MgO, SiO_2, Sc_2O_3, and WO_3, do not show any distinct chemical differences in the cassiterite from the mining area.

The Ta/(Ta+Nb) ratios of most cassiterite grains are lower than 0.5, whereas the Mn/(Mn+Fe) ratios are below 0.1 (Table 4.1 and Fig. 4.15 (A)). All the data from the cassiterite compositions plot along a linear array within the rare element pegmatite field, showing a good 2:1 ratio (Nb + Ta and Fe + Mn). Some of the cassiterite show a Nb + Ta and Fe + Mn ratio of 1:1 (Figure 4.15 (B).

Table 4. 1: Representative compositions of cassiterite from Nyagsagara, specifically from NYAG07, NYAG15, NYAG03, and NYAG04

	NYAG07 Average	NYAG15 Average	NYAG15 Light	NYAG15 Dark	NYAG03 Average	NYAG03 Light	NYAG03 Dark	NYAG04 Average	NYAG04 Light	NYAG04 Dark
MgO	0.16	0.17	0.16	0.12	0.17	0.17	0.19	0.16	0.18	0.14
SiO2	0.17	0.16	0.21	0.16	0.17	0.17	0.19	0.16	0.19	0.12
Sc2O3	0.00	0.00	0.00	0.00	0.00	0.00	0.00	0.00	0.00	0.00
TiO2	0.02	0.03	0.04	0.05	0.03	0.06	0.04	0.02	0.00	0.00
MnO	0.02	0.03	0.00	0.01	0.04	0.03	0.10	0.03	0.03	0.03
Fe2O3	0.60	0.61	0.55	0.86	0.67	0.47	1.07	0.74	0.53	1.12
SnO2	97.36	96.56	96.83	96.01	96.42	97.04	94.93	96.50	97.20	94.42
Ta2O5	0.64	0.70	0.26	0.93	0.81	0.58	1.37	0.89	0.78	2.22
WO3	0.01	0.01	0.00	0.00	0.02	0.00	0.04	0.02	0.00	0.00
Nb2O5	1.04	1.02	1.16	1.34	1.20	0.65	2.00	1.30	0.80	1.89
Total	100.04	99.30	99.21	99.48	99.51	99.17	99.93	99.83	99.71	99.94
Mg	0.007	0.006	0.006	0.004	0.006	0.006	0.007	0.006	0.007	0.005
Si	0.004	0.004	0.005	0.004	0.004	0.004	0.005	0.004	0.005	0.003
Sc	0.000	0.000	0.000	0.000	0.000	0.000	0.000	0.000	0.000	0.000
Ti	0.000	0.001	0.001	0.001	0.001	0.001	0.001	0.000	0.000	0.000
Mn	0.000	0.001	0.000	0.000	0.001	0.001	0.002	0.001	0.001	0.001
Fe	0.013	0.011	0.010	0.016	0.012	0.009	0.020	0.014	0.010	0.021
Sn	0.964	0.958	0.965	0.954	0.956	0.970	0.935	0.957	0.966	0.933
Ta	0.005	0.005	0.002	0.006	0.005	0.004	0.009	0.006	0.005	0.015
W	0.000	0.000	0.000	0.000	0.000	0.000	0.000	0.000	0.000	0.000
Nb	0.014	0.011	0.013	0.015	0.013	0.007	0.022	0.015	0.009	0.021
Ta/(Ta+Nb)	0.258	0.293	0.119	0.295	0.288	0.349	0.292	0.293	0.370	0.414
Mn/(Mn+Fe)	0.034	0.050	0.000	0.013	0.058	0.067	0.095	0.037	0.060	0.029

Average: Is the average for all the points analysed for that deposit; Light: Is the lighter zone; Dark: is the darker zone. Cation formula based on 2 atoms of oxygen.

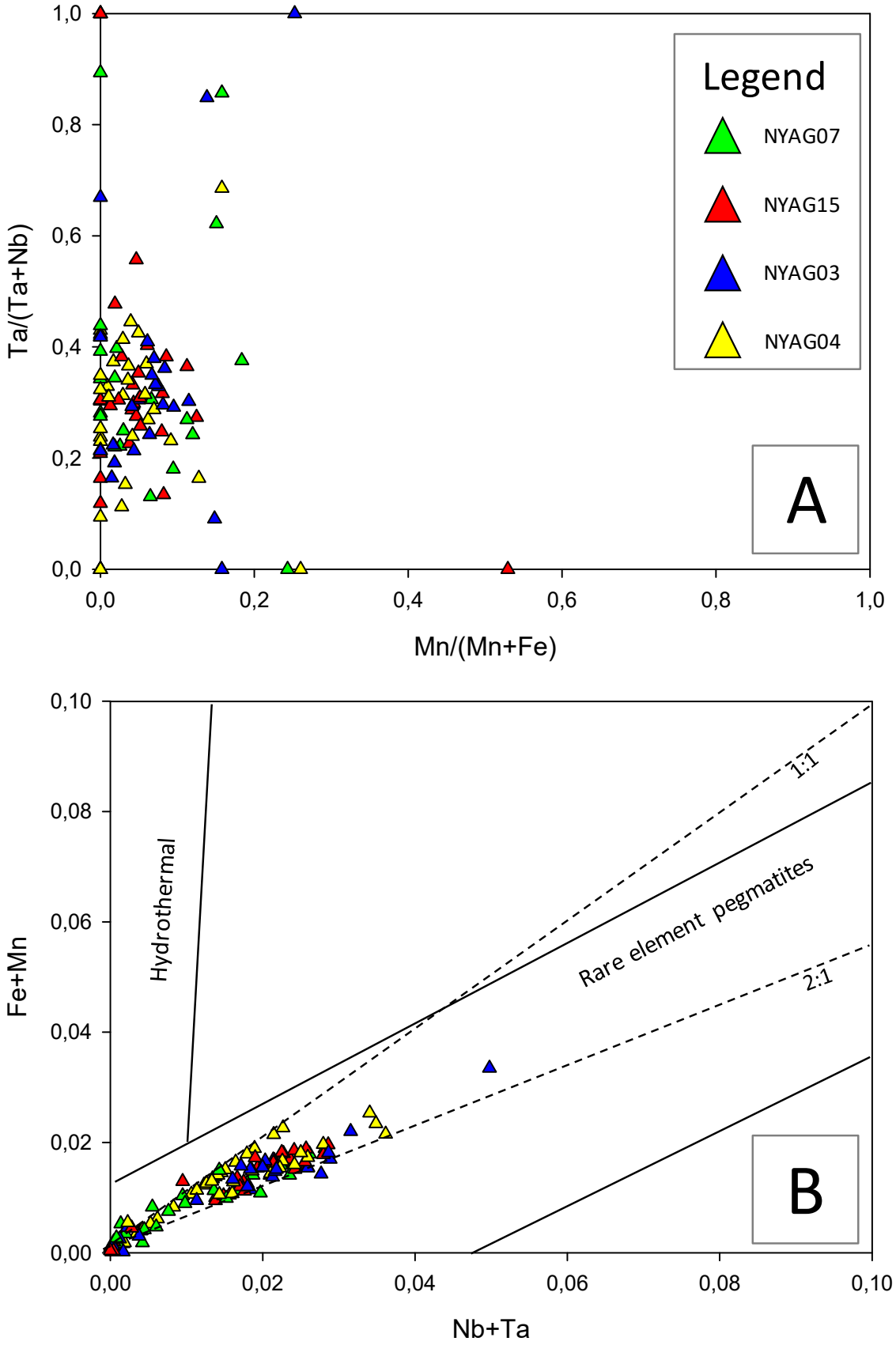


Figure 4. 15: Cassiterite analyses plotted in the columbite quadrilateral showing low Nb/Ta fractionation; (B) a binary diagram of (Nb + Ta) vs (Fe +Mn) for cassiterite from all the mining sites, NYAG07 (green), NYAG15 (red), NYAG03 (blue), NYAG04 (yellow). The fields of cassiterite in rare element pegmatites and of hydrothermal cassiterite were defined by Tindle and Breaks (1998).

The cassiterite from all the mining sites at Nyagasagara host a number of inclusions and/or exsolution products of coltan and one inclusion of zircon (Fig. 4.16 (A) - (C)). The exsolution products were identified where the cassiterite grains showed a depletion in Nb and Ta content next to the coltan grain, but showed an increase in Nb and Ta further away from the coltan grain. The Nb and Ta content of cassiterite hosting coltan inclusions, did not show this depletion in Nb and Ta content next to the coltan grain.

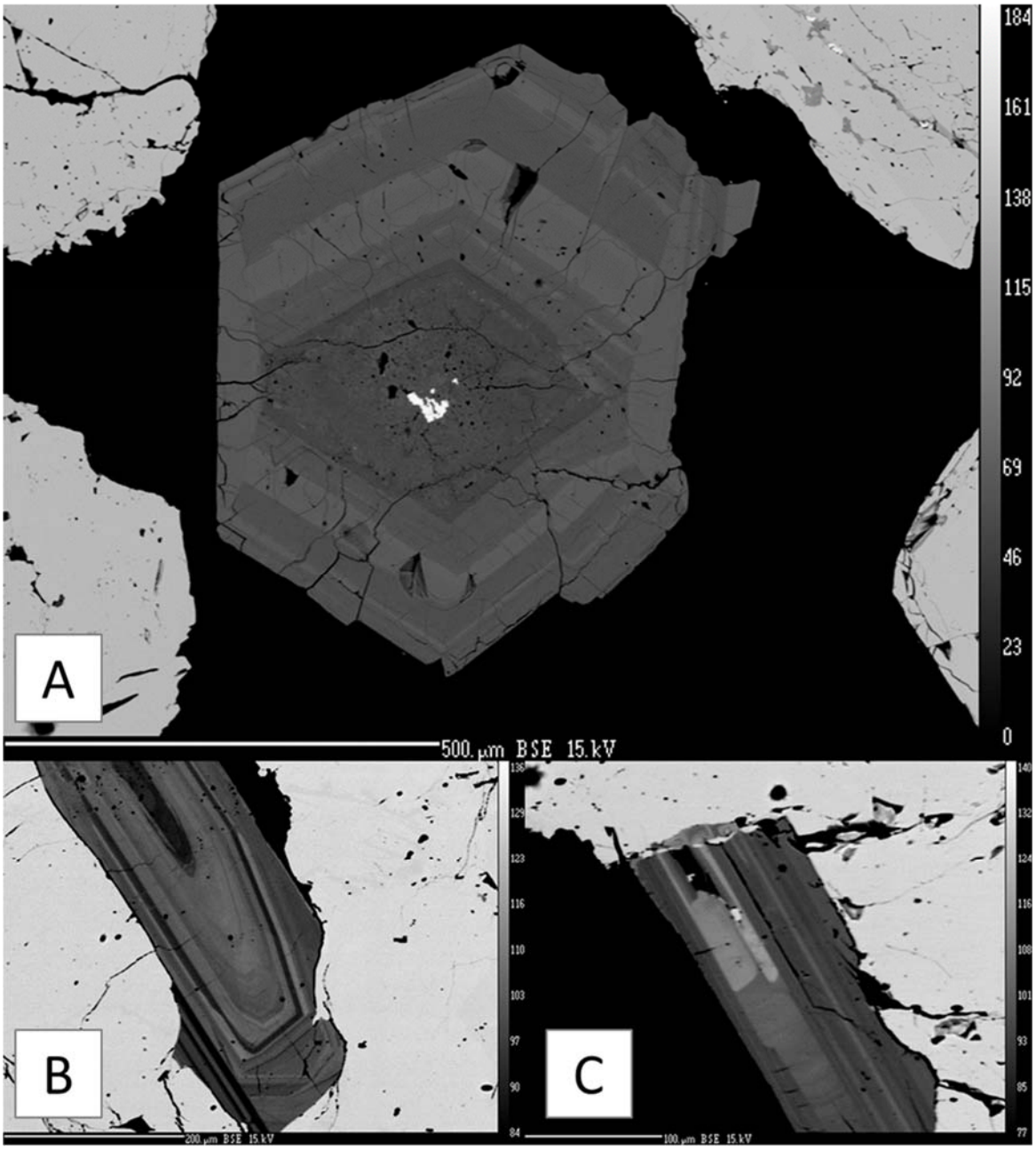


Figure 4. 16: Microphotographs of inclusions and/or exsolution products hosted in the cassiterite grains of Nyagasagara; A) zoned zircon grain, B) zoned coltan grain, C) zoned coltan grain.

4.5.2 Geochemistry of the coltan inclusions and products of exsolution

The compositions of the coltan minerals (inclusions and exsolution products) was plotted in terms of (Sn+Ti+W) – (Nb+Ta) – (Fe +Mn) triangular diagram (Fig. 4.17) The average Nb + Ta concentrations for the coltan inclusions and exsolution products range from 63.7% (NYAG07) to 61.1% (NYAG04) and 75% (NYAG15) to 65.2% (NYAG03) respectively (Fig. 4.17). All the coltan analysed, except for one in NYAG15, have higher Nb than Ta concentrations. The exsolved Ta>Nb coltan mineral (manganotantalite) also contains the highest Sn+Ti+W (0.074) concertation (7.4%) compared to the other coltan minerals with an average Sn+Ti+W concentration of 0.8%.

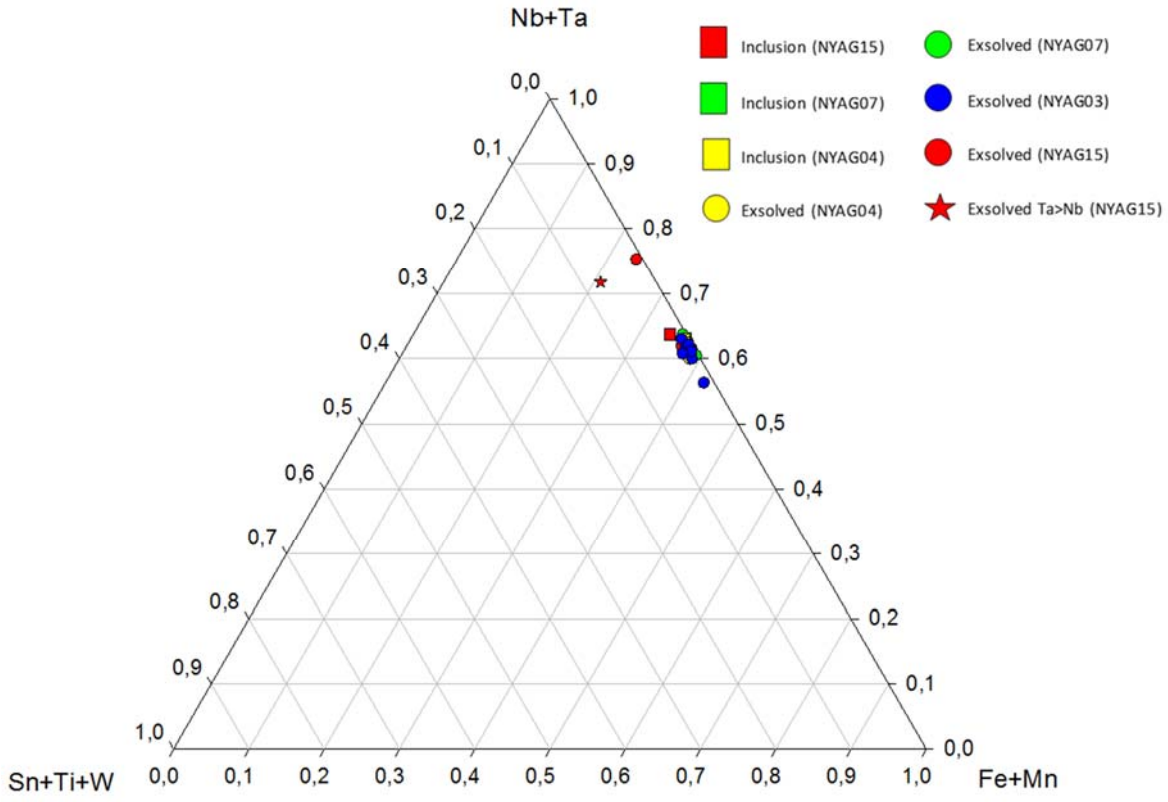


Figure 4. 17: Coltan analyses plotted in the (Sn+Ti+W) – (Nb+Ta) – (Fe+Mn) ternary diagram

Representative compositions of coltan inclusions and products of exsolution, as well as of the exsolved manganotantalite are given in Table 4.2. The colour zoning observed in the coltan (Fig. 4.16 (B) – (C), have different chemical compositions. The darker zones have more Fe_2O_3 and Nb_2O_5, and less Ta_2O_5 compared to the lighter zones. Table 4.2 shows that coltan inclusions have very little MgO, SiO_2 and Sc_2O_3 impurities and that it is generally below the detection limit of the electron microprobe conditions employed.

Table 4. 2: Representative compositions of coltan inclusions and exsolution products hosted in cassiterite from Nyagsagara, specifically from NYAG07, NYAG15, NYAG03, and NYAG04

	Coltan Inclusion			Exsolved Coltan								Ta>Nb
	NYAG07 Average	NYAG15 Average	NYAG04 Average	NYAG07 Average	NYAG15 Average	NYAG03 Average	NYAG03 C,Light	NYAG03 Darker	NYA04 Average	NYA04 C,Dark	NYA04 Light	NYAG15 Average
MgO	0.00	0.00	0.02	0.01	0.02	0.01	0.00	0.00	0.01	0.00	0.01	0.04
SiO2	0.00	0.00	0.00	0.00	0.00	0.00	0.00	0.00	0.00	0.00	0.00	0.00
Sc2O3	0.00	0.02	0.00	0.00	0.01	0.01	0.00	0.00	0.01	0.00	0.00	0.00
TiO2	0.22	0.22	0.28	0.22	0.20	0.41	0.36	0.19	0.26	0.24	0.28	0.72
MnO	9.71	10.77	8.41	10.19	10.01	7.10	9.19	9.82	11.07	8.91	10.48	6.80
Fe2O3	14.52	14.12	15.13	13.42	13.57	16.44	13.32	13.29	11.83	14.95	12.13	0.46
SnO2	0.27	0.22	0.37	0.19	0.22	0.25	0.19	0.19	0.19	0.18	0.12	4.06
Ta2O5	14.64	13.99	21.44	17.43	18.08	27.50	32.42	22.13	22.74	19.92	29.99	47.80
WO3	0.41	0.17	0.23	0.11	0.10	0.03	0.16	0.00	0.11	0.00	0.00	0.00
Nb2O5	61.45	61.67	54.43	58.97	57.93	47.62	44.23	53.68	53.87	55.35	48.30	17.58
Total	101.22	101.18	100.30	100.55	100.13	99.37	99.37	99.37	99.37	99.37	99.37	77.46
Mg	0.000	0.000	0.001	0.001	0.002	0.001	0.000	0.000	0.001	0.000	0.001	0.003
Si	0.000	0.000	0.000	0.000	0.000	0.000	0.000	0.000	0.000	0.000	0.000	0.000
Sc	0.000	0.001	0.000	0.000	0.000	0.000	0.000	0.000	0.000	0.000	0.000	0.000
Ti	0.009	0.009	0.012	0.010	0.009	0.019	0.017	0.009	0.011	0.011	0.013	0.031
Mn	0.470	0.522	0.410	0.508	0.506	0.367	0.488	0.502	0.530	0.448	0.543	0.325
Fe	0.625	0.608	0.656	0.595	0.610	0.755	0.629	0.603	0.503	0.668	0.558	0.020
Sn	0.006	0.005	0.008	0.004	0.005	0.006	0.005	0.005	0.004	0.004	0.003	0.091
Ta	0.228	0.218	0.336	0.279	0.294	0.456	0.553	0.363	0.350	0.322	0.499	0.733
W	0.006	0.003	0.003	0.002	0.001	0.001	0.003	0.000	0.002	0.000	0.000	0.000
Nb	1.588	1.595	1.417	1.571	1.564	1.313	1.254	1.464	1.377	1.486	1.336	0.448
Ta/(Ta+Nb)	0.125	0.120	0.192	0.151	0.158	0.258	0.306	0.199	0.203	0.178	0.272	0.621
Mn/(Mn+Fe)	0.429	0.462	0.385	0.461	0.453	0.327	0.437	0.454	0.513	0.401	0.493	0.943

Average: Is the average for all the points analysed for that depoit; C,Light: the lighter centre of the grain; C,Dark: the darker centre of the grain. Cation formula based on 6 atoms of oxygen.

The coltan inclusions and exsolution products, recognised in the cassiterite grains from Nyagasagara, have compositions ranging from ferrocolumbite to manganocolumbite, although most of the inclusions occur as ferrocolumbite. At NYAG015, one exsolved coltan with a composition of manganotanalite was observed (Table 4.2 and Fig. 4.18). The Ta/(Ta+Nb) ratios of most coltan inclusions and exsolution products are lower than 0.5, and are plotted along the 0.2 Ta ratio, whereas the Mn/(Mn+Fe) ratios range from 0.04 to 0.94 (Table 4.1 and Fig. 4.18).

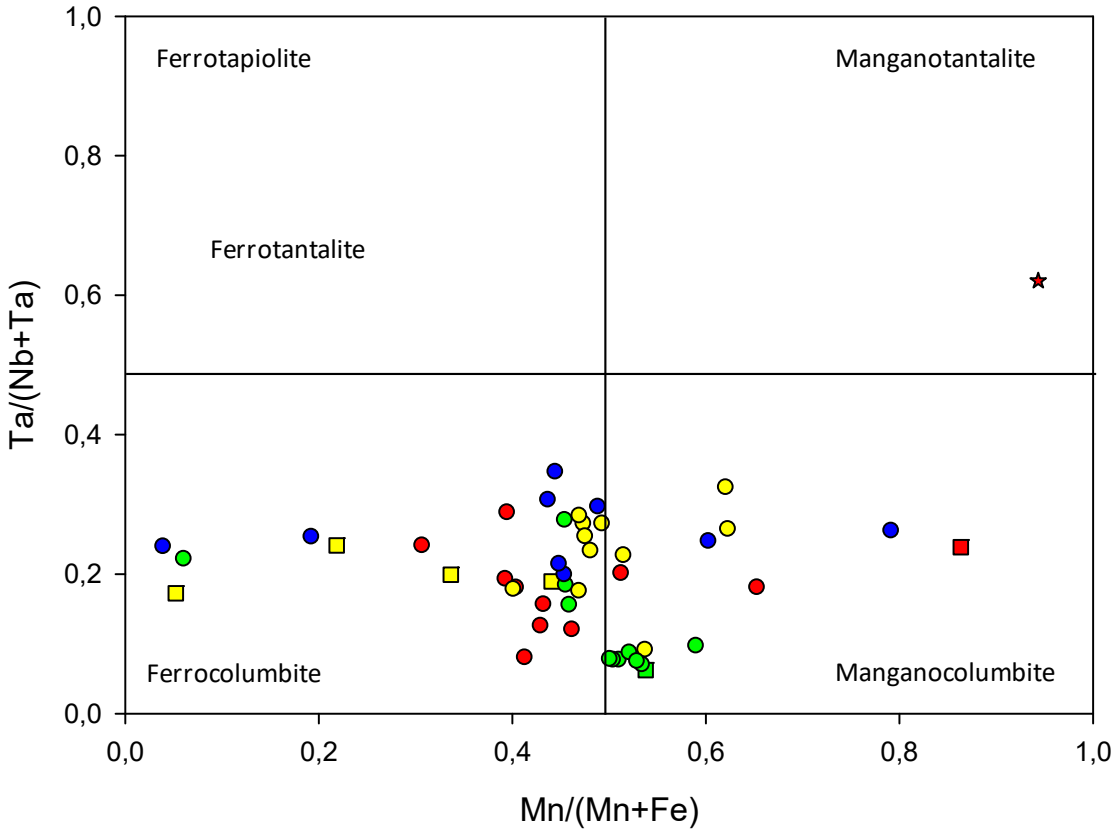


Figure 4. 18: Coltan minerals from the Nyagasagara mining area plotted in the columbite quadrilateral.

Chapter 5:

Discussion

5.1 Introduction

The HMR license, consists of four mining areas, known as Nyagasagara, Gakurazo, Kageyo, and Kageyo Extension. According to local information all four of these deposits are rare element pegmatite related and occur within an area of G4 granite and historical mining sites. The artisanal miners claim that all four mining sites contain Sn-W-Ta-Nb oxide minerals, however, production figures from HMR only indicates cassiterite and coltan for Nyagasagara and Kageyo respectively. No production data are available for Gakurazo and Kageyo Extension, but they too are believed to contain both cassiterite and coltan. Concentrate samples were selected from all four sites to determine the mineral grade at the various deposits. Of the deposits, Nyagasagara was investigated in detail.

5.2 HMR mining areas compared to other deposits in Rwanda

HMR mining areas, similar to most major cassiterite (Rutongo) and/or coltan (Gatumba) or wolframite (Nyakabingo) mining areas in Rwanda, occur in close proximity to large scale structures, G4 granites, and/or pegmatites. The HMR license area is located between the Bugesera syncline and the Bugesera granite, with both the Nyagasagara and Kageyo mining areas occurring adjacent to large scale quartzite/pegmatite veins. The Kageyo Extension is situated on the rim of the Bugesera granite, and Gakurazo is located between Nyagasagara and Kageyo. The Rutongo cassiterite deposits are situated on the Rutongo anticline and most of the mineralisation is associated with hydrothermal quartz veins within quartzites (Dewaele et al., 2009; De Clercq, 2012; Dewaele et al., 2013; Pohl et al., 2013). The Nyakabingo wolframite deposit, similar to Rutongo is also a hydrothermal vein deposit situated on the flanks of a large anticline, but the wolframite mineralisation is primarily hosted in black shales and not in quartzites (De Clercq et al., 2008; Hulsbosch et al., 2013; Dewaele et al., 2016; Hulsbosch et al., 2016). The Gatumba cassiterite and coltan deposit is hosted within rare metal pegmatites situated between two granitic batholiths (Dewaele et al., 2007; Lehmann et al., 2008; Dewaele et al., 2011; Dewaele et al., 2013). Thus, the HMR deposits are in a suitable regional geological setting for a Sn-W-Ta-Nb deposit to be found. However, the regional location alone is not enough to define the HMR deposit and other factors such as the ROM, host rock, grade, mineral size fraction, mineralisation style, oxide minerals present, and geochemistry of the oxide minerals present should be considered too.

At each one of the HMR mining sites the ROM material consisted of very weathered material, none of the sites intersected fresh granite and/or pegmatite material. This makes it difficult to determine whether the deposit is a primary or secondary deposit. When only looking at the weathered ROM, one is tempted to classify the HMR deposit as a secondary deposit (an eluvial and/or alluvial deposit). However, both Rutongo and Nyakabingo started as open pit mines, in the weathered material and progressively moved to underground mining of fresh material and they are classified as hydrothermal vein deposits (De Clercq et al., 2008; Dewaele et al., 2009). The weathered zone in Rwanda is quite deep and it is not uncommon to reach a depth of 30 m below surface, whereas the average mining depth for the HMR mining sites is not more than 15 m below surface and thus most probably are still in the weathered zone. Thus, even though a mining area started out as a secondary deposit, the presence of a primary deposits at depth is still possible. Further studies are needed to determine whether pegmatite and/or granite is situated deeper below the surface at the deposits.

The host rock for Nyagasagara Tunnel 1 and Gakurazo appeared to be very similar with the naked eye, both sites being hosted in very weathered, predominantly kaolinite-rich material. The other sites at Nyagasagara (Tunnel 2-5, Walking 1, and 2) appear to be hosted in a reddish laterite. At Kageyo and Kageyo Extension the host rock appears to be quartzite, thought to be similar to the Rutongo deposit, except that Rutongo is known for its vein type cassiterite deposits and coltan minerals are not commonly associated with vein type deposits. None of these sites had black shales as a host rock and according to De Clercq (2012) the major difference between cassiterite and wolframite deposits, is whether the host rock is a black shale or quartzite. He determined that cassiterite vein deposits in Rwanda are mostly hosted in quartzites, whereas wolframite vein deposits are mostly hosted in black shales. This is supported by (Dewaele et al., 2009; Hulsbosch et al., 2013; Pohl et al., 2013; Dewaele et al., 2016), who claim that in the KAB, primary mineralisation of Sn, Nb-Ta and W do not commonly occur in the same deposits, due to different host rocks at the various deposits, which influences the precipitation mechanisms of the elements. Based on the above-mentioned information and the lack of wolframite minerals in the HMR historical production data, the presence of wolframite at any of the HMR mining sites is highly unlikely.

The historical production data for the HMR deposits indicates that cassiterite is the main mineral mined for at Nyagasagara, whereas for Kageyo it is coltan. However, the artisanal miners believe that cassiterite and coltan is present at both mining sites. The historical data do not indicate whether Gakurazo was predominantly mined for cassiterite and/or coltan and no historical information is available for the Kageyo Extension. According to old internal company documents, the average grade for Nyagasagara and Kageyo were 5% cassiterite and 2% coltan respectively, whereas no information

is available for Gakurazo and Kageyo Extension. The 5% cassiterite grade is similar to grades reported for Rutongo where the grade ranges between 0.6% and 5% cassiterite. No known coltan grades are available in literature for Rwanda. However, the grades observed at all four mining areas during this study were very low and contradicts the old internal company documents. The grade for Nyagasagara ranged from 0.04% to 5.56% cassiterite, for Kageyo ranged from 0.01% to 0.03% coltan, for Gakurazo 0.04% cassiterite and/or coltan, and for Kageyo Extension 0.01% coltan. It could be that for Nyagasagara, the old company reports only referred to the cassiterite grade at Tunnel 1 (5.56%), but the reason for the major difference in grade at Kageyo is unknown. Only the Nyagasagara deposit was studied in further detail, due to the low grades at the other mining areas. The subsequent studies mainly focussed on the concentrate material sampled from Nyagasagara.

5.3 Nyagasagara deposit and its mineralisation

To further understand the Nyagasagara deposit, its mineralisation, and whether coltan and/or wolframite is present, subsequent studies focussed on the concentrate material from Tunnel 1-5, Walking 1, and 2. The studies included size fraction analysis, whole rock chemistry and geochemistry of the concentrate.

According to the size fraction analysis, almost 60% of the concentrate report to the coarse size fraction of +2 mm and +4 mm, whereas 30% report to +1 mm and the rest reports to the < 1 mm size fraction. The comparison between the average grain size distribution and cassiterite grade for the five mining sites on Nyagasagara, indicated a decrease in the average grain size with decreasing grade. This could be an indication that the areas with the highest grade were closest to the source of mineralisation or that the various mining sites differ from each other. The varying grain size distribution between the mining sites could be due to different processing techniques used by the artisanal miners, resulting in a loss and/or theft of certain grain sizes. To further investigate the mineralisation style, whether there is any significant difference between the five mining sites on Nyagasagara and the presence of coltan and wolframite, mineralogical and whole rock chemical analyses were performed on the concentrate samples.

Under transmitted light only cassiterite was identified in the thin sections, but no distinct differences were observed between the five mining sites. The cassiterite displayed similar optical characteristics at all the sites, compared to literature (Neiva, 1996; De Clercq, 2012) for Rwanda and in general. These included, colours ranging from dark reddish brown to colourless, zoning and moderate to intense pleochroism. The only difference observed optically was that the cassiterite minerals from Tunnel 2

appeared slightly darker compared to the cassiterite from the other four sites. The shape of the cassiterite grains are angular to very angular. Thus, the mining sites are most probably very close to the source of the mineralisation and can be classified as an eluvial deposit. The colour zonation and geochemistry of the cassiterite were further investigated with the electron microprobe.

The whole rock chemical data reported an average Sn content (weight percent) of 67.08% Sn over the four mining sites, with Nb, Ta, and W only reporting average concentrations of 0.73%, 0.61% and 150 ppm respectively. Thus, the optical microscopy data combined with the whole rock chemistry suggest that only cassiterite is present on Nyagasagara and that the Nb and Ta concentrations are probably related to coltan inclusions and/or exsolution products. This supports the finding, that Sn-Nb-Ta-W oxide minerals do not commonly occur in the same deposits in Rwanda (Dewaele et al., 2009; Hulsbosch et al., 2013; Pohl et al., 2013; Dewaele et al., 2016). Lithium was not present in significant amounts at any of the mining sites.

5.3.1 Geochemistry of cassiterite

The cassiterite grains analysed from Nyagasagara had an average SnO_2 concentration of 96.71 Wt. %, but with a few grains, especially in the lighter zones, showing considerable purity (SnO_2 > 99 Wt. %). The purity of the cassiterite displayed a decreasing trend with a decrease in grade at the mining sites, but the difference in SnO_2 concentrations is considered too small (< 1%), to be of major significance. Furthermore, some of the mining sites had a higher variance within the same site. Other significant concentrations recorded in the cassiterite were for Nb_2O_5, Ta_2O_5, and Fe_2O_3, whereas TiO_2, WO_3, and MnO are present as minor amounts. Most cassiterite grains had reported more Nb than Ta, except for one cassiterite grain at Tunnel 2, which recorded more Ta than Nb. According to literature, these concentrations can give an indication of the origin of the grains, whether it is related to hydrothermal vein deposits or rare element pegmatite and/or granite deposits (magmatic deposits). In hydrothermal vein deposits, Ti, Sc and V concentrations are elevated relative to Nb, Ta, Zr, Hf, and U (Oberthür et al., 2016). This is supported by data from cassiterite analysed at Rutongo, which reported Ti as the most abundant element, after SnO_2, with concentrations ranging around 0.6% TiO_2 (De Clercq, 2012). Cassiterite from magmatic deposits are enriched in Nb, Ta, Zr, Hf, Mn and Zn, with low Ti, Sc, and V concentrations and most pegmatite related cassiterite have more Ta than Nb (Cèrny and Ercit, 1985; Černý et al., 2004; Oberthür et al., 2016). Thus, the trace element signatures of the cassiterite grains from Nyagasagara predominantly point to an origin from magmatic deposits, specifically rare element granite deposits. This is supported by the fact that all the cassiterite at Nyagasagara plotted in the rare

element pegmatite/ granite field as defined by Tindle and Breaks (1998) on the binary diagram of (Fe + Mn) vs (Ta + Nb) (refer to Fig. 4.15 (B) chapter 4.5.1).

Most of the cassiterite analysed displayed colour zoning, which according to literature is controlled by the degree of substitution of tin by elements such as Nb, Ta, Fe, Ti, W and Zr. (Möller et al., 1988; Neiva, 1996; De Clercq, 2012). The light zones analysed in the Nyagasagara cassiterite had higher SnO_2 concentrations compared to the darker zones, which had lower SnO_2 concentrations, but higher Nb_2O_5, Ta_2O_5, and FeO concentrations.

Cassiterite is known to host a number of inclusions, such as coltan, rutile, zircon and ilmenite (Dewaele et al., 2013). In the grains from Nyagasagara however, only one inclusion of zircon, and numerous coltan inclusions and exsolution products were observed. No depletion in Nb, Ta, and Fe were observed in the cassiterite close to the inclusions. Whereas, the cassiterite grains close to the coltan exsolution products reported a depletion in Nb, Ta, and Fe concentrations. According to literature, it is not uncommon to find coltan inclusions and/or exsolution products in both hydrothermal vein type and pegmatite and/or granite type deposits and thus cannot be used to determine the origin of the cassiterite (Dewaele et al., 2013).

5.3.2 Geochemistry of coltan inclusions and exsolution products

Two types of coltan exsolution products were identified in the cassiterite, the first type had more Nb concentration than Ta, whereas the second type had more Ta than Nb. Note that only one exsolution product of the second type was observed in the cassiterite and that the total weight percentage of that grain only calculated to 77%, which could indicate an error in the results. Coltan inclusions were also observed in the cassiterite.

The average Nb + Ta concentrations for coltan inclusions compared to exsolution products, indicate that the coltan inclusions show less variability (61.1% to 63.7% Nb + Ta) than the coltan exsolution products (Ta + Nb). This is most probably related to the amount of Nb + Ta that got exsolved from the cassiterite, to form the exsolution product.

Both the coltan inclusions and exsolution products have similar compositions, ranging from ferrocolumbite to manganocolumbite, except for the Ta>Nb exsolved grain having a composition of manganotantalite. The Ta/(Ta +Nb) values tend to increase with increasing Mn/(Mn + Fe) from ferrocolumbite to mangantantalite (Černý, 1989; Neiva, 1996; Melcher et al., 2008). This trend is not

observed in the coltan grains from Nyagasagara, here the Ta/(Ta + Mn) values stay around 0.2 with an increase in Mn/(Mn + Fe) values. A possible reason for this is that Nyagasagara coltan grains are exsolution products and inclusions, instead of discrete coltan mineral grains (González et al., 2017).

Chapter 6:

Conclusions and Recommendations

The HMR project (Nyagasagara, Gakurazo, Kageyo, and Kageyo Extension) is located between the Bugesera syncline and the Bugesera granite, with both Nyagasagara and Kageyo occurring adjacent (<4 km) to known large scale structures, granites and/or pegmatites. The Kageyo Extension is located on the rim of the Bugesera granite, and Gakurazo is located in between Nyagasagara and Kageyo. It can be concluded that the HMR deposits are situated in a suitable regional geological setting for Sn-W-Ta-Nb oxide minerals to be found.

At each one of the HMR mining sites the ROM material consisted of very weathered material, none of the sites intersected fresh material such as granite and/or pegmatite. This is most probably due to the mining pits being too shallow. The host rocks at all the sites were also very weathered, except for the quartzites at Kageyo, which showed little weathering. None of the sites had black shales as host rocks, and it can be concluded that the presence of vein type wolframite is very unlikely.

The cassiterite and coltan grades reported for the four mining areas on the license, differed quite a bit. The highest grades recorded at Nyagasagara, Gakurazo, Kageyo and Kageyo Extension were 5.56% cassiterite, 0.08% cassiterite, 0.03% coltan, and 0.01% coltan respectively.

The cassiterite grade compared with the size fraction analysis at Nyagasagara, indicated a positive correlation between the grain size (in the +4 mm and < +500 µm size fractions) and the grade. As the cassiterite grade decreased (from Tunnel 1 to Walking 1), so did the average grain size. Nevertheless, most of the cassiterite from Nyagasagara reported to the coarse size fraction of +2 mm and +4 mm, which represented 60% of the cassiterite grains. Both the coarser (+ 2 mm) and finer (+ 500 µm) size fractions were studied under transmitted light and the shape of the cassiterite grains ranged from very angular to angular and displayed common optical characteristics such as zoning and pleochroism. There appeared to be no correlation between the grain size and the number of alternating zones in the cassiterite. Cassiterite was also the only mineral identified in the concentrate samples from Nyagasagara. Thus, the presence of coltan and wolframite as discrete minerals on Nyagasagara is very unlikely. This is supported by the whole rock chemistry and electron microprobe studies of the concentrate, which reported compositions of primarily SnO_2.

The trace element signatures of the cassiterite grains from Nyagasagara predominantly point to an origin from magmatic deposits. The Nb > Ta concentrations in the cassiterite suggest they originated

from a rare element granite deposits. The Fe, Nb, and Ta concentrations tend to differ across the colour zones observed in the cassiterite. The darker zones have more Fe, Nb, and Ta compared to the lighter zones.

Numerous coltan exsolution products and inclusions were observed in the cassiterite. They were differentiated by the Nb, Ta, and Fe concentrations in the cassiterite grains close to the exsolution products compared to further away. The composition of the cassiterite closest to the coltan exsolution products have depleted Nb, Ta, and Fe concentrations compared to further away, whereas for the inclusions it remained unchanged.

Based on all the evidence it can be concluded that the Nyagasagara deposit is an eluvial deposit consisting of only cassiterite minerals, which have a magmatic origin, believed to be related to rare element granites.

The following is recommended for future work:

- Perform whole rock chemistry and electron microprobe studies on the material from Gakurazo, Kageyo and Kageyo Extension to help further differentiate between the four mining areas and to determine whether coltan and/or cassiterite is present.

- Perform drilling, to determine whether primary mineralisation occurs at depth.

- Perform whole rock chemistry and electron microprobe studies on fresh pegmatite and/or granite material from the Bugesera district and to compare it with Gatumba and Rutongo.

References

Baudin, B., Zigirababili, J., Ziserman, A., and Petricec, V., 1982. Map of the mineral deposits of Rwanda. Scale: 1:250 000. Ministry of Natural Resources, Rwanda.

Bonham-Carter, G., 1994. GIS for Geoscientists: Modeling with GIS. New York. Elsevier.

Buurman, I., and Montjoie, R., 2016. Field sampling report. Unpublished company report, Umbono Capital, Johannesburg, South Africa.

Cahen, L., Snelling, N., Delhal, J., Vail, J., Bonhomme, M., and Ledent, D., 1984, The Geochronology and Evolution of Africa, Clarendon Press, Oxford, UK.

Černý, P., 1989, Characteristics of pegmatite deposits of tantalum, Lanthanides, and niobium, Springer, pp 195-239.

Cerny, P., Blevin, P., Cuney, M., and London, D., 2005. Granite-related ore deposits. Society of Economic Geologists, Vol. 100, pp 337-370.

Černý, P., Chapman, R., Ferreira, K., and Smeds, S.-A., 2004. Geochemistry of oxide minerals of Nb, Ta, Sn, and Sb in the Varuträsk granitic pegmatite, Sweden: The case of an “anomalous” columbite-tantalite trend. American Mineralogist, Vol. 89, pp 505-518.

Cèrny, P., and Ercit, T. S., 1985. Some recent advances in the mineralogy and geochemistry of Nb and Ta in rare-element granitic pegmatites. Bull. Minerals, Vol. 108, pp 499-532.

De Clercq, F., 2012. Metallogenesis of Sn and W vein-type deposits in the Karagwe-Ankole belt (Rwanda). PhD Thesis (unpublished), University of Leuven, Wetenschap and Technologie.

De Clercq, F., Muchez, P., Dewaele, S., and Boyce, A., 2008. The tungsten mineralisation at Nyakabingo and Gifurwe (Rwanda): preliminary results. Geologica Belgica, Vol. 11, pp 251-258.

Debruyne, D., Hulsbosch, N., Van Wilderode, J., Balcaen, L., Vanhaecke, F., and Muchez, P., 2015. Regional geodynamic context for the Mesoproterozoic Kibara Belt (KIB) and the Karagwe-Ankole Belt: evidence from geochemistry and isotopes in the KIB. Precambrian Research, Vol. 264, pp 82-97.

Dewaele, S., De Clercq, F., Hulsbosch, N., Piessens, K., Boyce, A., Burgess, R., and Muchez, P., 2016. Genesis of the vein-type tungsten mineralization at Nyakabingo (Rwanda) in the Karagwe–Ankole belt, Central Africa. Mineralium Deposita, Vol. 51, pp 283-307.

Dewaele, S., Goethals, H., and Tom, T., 2013. Mineralogical characterization of cassiterite concentrates from quartz vein and pegmatite mineralization of the Karagwe-Ankole and Kibara Belts, Central Africa. Geologica Belgica, Vol. 16, pp 66-75.

Dewaele, S., Henjes-Kunst, F., Melcher, F., Sitnikova, M., Burgess, R., Gerdes, A., Fernandez-Alonso, M., De Clercq, F., Muchez, P., and Lehmann, B., 2011. Late Neoproterozoic overprinting of the cassiterite and columbite-tantalite bearing pegmatites of the Gatumba area, Rwanda (Central Africa). Journal of African Earth Sciences, Vol. 61, pp 10-26.

Dewaele, S., Muchez, P., De Clercq, F., Boyce, A., Schneider, J., Burgess, R., and Fernandez-Alonso, M., 2009. Geology of the cassiterite mineralisation in the Rutongo area, Rwanda (Central Africa): current state of knowledge. Geologica Belgica, Vol. 13, pp 91-112.

Dewaele, S., Tack, L., Fernandez-Alonso, M., Boyce, A., and Muchez, P., (2007). Cassiterite and columbite mineralization in pegmatites of the northern part of the Kibara orogen (Central Africa): the Gatumba area (Rwanda), in Proceedings Irish Association for Economic Geology, pp 1489-1492.

Dyussembayeva, K., Baibatsha, A., Kassenova, A., Mamanov, E., and Assubayeva, S., 2014. Results of study the rare metal ore mineralization of the selected areas in Central Africa. International Multidisciplinary Scientific GeoConference: SGEM: Surveying Geology & Mining Ecology Management, Vol. 1, pp 299.

Evans, D., Boadi, I., Byemelwa, L., Gilligan, J., and Marcet, P., 2000. Kabanga magmatic nickel sulphide deposits, Tanzania: morphology and geochemistry of associated intrusions. Journal of African Earth Sciences, Vol. 30, pp 651-674.

Fernandez-Alonso, M., Cutten, H., De Waele, B., Tack, L., Tahon, A., Baudet, D., and Barritt, S., 2012. The Mesoproterozoic Karagwe-Ankole Belt (formerly the NE Kibara Belt): The result of

prolonged extensional intracratonic basin development punctuated by two short-lived far-field compressional events. Precambrian Research, Vol. 216, pp 63-86.

Fernandez-Alonso, M., and Theunissen, K., 1998. Airborne geophysics and geochemistry provide new insights in the intracontinental evolution of the Mesoproterozoic Kibaran belt (Central Africa). Geological Magazine, Vol. 135, pp 203-216.

GMD, 2010. Mining in Rwanda. Unpublished report, Geology and Mines Deparment, Kigali, Rwanda.

González, T. L., Polonio, F. G., Moro, F. J. L., Fernández, A. F., Contreras, J. L. S., and Benito, M. C. M., 2017. Tin-tantalum-niobium mineralization in the Penouta deposit (NW Spain): Textural features and mineral chemistry to unravel the genesis and evolution of cassiterite and columbite group minerals in a peraluminous system. Ore Geology Reviews, Vol. 81, pp 79-95.

Hulsbosch, N., Boiron, M.-C., Dewaele, S., and Muchez, P., 2016. Fluid fractionation of tungsten during granite–pegmatite differentiation and the metal source of peribatholitic W quartz veins: Evidence from the Karagwe-Ankole Belt (Rwanda). Geochimica et Cosmochimica Acta, Vol. 175, pp 299-318.

Hulsbosch, N., Hertogen, J., Dewaele, S., André, L., and Muchez, P., 2013. Petrographic and mineralogical characterisation of fractionated pegmatites culminating in the Nb-Ta-Sn pegmatites of the Gatumba area (western Rwanda). Geologica Belgica, Vol. 16, pp 105-117.

Hulsbosch, N., Hertogen, J., Dewaele, S., André, L., and Muchez, P., 2014. Alkali metal and rare earth element evolution of rock-forming minerals from the Gatumba area pegmatites (Rwanda): Quantitative assessment of crystal-melt fractionation in the regional zonation of pegmatite groups. Geochimica et Cosmochimica Acta, Vol. 132, pp 349-374.

Kinnaird, J. A., Nex, P. A., and Milani, L., 2016. Tin in Africa. Episodes, Vol. 39, pp 361-380.

Klerkx, J., Liégeois, J. P., Lavreau, J., and Claessens, W., 1987. Crustal evolution of the northern Kibaran belt, eastern and central Africa. Proterozoic Lithospheric Evolution, Vol., pp 217-233.

Lehmann, B., Halder, S., Munana, J. R., Ngizimana, J. de la., and Biryabarema, M., 2014. The geochemical signature of rare-metal pegmatites in Central Africa: Magmatic rocks in the Gatumba tin–tantalum mining district, Rwanda. Journal of Geochemical Exploration, Vol. 144, pp 528-538.

Lehmann, B., Melcher, F., Sitnikova, M., and Ruzindana Munana, J., 2008. The Gatumba rare-metal pegmatites: chemical signature and environmental impact. Etudes Rwandaises, Vol. 16, pp 25-40.

Melcher, F., Graupner, T., Gäbler, H.-E., Sitnikova, M., Henjes-Kunst, F., Oberthür, T., Gerdes, A., and Dewaele, S., 2015. Tantalum–(niobium–tin) mineralisation in African pegmatites and rare metal granites: constraints from Ta–Nb oxide mineralogy, geochemistry and U–Pb geochronology. Ore Geology Reviews, Vol. 64, pp 667-719.

Melcher, F., Graupner, T., Henjes-Kunst, F., Oberthür, T., Sitnikova, M., Gäbler, E., Gerdes, A., Brätz, H., Davis, D., and Dewaele, S., (2008). Analytical fingerprint of columbite-tantalite (coltan) mineralization in pegmatites: Focus on Africa, in Proceedings, ninth international congress for applied mineralogy (ICAM), pp 615-624.

Melcher, F., Graupner, T., Sitnikova, M., Henjes-Kunst, F., Gäbler, H.-E., and Oberthür, T., 2009. African rare-element pegmatite provinces: mineralogy and geochemistry of Nb-Ta minerals. Estudos Geológicos, Vol. 19, pp 217.

Möller, P., Dulski, P., Szacki, W., Malow, G., and Riedel, E., 1988. Substitution of tin in cassiterite by tantalum, niobium, tungsten, iron and manganese. Geochimica et Cosmochimica Acta, Vol. 52, pp 1497-1503.

Montjoie, R., 2014. Geological and Exploration Report. Unpublished company report, Umbono Capital, Johannesburg, South Africa.

Muchez, P., Hulsbosch, N., and Dewaele, S., 2014, Geological mapping and implications for Nb-Ta, Sn and W prospection in Rwanda, Tervuren: Royal Museum for Central Africa (RMCA), Vol. 60, pp 515-530.

Neiva, A. M. R., 1996. Geochemistry of cassiterite and its inclusions and exsolution products from tin and tungsten deposits in Portugal. The Canadian Mineralogist, Vol. 34, pp 745-768.

Ngaruye, J.-C., 2011. Petrographic and geochemical investigation of Sn-W-Nb-Ta pegmatites and mineralized quarts veins in southeastern Rwanda. MSc Thesis (unpublished), University of the Free State, Faculty of Natural and Agricultural sciences.

Nieder, R., Weber, T. K., Paulmann, I., Muwanga, A., Owor, M., Naramabuye, F.-X., Gakwerere, F., Biryabarema, M., Biester, H., and Pohl, W., 2014. The geochemical signature of rare-metal pegmatites in the Central Africa Region: Soils, plants, water and stream sediments in the Gatumba tin–tantalum mining district, Rwanda. Journal of Geochemical Exploration, Vol. 144, pp 539-551.

Oberthür, T., Melcher, F., Goldmann, S., Wotruba, H., Gerdes, A., Dijkstra, A., and Dale, C. W., 2016. Mineralogy and mineral chemistry of detrital heavy minerals from the Rhine River in Germany as evidence to their provenance, sedimentary and depositional history: focus on platinum-group minerals and remarks on cassiterite, columbite-group minerals and uraninite. International Journal of Earth Sciences, Vol. 105, pp 637-657.

OGMR, 2010. Strategic Plan 2010-2013. Unpublished Report, Rwanda Geology and Mining Authority, Kigali, Rwanda.

Perks, R., 2013. Digging into the past: critical reflections on Rwanda's pursuit for a domestic mineral economy. Journal of Eastern African Studies, Vol. 7, pp 732-750.

Pohl, W., 1994. Metallogeny of the northeastern Kibara belt, Central Africa—Recent perspectives. Ore Geology Reviews, Vol. 9, pp 105-130.

Pohl, W., Biryabarema, M., and Lehmann, B., 2013. Early Neoproterozoic rare metal (Sn, Ta, W) and gold metallogeny of the Central Africa Region: a review. Applied Earth Science, Vol. 122, pp 66-82.

Pohl, W., and Günther, M., 1991. The origin of Kibaran (late Mid-Proterozoic) tin, tungsten and gold quartz vein deposits in Central Africa: a fluid inclusions study. Mineralium Deposita, Vol. 26, pp 51-59.

Pollard, P., and Taylor, R., 1986. Progressive evolution of alteration and tin mineralization; controls by interstitial permeability and fracture-related tapping of magmatic fluid reservoirs in tin granites. Economic Geology, Vol. 81, pp 1795-1800.

Schlüter, T., 2008. Geological atlas of Africa with Notes on Stratigraphy, Tectonics, Economic Geology, Geohazards, Geosites and Geoscientific Education of Each Country. Berlin. Springer-Verlag.

Tack, L., Liégeois, J.-P., Deblond, A., and Duchesne, J.-C., 1994. Kibaran A-type granitoids and mafic rocks generated by two mantle sources in a late orogenic setting (Burundi). Precambrian Research, Vol. 68, pp 323-356.

Tack, L., Wingate, M., De Waele, B., Meert, J., Belousova, E., Griffin, B., Tahon, A., and Fernandez-Alonso, M., 2010. The 1375 Ma “Kibaran event” in Central Africa: Prominent emplacement of bimodal magmatism under extensional regime. Precambrian Research, Vol. 180, pp 63-84.

Woldai, T., Pistocchi, A., and Master, S., 2006. Validation and sensitivity analysis of a mineral potential model using favourability functions. Applied GIS, Vol. 2, pp article no. 2, pp 1-19.

U.S. Geological Survey, 2016. Mineral Commodity Summaries. U.S Geological Survey, 202 p., http://dx.doi.org/10.3133/70140094

Appendix A: Annual exports, earnings and contribution to total exports from 1930 to 2015 (GMD, 2010; OGMR, 2010; Ngaruye, 2011; USGS, 2016)

Year	Volume (tonnes)	Export earnings USD$	% of Total exports
1930	No data	No data	20
1968	No data	No data	42.5
1973	No data	No data	21.6
1985	No data	No data	<10
1995	No data	1.5	3.0
1996	No data	2.3	3.7
1997	No data	3.8	4.1
1998	No data	4.7	7.3
1998	No data	6.9	11.2
1999	943	12.6	18.2
2000	1012	15.9	23.6
2001	2102	42.6	45.6
2002	2083	15.6	23.6
2003	2599	11.1	17.5
2004	50825	29.3	29.9
2005	6465	37.3	29.9
2006	6187	37.0	24.8
2007	8283	70.6	40.0
2008	7364	94.0	40.0
2009	7960	54.6	30.0
2010	8406	71.0	30.0
2011	9697	158.0	30.0
2012	7588	136.3	28.3
2013	7639	226.2	31.0
2014	4200	No data	No data
2015	3700	No data	No data

Appendix B: Summary of Rwanda's mining history

Year	Summary
1930-1931	Cassiterite was discovered in Rwinkwavu and Rutongo concessions
1931-1941	Cassiterite and coltan were discovered in Bisesero, Gatumba, Ntunga, Mugesera and Bugesera mining concessions
1933	Discovery at Rutsiro
1940-1950	Wolframite was discovered in Gifurwe, Nyakabingo and Bugarama
1968-1985	Discoveries in Gisenyi, Kibuye, Ruhengeri, Kigali Rural and Cas&Coltan in Muhanga, Karongi, Ngoma, Nyagatare and Rusizi
1978-1979	Wolfram in Bugarama, Gifurwe and Nyakabingo
1981	Sanders carried out long range magnetic and radiometric survey of Rwanda with a flight line spacing of 500m (W-W survey parameters)
1994	The Rwandan genocide had a devasting effect on the country, its people and economy. Between 1994 to 1998 the export earnings of the Rwandan mining industry as a percentage of total exports dropped to its lowest levels in recorded history
2008	Government contracted, new resolutions geophysics (NRG), a south African company, to carry out an aerial survey covering almost the whole country to acquire gravity and new magnetic data, for further understanding of the subsurface and possible associated mineral potential

Appendix C: Sample list from the four mining areas

SampleID	Site	Mine site name	Sample Type	Mass before Splitting (grams)
NYAG06	NYAGASAGARA	Tunnel V	RoM	706
NYAG08	NYAGASAGARA	Tunnel V	Concentrate	453.6
NYAG10	NYAGASAGARA	Tunnel V	Tailings	951
NYAG14	NYAGASAGARA	Tunnel IV	RoM	677
NYAG16	NYAGASAGARA	Tunnel IV	Concentrate	71.1
NYAG13	NYAGASAGARA	Tunnel IV	Tailings	915
NYAG05	NYAGASAGARA	Tunnel I	RoM	570
NYAG07	NYAGASAGARA	Tunnel I	Concentrate	419.4
NYAG09	NYAGASAGARA	Tunnel I	Tailings	653
NYA1002	NYAGASAGARA	Tunnel I	Bottom of sluice pond	526
NYAG01	NYAGASAGARA	Walking 1	RoM	682
NYAG04	NYAGASAGARA	Walking 1	Concentrate	426
NYAG12	NYAGASAGARA	Walking 1	Tailings	1012
NYAG02	NYAGASAGARA	Walking 2	RoM	685
NYAG03	NYAGASAGARA	Walking 2	Concentrate	506
NYAG11	NYAGASAGARA	Walking 2	Tailings	458
NYAG19	NYAGASAGARA	Walking 2	Bottom of sluice pond	554
NYAG17	NYAGASAGARA	Tunnel II	RoM	493
NYAG15	NYAGASAGARA	Tunnel II	Concentrate	479.2
NYAG18	NYAGASAGARA	Tunnel II	Tailings	868
KAG01	KAGEYO	Kageo 1	RoM	666.2
KAG03	KAGEYO	Kageo 1	Concentrate	258.6
KAG10	KAGEYO	Kageo 1	Tailings	646.5
KA1001	KAGEYO	Kageo 1	Hand Speciman	629
KAG05	KAGEYO	Kageo 2	RoM	618.1
KAG04	KAGEYO	Kageo 2	Concentrate	12
KAG11	KAGEYO	Kageo 2	Tailings	603
KA2001	KAGEYO	Kageo 2	Hand Speciman	724
KAG02	KAGEYO	Kageo 3	RoM	398
KAG06	KAGEYO	Kageo 3	Concentrate	201.6
KAG09	KAGEYO	Kageo 3	Tailings	640.5
KA3001	KAGEYO	Kageo 3	Hand Speciman	764.3
KAGEXT01	KAGEYO EXTENTION	Laterite	RoM	680
KAGEXT03	KAGEYO EXTENTION	Laterite	Concentrate	177.7
KAGEXT02	KAGEYO EXTENTION	Laterite	Tailings	590.2
GAK05	GAKURAZO	Gakurazo	RoM	700

GAK01	GAKURAZO	Gakurazo	Concentrate	208
GAK09	GAKURAZO	Gakurazo	Tailings	700
GA1001	GAKURAZO	Gakurazo	Hand Speciman	723.4

Appendix D: Sample list sent to Setpoint and work program

SampleID	Mass (grams)	Drying	Splitting	Size Fraction Analysis	31 Elements+ XRF (Sn, Ta, Nb)	ICP-OES (for Li)
NYAG07	419.4	x	x	x	x	
NYAG15	479.2	x	x	x	x	
NYAG08	453.6	x	x	x	x	
NYAG04	426	x	x	x	x	
NYAG03	506	x	x	x	x	
NYAG05	570	x	x		x	x
NYAG17	493	x	x		x	x
NYAG06	706	x	x		x	x
NYAG01	682	x	x		x	x
NYAG02	685	x	x		x	x
NYAG09	653	x	x		x	
NYAG18	868	x	x		x	
NYAG10	951	x	x		x	
NYAG12	1012	x	x		x	
NYAG11	458	x	x		x	

Appendix E: List of thin sections from Nyagasagara concentrate

Thick Section Number	SampleID	Size Fraction	unit
1	NYAG03	1	mm
2	NYAG07	1	mm
3	NYAG08	1	mm
4	NYAG04	500	um
5	NYAG15	1	mm
6	NYAG04	1	mm
7	NYAG08	2	mm
8	NYAG03	2	mm
9	NYAG15	2	mm
10	NYAG07	2	mm
11	NYAG04	2	mm
12	NYAG08	4	mm
13	NYAG03	4	mm
14	NYAG15	4	mm
15	NYAG07	4	mm
16	NYAG04	4	mm
17	NYAG04	250	um
18	NYAG08	500	um
19	NYAG03	500	um
20	NYAG15	500	um
21	NYAG07	500	um
22	NYAG15	250	mm
23	NYAG07	250	mm
24	NYAG04	150	um
25	NYAG07	150	um
26	NYAG15	150	um
27	NYAG07	53	um
28	NYAG15	53	um

Appendix F: Cassiterite grades at the Nyagasagara and Coltan grades Kageyo, Kageyo Extension and Gakurazo mining sites.

Site Name	Material	Total ROM mass (kg)	Total concentrate mass (kg)	Grade (%)
Tunnel 1	Cassiterite	252	14	5.56
Tunnel 2	Cassiterite	172	0.4792	0.28
Tunnel 3	No production	No production	No production	No production
Tunnel 4	Cassiterite	160	0.0711	0.04
Tunnel 5	Cassiterite	1100	1.75	0.16
Walking site 1	Cassiterite	360	0.426	0.12
Walking site 2	Cassiterite	702	1.25	0.18
Kageyo 1	Coltan	2192	0.5317	0.02
Kageyo 2	Coltan	99.6	0.012	0.01
Kageyo 3	Coltan	1477.1	0.4053	0.03
Kageyo Extension	Coltan	1280.4	0.1777	0.01
Gakurazo	Coltan and Cassiterite	1202	1.0161	0.08

Appendix G: Cassiterite Size Fraction Analysis

Fraction	+4 mm	+2 mm	+1 mm	+500 um	+250 um	+150 um	+53 um	-53 µm
Units	%	%	%	%	%	%	%	%
NYAG07	37.2	18.4	14.2	12.9	11.1	4.0	1.8	0.4
NYAG15	25.0	37.0	23.7	9.1	3.4	0.8	0.2	0.9
NYAG08	8.4	56.1	31.9	3.0	0.1	0.1	0.1	0.3
NYAG04	5.3	27.9	51.9	11.5	2.9	0.3	0.0	0.2
NYAG03	11.8	58.9	27.8	1.3	0.0	0.0	0.0	0.1

Appendix H: Whole rock chemical data from the cassiterite concentrates of Nyagasagara

SAMPLEID	Mine_site	Sample Type	XRF Fusion Sn (%)	XRF Fusion Ta (%)	XRF Fusion Nb (%)
NYAG06	Nyagasagara_Tunnel 5	ROM	0.11	0.015	0.060
NYAG08	Nyagasagara_Tunnel 5	CONC	68.3	0.572	0.651
NYAG10	Nyagasagara_Tunnel 5	TAIL	0.04	0.015	0.059
NYAG05	Nyagasagara_Tunnel 1	ROM	0.06	0.032	0.124
NYAG07	Nyagasagara_Tunnel 1	CONC	70.5	0.551	0.634
NYAG09	Nyagasagara_Tunnel 1	TAIL	0.40	0.015	0.059
NYAG01	Nyagasagara_Walking 1	ROM	0.06	0.015	0.061
NYAG04	Nyagasagara_Walking 1	CONC	63.5	0.627	0.809
NYAG12	Nyagasagara_Walking 1	TAIL	0.03	0.016	0.060
NYAG02	Nyagasagara_Walking 2	ROM	0.10	0.015	0.061
NYAG03	Nyagasagara_Walking 2	CONC	67.3	0.647	0.793
NYAG11	Nyagasagara_Walking 2	TAIL	0.06	0.015	0.059
NYAG17	Nyagasagara_Tunnel 2	ROM	0.10	0.015	0.057
NYAG15	Nyagasagara_Tunnel 2	CONC	65.8	0.644	0.767
NYAG18	Nyagasagara_Tunnel 2	TAIL	0.08	0.013	0.054
NYAG14	Nyagasagara_Tunnel 4	ROM	**Decided not to analyse because of it's low grade**		
NYAG16	Nyagasagara_Tunnel 4	CONC	**Decided not to analyse because of it's low grade**		
NYAG13	Nyagasagara_Tunnel 4	TAIL	**Decided not to analyse because of it's low grade**		

Appendix I: Whole rock chemical data from the cassiterite concentrates of Nyagasagara

SAMPLEID	NYAG														
	6	8	10	5	7	9	1	4	12	2	3	11	17	15	18
Sample Type	ROM	CONC	TAIL	ROM	CONC	TAIL	ROM	CONC	TAIL	ROM	CONC	TAIL	ROM	CONC	TAIL
Li (ppm)	<10.5			<10.5			10.5			11.2			13.8		
As (ppm)	19	<3	31	15	<3	14	21	9	22	10	3	26	16	<3	6
Bi (ppm)	4	32	7	10	34	10	11	33	12	9	37	16	8	34	6
Co (ppm)	7	51	4	3	6	4	24	24	<3	12	11	4	<3	24	<3
Cu (ppm)	22	30	21	<10	19	<10	30	23	29	32	17	26	<10	15	10
Ni (ppm)	11	57	10	31	56	36	18	52	13	15	65	12	36	67	24
Mo (ppm)	<4	106	<4	4	109	<4	<4	110	<4	<4	112	<4	<4	109	<4
Pb (ppm)	80	-	130	47	-	313	60	-	12	70	-	48	65	-	103
Pb (%)	-	1.80	-	-	1.88	-	-	1.78	-	-	1.81	-	-	1.78	-
Rb (ppm)	82	<4	81	882	17	977	44	4	36	78	5	75	914	13	662
Se (ppm)	<3	74	3	<3	66	<3	3	72	<3	<3	81	3	<3	70	<3
Sr (ppm)	12	114	14	28	116	17	15	114	12	11	113	12	13	120	10
ThO2 (ppm)	32	<10	24	<10	<10	<10	11	<10	<10	19	<10	20	<10	<10	<10
U3O8 (ppm)	<7	37	<7	<7	<7	<7	<7	<7	<7	<7	<7	<7	<7	<7	<7
W (ppm)	<10	119	15	17	131	14	<10	116	15	21	113	18	11	272	16
Y (ppm)	9	<3	7	4	<3	<3	13	<3	11	10	<3	10	5	46	6
Yb (ppm)	<8	<8	<8	<8	<8	<8	<8	20	<8	<8	<8	<8	<8	8	<8
Zn (ppm)	32	27	32	45	26	40	35	39	30	33	33	30	66	25	51
Zr (ppm)	400	924	358	20	833	24	234	837	216	273	784	263	135	767	126
Ag (ppm)	<10	347	<10	<10	351	<10	<10	356	<10	<10	375	<10	<10	345	<10
Cd (ppm)	36	-	49	<10	-	60	31	-	21	44	-	34	<10	-	22
Cd (%)		0.37			0.37			0.37			0.38			0.36	
Sb (ppm)	<10	<10	<10	<10	<10	<10	<10	<10	<10	<10	<10	<10	<10	<10	<10

Appendix J: EMPA data from all the grains analysed from Nyagasagara concentrate

DataSet/ Point	Sample ID	Cass grain	Incl	Close	Far	MgO	SiO2	Sc2O3	TiO2	MnO	Fe2O3	SnO2	Ta2O5	WO3	Nb2O5
133 / 1 .	NYAG03		x			0	0	0	0.56	0.88	24.01	0.22	25.39	0	48.56
134 / 1 .	NYAG03	x		x		0.13	0.19	0	0	0.05	0.11	98.79	0.34	0	0.07
135 / 1 .	NYAG03	x			x	0.17	0.19	0	0.03	0	0.62	96.83	0.53	0	0.97
136 / 1 .	NYAG03	x				0.18	0.18	0	0.01	0.04	0.69	96.4	1.29	0	1.12
137 / 1 .	NYAG03	x				0.14	0.15	0	0.04	0.06	0.74	96.38	0.98	0	1.04
138 / 1 .	NYAG03	x				0.17	0.14	0	0.05	0.07	1.73	92.33	1.59	0.01	3.52
139 / 1 .	NYAG03		x			0.07	0	0	0.51	12.38	9.17	0.15	27.44	0.08	50.36
140 / 1 .	NYAG03	x		x		0.13	0.21	0	0.06	0.03	0.06	99.25	0	0	0
141 / 1 .	NYAG03	x			x	0.15	0.15	0	0	0.03	0.69	96.78	0.58	0	1.17
142 / 1 .	NYAG03	x				0.17	0.14	0	0.05	0	0.64	96.77	1.11	0	0.93
143 / 1 .	NYAG03	x				0.21	0.16	0	0.03	0.05	0.73	95.89	1.06	0.09	1.28
144 / 1 .	NYAG03	x				0.17	0.14	0	0.04	0.09	0.78	95.4	0.9	0	1.25
145 / 1 .	NYAG03		x			0	0	0	0.36	9.19	13.32	0.19	32.42	0.16	44.23
146 / 1 .	NYAG03		x			0	0	0	0.46	9.04	12.7	0.3	36.11	0.01	41.04
147 / 1 .	NYAG03		x			0	0	0	0.19	9.82	13.29	0.19	22.13	0	53.68
148 / 1 .	NYAG03		x			0	0	0	0.29	9.98	13.81	0.15	23.57	0.11	52.01
149 / 1 .	NYAG03	x		x		0.19	0.19	0	0	0.05	0.11	98.2	0	0	0.02
150 / 1 .	NYAG03	x			x	0.19	0.23	0	0	0.02	0.14	98.29	0.1	0	0.03
151 / 1 .	NYAG03	x				0.16	0.18	0	0	0.03	0.79	95.89	0.86	0.02	1.25
152 / 1 .	NYAG03					0.16	0.17	0.01	0.02	0.08	112.89	0	0	0.01	0
153 / 1 .	NYAG03	x				0.16	0.16	0	0.03	0.07	0.89	94.94	1.25	0	1.79
154 / 1 .	NYAG03	x		x		0.15	0.15	0	0.04	0.03	0.98	96.36	0.73	0	1.72
155 / 1 .	NYAG03	x			x	0.16	0.12	0	0.01	0	0.72	95.83	0.63	0	1.42
156 / 1 .	NYAG03	x				0.17	0.17	0	0.06	0.03	0.47	97.04	0.58	0	0.65

DataSet/ Point	Sample ID	Cass grain	Incl	Close	Far	MgO	SiO2	Sc2O3	TiO2	MnO	Fe2O3	SnO2	Ta2O5	WO3	Nb2O5
157 / 1 .	NYAG03	x				0.19	0.19	0	0.04	0.1	1.07	94.93	1.37	0.04	2
158 / 1 .	NYAG03		x			0	0	0	0.59	16.7	4.94	1.22	27.87	0	47.3
159 / 1 .	NYAG03	x		x		0.16	0.19	0	0.02	0.02	0.12	98.45	0.23	0	0.08
160 / 1 .	NYAG03	x			x	0.18	0.17	0	0	0.05	0.15	98.73	0.37	0	0.06
161 / 1 .	NYAG03	x				0.16	0.15	0	0.01	0.04	0.66	96.02	0.57	0	1.07
162 / 1 .	NYAG03	x				0.2	0.15	0	0	0.05	0.75	95.97	1.22	0	1.2
163 / 1 .	NYAG03		x			0	0	0	0.21	10.68	12.15	0.17	24.73	0.21	51.95
164 / 1 .	NYAG03	x		x		0.16	0.23	0	0.04	0.12	0.15	98.32	0.21	0.01	0.07
165 / 1 .	NYAG03	x			x	0.13	0.21	0	0	0	0.12	98.88	0.01	0	0.04
166 / 1 .	NYAG03	x				0.15	0.22	0	0.02	0	0.84	96.5	0.54	0.07	1.2
167 / 1 .	NYAG03		x			0.02	0	0	0.62	12.11	14.25	0.45	30.26	0.11	43.26
168 / 1 .	NYAG03	x		x		0.21	0.19	0	0.03	0.01	0.19	98.01	0.17	0	0.06
169 / 1 .	NYAG03	x			x	0.15	0.11	0	0.05	0.01	1.09	93.94	1.99	0	1.89
50 / 1 .	NYAG03		x			0	0	0.01	0.37	4.18	19.7	0.14	26.86	0.01	47.69
51 / 1 .	NYAG03	x		x		0.18	0.19	0	0.02	0.03	0.18	98.43	0.16	0.02	0.05
52 / 1 .	NYAG03	x			x	0.14	0.1	0	0.1	0.07	1.3	94.39	1.99	0	2.18
53 / 1 .	NYAG03	x				0.18	0.2	0	0.03	0.01	0.06	98.63	0	0	0.03
54 / 1 .	NYAG03	x				0.19	0.12	0	0.05	0.04	0.86	96.75	0.97	0	1.33
55 / 1 .	NYAG03	x				0.21	0.18	0	0	0.01	0.6	96.74	0.52	0.01	1.32
56 / 1 .	NYAG03	x				0.17	0.2	0	0.03	0	0.01	98.92	0.25	0	0
57 / 1 .	NYAG03	x				0.13	0.21	0	0.04	0.03	0.1	98.87	0.18	0.04	0
58 / 1 .	NYAG03	x				0.19	0.17	0	0	0	0.16	98.46	0.37	0	0.11
59 / 1 .	NYAG03	x				0.15	0.15	0	0.03	0.01	0.75	95.28	0.67	0	2.05
60 / 1 .	NYAG03	x				0.17	0.19	0	0.02	0.03	0.21	98.39	0.28	0	0.03
61 / 1 .	NYAG03	x				0.15	0.2	0	0.03	0.11	0.71	96.18	0.35	0.08	2.11
62 / 1 .	NYAG03	x				0.17	0.19	0	0.02	0.01	0.67	96.77	0.56	0	1.17
63 / 1 .	NYAG03	x				0.18	0.13	0	0.07	0.01	0.9	95.49	1.31	0.07	1.79
64 / 1 .	NYAG03	x				0.17	0.19	0	0	0	0.83	96.42	1.17	0	1.62

DataSet/ Point	Sample ID	Cass grain	Incl	Close	Far	MgO	SiO2	Sc2O3	TiO2	MnO	Fe2O3	SnO2	Ta2O5	WO3	Nb2O5
65 / 1 .	NYAG03	x				0.15	0.14	0	0	0.05	0.69	95.65	1.01	0	1.24
1 / 1 .	NYAG04	x				0.17	0.15	0	0.02	0	0.33	98.45	0.59	0	0.47
2 / 1 .	NYAG04	x				0.2	0.18	0	0.03	0.03	0.18	99.61	0.29	0.07	0.08
3 / 1 .	NYAG04	x				0.15	0.16	0	0.02	0	0.78	96.42	0.32	0	1.85
4 / 1 .	NYAG04	x				0.18	0.15	0	0	0.04	0.68	97.07	1.01	0.02	1.65
5 / 1 .	NYAG04	x				0.15	0.17	0	0.01	0	0.57	97.27	0.67	0.01	1.29
6 / 1 .	NYAG04	x				0.18	0.17	0	0	0.05	0.16	99.02	0	0	0.38
7 / 1 .	NYAG04	x				0.18	0.16	0	0	0.01	0.65	97.19	1.14	0	1.15
8 / 1 .	NYAG04	x				0.19	0.1	0	0.09	0.01	1.21	94.94	1.64	0	2.01
9 / 1 .	NYAG04	x				0.18	0.19	0	0	0.06	0.67	97.51	0.45	0.06	0.9
10 / 1 .	NYAG04	x				0.16	0.13	0	0	0.03	1.12	95.5	1.37	0.01	1.81
11 / 1 .	NYAG04	x				0.18	0.22	0	0.06	0.02	0.79	96.74	0.36	0.1	1.71
12 / 1 .	NYAG04	x				0.19	0.17	0	0.03	0	0.89	96.5	0.96	0	1.93
13 / 1 .	NYAG04		x			0	0	0	0.12	12.04	11.66	0.18	10.73	0.3	64.42
14 / 1 .	NYAG04		x			0.04	0	0.02	0.32	10.97	11.62	0.27	25.16	0.14	51.69
15 / 1 .	NYAG04	x		x		0.18	0.17	0	0.03	0.02	0.13	99.13	0.32	0	0.07
16 / 1 .	NYAG04	x			x	0.15	0.17	0	0	0	0.74	96.85	1.32	0.05	1.29
92 / 1 .	NYAG04		x			0	0	0	0.24	8.91	14.95	0.18	19.92	0	55.35
93 / 1 .	NYAG04		x			0.01	0	0	0.28	10.48	12.13	0.12	29.99	0	48.3
94 / 1 .	NYAG04		x			0.01	0	0.01	0.27	10.03	12.54	0.16	29.7	0	47.8
95 / 1 .	NYAG04		x			0	0	0.01	0.3	10.1	12.53	0.12	27.71	0	49.03
96 / 1 .	NYAG04		x			0	0	0	0.28	9.69	12.32	0.09	31.29	0	47.6
97 / 1 .	NYAG04		x			0.02	0	0	0.24	10.23	12.42	0.08	26.15	0	51.76
98 / 1 .	NYAG04		x			0.02	0	0.01	0.32	9.73	13.9	0.33	21.51	0	55.28
99 / 1 .	NYAG04	x		x		0.19	0.21	0	0	0.07	0.14	99.07	0.06	0	0.13
100 / 1 .	NYAG04	x			x	0.17	0.23	0	0	0.03	0.08	98.8	0.15	0	0.03
101 / 1 .	NYAG04	x				0.15	0.17	0	0.07	0	0.89	95.97	1.08	0	1.36
102 / 1 .	NYAG04	x				0.11	0.17	0	0.05	0	0.77	96.62	0.79	0.01	1.4

DataSet/ Point	Sample ID	Cass grain	Incl	Close	Far	MgO	SiO2	Sc2O3	TiO2	MnO	Fe2O3	SnO2	Ta2O5	WO3	Nb2O5
103 / 1 .	NYAG04	x				0.16	0.17	0	0	0.09	0.69	96.38	0.45	0	1.38
104 / 1 .	NYAG04	x				0.18	0.15	0	0.04	0	0.29	97.99	0	0	0.2
105 / 1 .	NYAG04	x				0.14	0.12	0	0	0.03	1.12	94.42	2.22	0	1.89
106 / 1 .	NYAG04	x				0.1	0.17	0	0	0.03	0.82	95.79	1.59	0.08	1.19
107 / 1 .	NYAG04	x				0.18	0.19	0	0	0.03	0.53	97.2	0.78	0	0.8
108 / 1 .	NYAG04	x				0.13	0.14	0	0.04	0.04	1.21	94.26	1.76	0	2.05
109 / 1 .	NYAG04	x				0.17	0.17	0	0	0.03	0.89	95.45	1.4	0	1.46
110 / 1 .	NYAG04		x			0.02	0	0.01	0.7	10.87	13.84	0.43	19.57	0.07	55.3
111 / 1 .	NYAG04	x		x		0.21	0.22	0	0.01	0.2	0.14	100.25	0	0	0.02
112 / 1 .	NYAG04	x			x	0.17	0.19	0	0	0.05	0.02	98.86	0.15	0.04	0
113 / 1 .	NYAG04	x				0.16	0.23	0	0.01	0.02	0.67	96.93	0.3	0	1
114 / 1 .	NYAG04	x				0.16	0.2	0	0	0.03	0.78	95.12	0.78	0	1.49
115 / 1 .	NYAG04		x			0.04	0	0.02	0.48	1.09	22.26	0.14	19.2	0.14	55.39
116 / 1 .	NYAG04	x		x		0.17	0.19	0	0	0.2	0.52	97.2	0.97	0	0.3
117 / 1 .	NYAG04	x			x	0.2	0.14	0	0.01	0	0.39	98.39	0.44	0	0.24
118 / 1 .	NYAG04		x			0.01	0	0.01	0.34	4.82	19.39	0.22	26.45	0	50.09
119 / 1 .	NYAG04	x		x		0.12	0.24	0	0	0	0.18	99.4	0.06	0.09	0
120 / 1 .	NYAG04	x			x	0.13	0.24	0	0.01	0.03	0.03	98.78	0.04	0.01	0
121 / 1 .	NYAG04	x				0.13	0.14	0	0	0.06	0.9	95.51	1.06	0	1.58
122 / 1 .	NYAG04	x				0.18	0.18	0	0	0	0.57	96.6	0.82	0	0.92
123 / 1 .	NYAG04		x			0.18	0	0	0.39	7.25	16.1	0.41	22.55	0.08	54.55
124 / 1 .	NYAG04	x		x		0.14	0.17	0	0	0.05	1	94.66	0.82	0	2.16
125 / 1 .	NYAG04	x			x	0.15	0.21	0	0.02	0.07	0.72	96.25	0.57	0.02	1.44
126 / 1 .	NYAG04		x			0	0	0	0.23	12.87	8.76	0.07	29.19	0	48.93
127 / 1 .	NYAG04		x			0	0	0.01	0.16	12.62	8.67	0.13	34.27	0	43.02
128 / 1 .	NYAG04	x		x		0.15	0.15	0	0.02	0.1	0.03	99.19	0	0	0.02
129 / 1 .	NYAG04	x			x	0.17	0.11	0	0	0	1.01	94.93	1.28	0	1.7

DataSet/ Point	Sample ID	Cass grain	Incl	Close	Far	MgO	SiO2	Sc2O3	TiO2	MnO	Fe2O3	SnO2	Ta2O5	WO3	Nb2O5
130 / 1 .	NYAG04	x				0.17	0.09	0	0.1	0.07	1.28	94.23	1.59	0	2.08
131 / 1 .	NYAG04	x				0.15	0.16	0	0.03	0.03	0.65	96.45	1.01	0	0.82
132 / 1 .	NYAG04	x				0.14	0.16	0	0.05	0.01	1.03	94.19	1.27	0.05	1.7
51 / 1 .	NYAG07	x				0.14	0.22	0	0	0.05	0.81	96.95	0.44	0.02	1.76
52 / 1 .	NYAG07	x				0.13	0.21	0	0	0	0.58	96.83	0.82	0	1.26
53 / 1 .	NYAG07	x				0.14	0.2	0	0	0.02	0.12	99.23	0.1	0	0.01
54 / 1 .	NYAG07	x				0.16	0.19	0	0.02	0	0.55	97.47	0.3	0.03	0.66
55 / 1 .	NYAG07		x			0	0	0	0.18	11.61	12.54	0.47	9.14	0.33	66.36
56 / 1 .	NYAG07	x		x		0.18	0.26	0	0	0.01	0.28	98	0.42	0	0.43
57 / 1 .	NYAG07		x			0	0	0	0.21	11.56	11.95	0.41	10.5	0.47	66.31
58 / 1 .	NYAG07	x		x		0.19	0.19	0	0	0.08	0.24	98.47	0.21	0	0.37
59 / 1 .	NYAG07	x			x	0.13	0.16	0	0	0.05	0.86	96.35	1.33	0.05	1.32
60 / 1 .	NYAG07	x				0.17	0.21	0	0	0	0.25	98.56	0.39	0	0.3
61 / 1 .	NYAG07	x				0.16	0.21	0	0	0	0.4	98.04	0.31	0.01	0.49
62 / 1 .	NYAG07	x				0.16	0.16	0	0.01	0.08	0.71	97.3	0.57	0	0.93
63 / 1 .	NYAG07		x			0	0	0	0.33	10.24	13.58	0.21	17.68	0.09	57.78
64 / 1 .	NYAG07	x		x		0.15	0.2	0	0	0.03	0.17	99.91	0.14	0	0.09
65 / 1 .	NYAG07	x			x	0.15	0.16	0	0	0.04	0.48	97.48	0.64	0	0.85
66 / 1 .	NYAG07		x			0	0	0	0.17	12.15	11.92	0.35	8.38	0.21	67.12
67 / 1 .	NYAG07	x		x		0.15	0.12	0	0.02	0.04	0.71	97.12	1.07	0	0.99
68 / 1 .	NYAG07	x			x	0.16	0.13	0	0	0.06	0.82	96.57	1.38	0	1.21
69 / 1 .	NYAG07		x			0.02	0	0.01	0.17	11.46	12.67	0.42	9.12	0.25	66.01
70 / 1 .	NYAG07	x		x		0.11	0.11	0	0.01	2.17	1.02	96.4	0.85	0	0.8
71 / 1 .	NYAG07		x			0	0	0.01	0.15	11.37	12.75	0.35	9.26	0.37	66.16
72 / 1 .	NYAG07	x		x		0.16	0.14	0	0.03	0.11	0.72	97.94	1.15	0	1.02
73 / 1 .	NYAG07	x			x	0.14	0.19	0	0.04	0.03	0.9	96.38	1.1	0.1	1.51
74 / 1 .	NYAG07		x			0	0	0.01	0.12	11.99	12.01	0.22	8.92	0.12	66.61
75 / 1 .	NYAG07	x		x		0.18	0.21	0	0.02	0.02	0.1	99.92	0.12	0.03	0.04

DataSet/ Point	Sample ID	Cass grain	Incl	Close	Far	MgO	SiO2	Sc2O3	TiO2	MnO	Fe2O3	SnO2	Ta2O5	WO3	Nb2O5
76 / 1 .	NYAG07	x			x	0.14	0.16	0	0	0	0.26	98.83	0.39	0.01	0.4
77 / 1 .	NYAG07		x			0	0	0	0.2	9.67	13.07	0.22	30.19	0	47.39
78 / 1 .	NYAG07	x		x		0.16	0.21	0	0.03	0.02	0.12	99	0.44	0	0.01
79 / 1 .	NYAG07	x			x	0.15	0.23	0	0	0.01	0.11	98.99	0.34	0	0.07
80 / 1 .	NYAG07		x			0.15	0	0	0.25	12.64	9.88	0.13	11.4	0	64.08
81 / 1 .	NYAG07	x		x		0.16	0.15	0	0	0.04	0.88	95.65	1	0	1.48
82 / 1 .	NYAG07	x				0.15	0.17	0	0.05	0.04	0.43	97.45	0.26	0	0.71
83 / 1 .	NYAG07	x				0.15	0.14	0	0.04	0	0.85	96.05	1.3	0.02	1.21
84 / 1 .	NYAG07	x				0.17	0.18	0	0	0.01	0.52	97.95	0.9	0	0.82
85 / 1 .	NYAG07	x				0.16	0.17	0	0.01	0.01	0.59	97.16	0.69	0	0.79
86 / 1 .	NYAG07		x			0	0	0	0.12	12.16	11.76	0.31	7.57	0.1	68.63
87 / 1 .	NYAG07	x		x		0.12	0.13	0	0	0.09	0.64	96.67	0.94	0	0.89
88 / 1 .	NYAG07	x			x	0.18	0.2	0	0.03	0.03	0.53	97.33	0.62	0.03	0.83
89 / 1 .	NYAG07		x			0.01	0	0.01	0.19	1.37	23.82	0.04	23.87	0	50.47
90 / 1 .	NYAG07	x		x		0.1	0.21	0	0.01	0.03	0.1	100.04	0.33	0	0.08
91 / 1 .	NYAG07	x			x	0.16	0.19	0	0	0.03	0.23	98.41	0.45	0.01	0.37
17 / 1 .	NYAG07	x				0.02	0.18	0	0	0	0.09	100.49	0.06	0.01	0.05
18 / 1 .	NYAG07	x				0.16	0.2	0	0.03	0	0.19	99.28	0	0.1	0.16
19 / 1 .	NYAG07	x				0.21	0.16	0	0	0	0.01	100.4	0.11	0.02	0
20 / 1 .	NYAG07	x				0.12	0.21	0	0	0	0.1	100.05	0.56	0.04	0.04
21 / 1 .	NYAG07	x				0.18	0.14	0	0	0.02	0.73	96.58	0.69	0	1.25
22 / 1 .	NYAG07	x				0.16	0.24	0	0	0.03	0.19	99.11	0.41	0	0.15
23 / 1 .	NYAG07		x			0	0	0	0.25	9.97	13.42	0.1	21.02	0.04	56.12
24 / 1 .	NYAG07	x		x		0.15	0.24	0	0.04	0	0.04	99.36	0.09	0	0.01
25 / 1 .	NYAG07	x			x	0.16	0.15	0	0.01	0	0.68	97.87	0.92	0.01	1.06
26 / 1 .	NYAG07	x				0.16	0.19	0	0	0.06	0.95	95.68	1.28	0	1.75
27 / 1 .	NYAG07	x				0.16	0.24	0	0.08	0.01	0.43	97.88	0.18	0	0.38
28 / 1 .	NYAG07	x				0.17	0.16	0	0	0.01	0.59	96.32	0.54	0.02	1.15

DataSet/ Point	Sample ID	Cass grain	Incl	Close	Far	MgO	SiO2	Sc2O3	TiO2	MnO	Fe2O3	SnO2	Ta2O5	WO3	Nb2O5
29 / 1 .	NYAG07	x				0.15	0.1	0	0.06	0.08	0.66	95.81	0.84	0	1.58
30 / 1 .	NYAG07	x				0.17	0.15	0	0	0	0.96	95.72	1.18	0	1.62
31 / 1 .	NYAG07	x				0.16	0.23	0	0.06	0.03	0.15	99.05	0.11	0	0.11
32 / 1 .	NYAG07	x				0.18	0.2	0	0.05	0.06	0.21	98.01	0	0	0.12
1 / 1 .	NYAG15		x			0.01	0	0	0.25	8.57	14.78	0.15	30.85	0	45.87
2 / 1 .	NYAG15		x			0	0	0	0.33	8.22	4.91	0.19	22.2	0.15	60.59
3 / 1 .	NYAG15	x		x		0.18	0.19	0	0.01	0.03	0.07	98.67	0.01	0	0
4 / 1 .	NYAG15	x			x	0.18	0.2	0	0	0	0.35	97.22	0.34	0	0.44
5 / 1 .	NYAG15		x			0.01	0	0.01	1	16.89	3.01	0.73	27.14	0	52.09
6 / 1 .	NYAG15	x		x		0.16	0.18	0	0	0.03	0.85	95.1	0.93	0	1.46
7 / 1 .	NYAG15	x			x	0.15	0.15	0	0	0.02	0.85	94.83	1.67	0	1.42
8 / 1 .	NYAG15		x			0	0	0	0.11	11.36	12.15	0.37	22.21	0.29	53.19
9 / 1 .	NYAG15	x		x		0.21	0.17	0	0	0	0.42	96.94	0.4	0	0.57
10 / 1 .	NYAG15	x			x	0.18	0.19	0	0	0	0.75	95.62	1.21	0.13	1.63
11 / 1 .	NYAG15	x				0.14	0.2	0	0	0	0.51	98.52	0.43	0	0.98
12 / 1 .	NYAG15	x				0.16	0.14	0	0	0.08	0.63	96.58	0.67	0	1.07
13 / 1 .	NYAG15	x				0.22	0.16	0	0.01	0.03	0.79	95.6	0.89	0	1.33
14 / 1 .	NYAG15	x				0.19	0.21	0	0.02	0	0.02	98.55	0.06	0.03	0
15 / 1 .	NYAG15	x				0.18	0.17	0	0.02	0.07	0.91	95.31	0.88	0	1.61
16 / 1 .	NYAG15		x			0.04	0	0	0.72	6.8	0.46	4.06	47.8	0	17.58
17 / 1 .	NYAG15	x		x		0.16	0.19	0	0	0	0.06	98.37	0.01	0	0
18 / 1 .	NYAG15				x	0.18	0.21	0	0	0.02	0.89	95.21	0.79	0	2.01
19 / 1 .	NYAG15	x				0.15	0.18	0	0	0.01	0.58	95.98	1.23	0	0.81
20 / 1 .	NYAG15	x				0.14	0.12	0	0	0.02	0.79	95.72	1.08	0	1.05
21 / 1 .	NYAG15	x				0.19	0.13	0	0.02	0.07	0.84	96.11	1.07	0	1.04
22 / 1 .	NYAG15	x				0.14	0.17	0	0	0	0.64	96.79	1.06	0	0.87
23 / 1 .	NYAG15	x				0.19	0.1	0	0	0.03	0.65	96.96	0.49	0	0.54

DataSet/ Point	Sample ID	Cass grain	Incl	Close	Far	MgO	SiO2	Sc2O3	TiO2	MnO	Fe2O3	SnO2	Ta2O5	WO3	Nb2O5
24 / 1 .	NYAG15	x				0.2	0.15	0	0.01	0.02	0.93	95.25	1.26	0	1.73
25 / 1 .	NYAG15		x			0.01	0	0	0.19	9.49	15.17	0.39	9.54	0.28	65.92
26 / 1 .	NYAG15	x		x		0.15	0.2	0	0	0.04	0.25	98.2	0.38	0	0.16
27 / 1 .	NYAG15		x			0	0	0.02	0.22	10.77	14.12	0.22	13.99	0.17	61.67
28 / 1 .	NYAG15	x		x		0.15	0.21	0	0	0.07	0.28	98.02	0.14	0.01	0.44
29 / 1 .	NYAG15					0.2	0.18	0	0	0.01	0.27	98.38	0.32	0	0.23
30 / 1 .	NYAG15		x			0	0	0	0.22	9.71	14.52	0.27	14.64	0.41	61.45
31 / 1 .	NYAG15	x		x		0.19	0.2	0	0	0	0.06	98.09	0.02	0	0.03
32 / 1 .	NYAG15	x			x	0.2	0.23	0	0.03	0.06	0.17	97.68	0.39	0.05	0.17
33 / 1 .	NYAG15		x			0.02	0	0	0.19	10	14.77	0.09	18.05	0.1	58.65
34 / 1 .	NYAG15		x			0	0	0	0.41	8.68	14.39	0.73	20.3	0.57	55.56
35 / 1 .	NYAG15	x		x		0.2	0.21	0	0.01	0.06	0.06	98.28	0	0	0.02
36 / 1 .	NYAG15		x			0.01	0	0	0.22	8.2	14.25	0.51	21.65	0.25	54.63
37 / 1 .	NYAG15	x			x	0.12	0.22	0	0	0.03	0.17	98.23	0.01	0	0.1
38 / 1 .	NYAG15	x		x		0.16	0.23	0	0	0.02	0.03	98.74	0	0	0.06
39 / 1 .	NYAG15	x				0.14	0.17	0	0.02	0.04	0.92	95.19	0.91	0.09	1.44
40 / 1 .	NYAG15	x				0.19	0.15	0	0.03	0.03	0.52	96.06	0.92	0	0.82
41 / 1 .	NYAG15		x			0.03	0	0	0.31	6.74	17.12	0.14	25.75	0	48.87
42 / 1 .	NYAG15	x		x		0.16	0.17	0	0.05	0.02	0.03	98.78	0.45	0	0.02
43 / 1 .	NYAG15	x			x	0.14	0.19	0	0.02	0.05	0.09	98.41	0.56	0	0.04
44 / 1 .	NYAG15	x				0.17	0.14	0	0.01	0	1	94.9	1.15	0	1.58
45 / 1 .	NYAG15	x				0.18	0.23	0	0.04	0.01	0.23	99.39	0.23	0.06	0.11
46 / 1 .	NYAG15	x				0.19	0.19	0	0	0	0.02	99.07	0	0.1	0
47 / 1 .	NYAG15	x				0.18	0.12	0	0.08	0.04	0.82	95.59	0.86	0	1.49
48 / 1 .	NYAG15	x				0.12	0.14	0	0	0.04	0.83	95.19	1.16	0	1.56
49 / 1 .	NYAG15	x				0.16	0.21	0	0.04	0	0.55	96.83	0.26	0	1.16
50 / 1 .	NYAG15	x				0.12	0.16	0	0.05	0.01	0.86	96.01	0.93	0	1.34

DataSet/ Point	Sample ID	Cass grain	Incl	Close	Far	MgO	SiO2	Sc2O3	TiO2	MnO	Fe2O3	SnO2	Ta2O5	WO3	Nb2O5
33 / 1 .	NYAG15					0.02	30.42	0	0.08	0.33	0.15	0.06	0	0	0
34 / 1 .	NYAG15					0.07	26.54	0	0.09	0.98	1.69	0.07	0	0	0
35 / 1 .	NYAG15					0	31.36	0.01	0.04	0.1	0.38	0.02	0	0	0
36 / 1 .	NYAG15					0.13	25.6	0	0.16	0.98	1.91	0.08	0	0	0
37 / 1 .	NYAG15					0.16	26.01	0	0.15	1.02	1.58	0.16	0	0	0
38 / 1 .	NYAG15					0.03	18.18	0.08	0.29	0.61	4.17	0.12	0	0	0.63
39 / 1 .	NYAG15	x				0.19	0.15	0	0.04	0	0.05	98.79	0	0	0
40 / 1 .	NYAG15	x				0.19	0.14	0	0.1	0.09	0.8	95.32	1.27	0	1.33
41 / 1 .	NYAG15	x				0.18	0.16	0	0.03	0.03	0.77	95.19	1.18	0.03	1.43
42 / 1 .	NYAG15	x				0.16	0.17	0	0	0.02	0.51	96.88	0.6	0	0.86
43 / 1 .	NYAG15	x				0.15	0.15	0	0.03	0	0.68	95.9	0.42	0.11	1.29
44 / 1 .	NYAG15	x				0.15	0.14	0	0.04	0.04	1	94.87	1.26	0	1.78
45 / 1 .	NYAG15	x				0.17	0.21	0	0	0.05	0.05	98.59	0	0.01	0.04
46 / 1 .	NYAG15	x				0.15	0.16	0	0.21	0.03	0.86	95.72	0.72	0	1.48
47 / 1 .	NYAG15	x				0.15	0.19	0	0.03	0.07	0.88	95.36	0.45	0	1.74
48 / 1 .	NYAG15	x				0.13	0.18	0	0.02	0.06	0.77	95.36	1.2	0	1.56
49 / 1 .	NYAG15					0.01	0.51	0	0.02	1.04	153.74	0.02	0.01	0	0